Insulin and chromogranin B secretory granules in cell lines under physiological and stress conditions

Thesis

UNRESTRICTED

Tiziana Giordano

Insulin and Chromogranin B secretory granules in β cell lines under physiological and stress conditions

Thesis submitted for the degree of

Doctor of Philosophy

In

Molecular and Cell Biology

30th April 2006

DIBIT

Department of Biological and Technological Research

San Raffele Scientific Institute

Milan, Italy

DATE OF SUBMISSION 05 APRIL 2006

DATE OF AWARD 18 DECEMBER 2006

ProQuest LLC.
789 East Eisenhower Parkway
P.O. Box 1346
Ann Arbor, MI 48106 – 1346

CONTENTS

Discussion

Materials and methods

ABBREVIATIONS USED

ARE	antioxidant response element
ATF4	activating transcription factor 4
ATF6	activating transcription factor 6
BAT	brown adipose tissue
CaMKII	Ca^{2+}/calmodulin kinase II
CART	cocaine- and amphetamine-regulated transcript
CasKII	casein kinase II
Cch	carbachol (carbamylcholine chloride)
Cg/Sg family	chromogranin/secretogranin family
CgA	chromogranin A
CgB	chromogranin B
CGP-37157	7-Chloro-5-(2-chlorophenyl)-1,5-dihydro-4,1-benzothiazepin-2(3H)-one
CHOP	C/EBP homologous protein
CHX	cycloheximide
CPE	carboxypeptidase E
CY5	indodicarbocyanine
Cyt c	cytochrome c
$\Delta\mu_{H+}$	electrochemical gradient
$\Delta\Psi_m$	mitochondrial membrane potential
DAG	diacyl glycerol
DAPI	2-(4-Amidinophenyl)-6-indolecarbamidine dihydrochloride
DBH	dopamine-β-hydroxylase
DCSGs	dense-core secretory granules
EDEM	ER degradation-enhancing α-mannosidase-like protein
EM	electron microscopy
ER	endoplasmic reticulum
ERAD	ER-associated degradation
ERSE	ER stress response element

ETC	electron transport chain
FA	fatty acids
FCCP	carbonyl-cyanide 4-(trifluoromethoxy)phenylhydrazone
FITC	fluoresceine
GABA	γ-aminobutyric acid
GC	Golgi complex
GK	glucokinase
Gluc	glucose
GSDB	goat serum dilution buffer
GSIS	glucose-stimulated insulin secretion
H_2O_2	hydrogen peroxide
HCSP	highly calcium-sensitive pool
HRP	horse-radish peroxidase
Hsp	heat shock protein
IAPP	islet amyloid polypeptide
IBMX	isobutylmethylxantine
IEM	immunoelectron microscopy
IL1β	interleukin 1
Ins	insulin
Ins1, Ins2	Insulin 1 and Insulin 2 genes
Ionomycin	iono
IP3	inositol trisphosphate
IRE1	inositol requiring 1/ERN1 [ER to nucleus signalling 1]
ISG	immature secretory granule
JNK	c-jun N-terminal kinase
K_{ATP} channels	ATP-sensitive K^+ channels
KRH	Krebs-Ringer bicarbonate buffer
MG	megamitochondria
Mt	mitochondrial
NMDA	N-Methyl-D-aspartate
·NO	nitric oxide
NSF	NEM sensitive factor
OD	optical density

$^{\cdot}O_2^-$	superoxide
$^{\cdot}OH$	hydroxyl radical
PANDER	pancreatic-derived factor
PC	proconvertase
PDI	protein disulfide isomerase
PERK	double-stranded RNA-activated protein kinase [PKR]-like endoplasmic reticulum kinase
PEK	pancreatic eukaryotic initiation factor 2α (eIF2α) kinase
PI	propidium iodide
PKA	nucleotide-dependent protein kinase
PKC	Ca^{2+}/phospholipid-dependent protein kinase
PLC	phospholipase C
PMA	phorbol 12-myristate 13-acetate
PPAR-γ	peroxisome proliferator-activated receptor γ
proIns	proinsulin
PTP	permeability transition pore
RaM	rapid uptake mode
RICS	Rho GAP involved in the ß-catenin-N-cadherin and NMDA receptor signalling
Rim	Rab3-interacting molecule
RNS	nitrogen reactive species
ROS	oxygen reactive species
RRP	ready-releasable pool
RSPs	regulated secretory proteins
RT	room temperature
S.I.	secretion index
SG	secretory granule
SgII	secretogranin II
SLMVs	synaptic-like microvesicles
SM	secretagogue mix
SNAP	soluble NSF attachment proteins
SNAREs	soluble N-ethylmaleimide-sensitive factor attachment protein receptors

SOD	superoxide dismutase
SR/ER	sarco/endoplasmic reticulum
SSVs	small synaptic vesicles
Stx	syntaxin
SYP	synaptophysin I
TCA	tricarboxylic acid cycle
Tg	thapsigargin
TGN	trans-Golgi network
Tiam-1	T-lymphoma invasion and metastasis 1
TMRM	tetramethylrhodamine methyl ester
TRITC	rhodamine
UCP	uncoupling protein
UPR	unfolded protein response
UPRE	unfolded protein response element
v-, t-SNAREs	vesicle-, target-SNAREs
VAMP	vesicle-associated membrane proteins
W/V	weight/volume
XBP-1	X-box binding protein
%	percentage

LIST OF FIGURES AND TABLES

ABSTRACT

The present work provides insights into several aspects of the regulated secretion in pancreatic β cells. We demonstrated a partial intracellular dissociation of two secretory granule (SG) markers, insulin (Ins) and chromogranin B (CgB), implicating distinct SG populations. In addition, we observed for the first time a redistribution of CgB, shifting from the SG core to the halo upon secretagogues application. We also found that upon ionomycin stimulation, CgB was preferentially released, possibly reflecting a higher sensitivity to Ca^{2+}. These findings suggest a differential regulation of Ins and CgB at multiple levels.

Furthermore, we observed heterogeneous Ins and CgB expression levels in the rat insulinoma Rin-5AH cell line. Among the sub-clones isolated therefrom, two displayed interesting features. The D2 sub-clone, showing nearly undetectable CgB levels and a lower Ins release compared to parental cells, suggested that CgB expression or secretion might affect Ins release. The Q2 sub-clone displayed high CgB content, accumulation of Ins and CgB in the Golgi complex and a poor secretion of both proteins; in addition, it showed a proportion of constitutively released Ins, suggesting a partial impairment of the secretory pathway. Q2 cells also displayed some features suggestive of oxidative stress, i.e. impaired ATP production upon stimulation of Ins secretion and altered mitochondrial morphology and functionality. Such features were also observed in patients with type 2 diabetes (T2D), thus we propose the Q2 sub-clone as a model of T2D.

Next, we assessed whether a cell model bearing oxidative stress is more susceptible to endoplasmic reticulum (ER) stress. We induced a sub-lethal ER stress in Q2 cells and compared them to INS1-E. Our results showed a higher sensitivity of Q2 cells to activation of apoptosis. Further studies of this sub-clone might shed light on the still unclear correlation between oxidative and ER stress in diabetes.

INTRODUCTION

The study of the molecular mechanisms of regulated secretion in pancreatic β cells has provided valuable insights into the pathology of diabetes mellitus. Insulin (Ins) is secreted by a regulated pathway that is widely used in neuronal and neuroendocrine cells. This ability to store secretory products (i.e. neurotransmitters and hormones) in membrane-bound organelles (secretory granules, SGs) and to release them upon appropriate stimulation is termed neurosecretion competence [1].

Ins is the main secretory product of pancreatic β cells, although other secretory products are co-stored in the SGs and co-released along with it. Any condition affecting secretory granules biogenesis, maturation and exocytosis may lead to an impairment of β cell function as seen in type 2 diabetes. In the last few years diabetes and β cell dysfunction have been associated with oxidative stress, i.e. a severe imbalance of the intracellular redox equilibrium. There is also a correlation between type 2 diabetes and a massive perturbation of the endoplasmic reticulum (ER) homeostasis, referred to as ER stress. The causes, the targets and the interrelations of oxidative and ER stress are only partially known, however their impact on β cell function is dramatic. They can affect multiple steps, including Ins synthesis, processing and correct folding, the signal transduction pathways implicated in the stimulus-secretion coupling, and late exocytotic events.

The major objectives of the work described in this thesis were to understand better the rules regulating the storage and secretion of Ins along with other secretory granule cargo

molecules in β cell models and to investigate the role of oxidative and ER stress on neurosecretion competence using β-cells as a model system. We used Rin-5AH β-cell lines that differed in their secretory response to glucose.

The following sections provide an overview of the secretory pathway and the mechanisms of exocytosis in endocrine cells, focusing on the pathways followed by Ins and chromogranin B from granule biogenesis to secretion. Insights will be provided on the complexity of Ins granule regulation and secretion. Next, the possible causes and effects of oxidative stress will be presented, with regard to their correlation with pancreatic β cell function. Finally, a brief introduction to the ER stress response and its implications in diabetes will be provided.

1. Mechanisms of neurosecretion in endocrine cells

1.1 The secretory pathway

Nascent polypeptide chains are translocated from the ER membrane-bound ribosomes into the ER lumen, where the complete proteins are properly folded and, depending on the signal sequence contained, either retained in the ER or targeted to other compartments. Proteins destined for secretion progress and mature along the so-called secretory pathway, which is composed of different intracellular compartments (ER; Golgi complex, GC; trans-Golgi network, TGN). They are then sorted into secretory vesicles and targeted to their final location. Differently from peptides, low-molecular weight molecules, typically neurotransmitters, are not synthesised in the ER but in the cytoplasm, and are taken up by transporters into secretory vesicles leaving the TGN [2].

This mechanism allows for a rapid, local recycling and refilling of secretory vesicles [3]. Secretory proteins are finally discharged by the secretory vesicles by exocytosis, i.e. the process by which SGs fuse with the plasma membrane and their soluble content is released extracellularly, whereas the luminal membrane-bound proteins are exposed on the cell surface. In eukaryotic cells, exocytosis can take place either at a constant rate (constitutive secretion) or in a regulated manner (regulated secretion).

Trafficking from ER to GC - Transport from one compartment to another through the secretory pathway is mediated by carrier vesicles that collect the 'cargo' proteins in buds arising from the membrane of the donor compartment and deliver them to the target compartment by fusing with its membrane [4]. After discharging their content, the transport vesicles return to the donor compartment and are recycled for a new cycle of transport [5]. Adaptor proteins on the cytoplasmic side of the vesicle membrane allow the appropriate cargoes to enter the forming vesicle [6] in a process called 'sorting'. Vesicles budding from the ER and moving to the GC are equipped with a specific 'COPII' coat [7], whereas vesicles moving into the retrograde direction from the GC to the ER have a 'COPI' coat [8]. As they progress through the *cis, medial* and *trans* cisternae of the GC, proteins undergo modifications such as oligosaccharide remodelling, proteolytic cleavage, phosphorylation, or sulfation. There are two possible mechanisms of protein transport through the GC [9, 10]. In the 'anterograde vesicle' hypothesis the cisternae are stable structures and transport vesicles move from stack to stack by anterograde transport, followed by COPI-coated vesicles-mediated recycling. According to the 'cisternal maturation' hypothesis, *cis*-Golgi cisternae move and mature through the GC becoming progressively *medial*- and *trans*-Golgi cisternae. The modifying enzymes are continuously delivered, sorted and retrogradally transported by COPI-coated vesicles. Both models may be valid for different proteins [11, 12].

The post-Golgi compartment - After progression and maturation through the GC, proteins are transported to a collection of cisternae, tubules and vesicles, known as the TGN, which represents the major sorting station of the secretory pathway [13]. From this compartment proteins are sorted, packaged into vesicles and targeted to different organelles: lysosomes and endosomes (through clathrin-coated vesicles), plasma membrane (through constitutive secretory vesicles or, according to recent findings, tubular structures that move along microtubules [14-16]) and SGs destined for regulated secretion.

After exocytosis, membranes and proteins are retrieved by endocytosis in clathrin-coated vesicles called endosomes, which move retrogradally to be recycled.

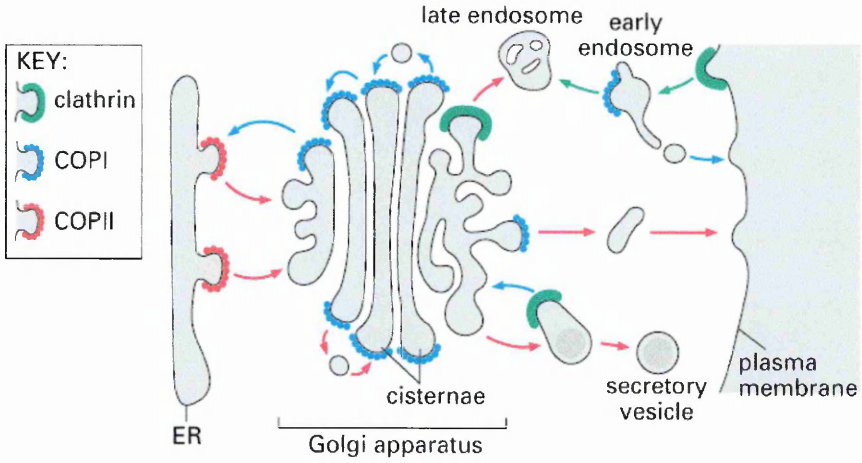

Fig. 1 - Schematic model of the secretory pathway. See text for details. Molecular Biology of the Cell, 4th Edition.

Molecular mechanisms of vesicle fusion - Transport vesicles and target membranes are provided with a molecular machinery aimed at recognising each other: the v- (vesicle)

and t- (target) SNARE (soluble N-ethylmaleimide [NEM]-sensitive factor attachment protein receptors) proteins. The SNAREs involved in intracellular and exocytotic trafficking, both constitutive and regulated, are homologs [17, 18]. The SNARE family is characterised by a 'SNARE motif', i.e. a 60 amino acid sequence that can form supercoiled structures. The interaction between the SNARE motifs of v- and t-SNAREs leads to the formation of a complex where the vesicles are 'docked' to the target membrane [19]. Once the SNARE complex has been assembled, the vesicle membrane lipids fuse with the target membrane. Following membrane fusion, the SNARE complex is disassembled by factors, such as the ATPase NSF (NEM sensitive factor) [19] and α-, β-, γ-SNAP (soluble NSF attachment proteins) [20], and its components are recycled.

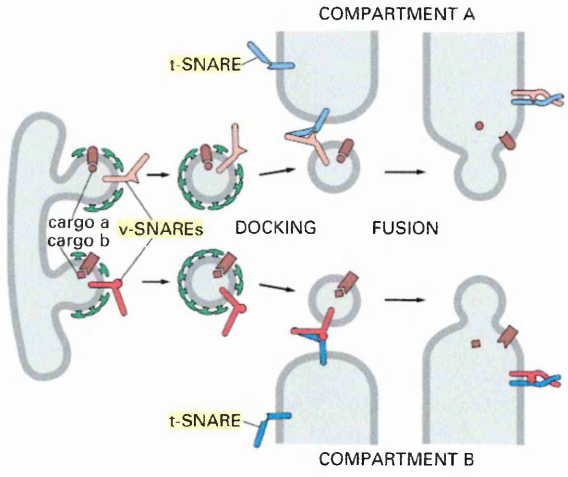

Fig. 2 – Model of vesicles docking and fusion with the target membrane. See text for details. Molecular Biology of the Cell, 4th Edition.

1.2 Granule biogenesis

Immature vesicles budding, or just budded, from the TGN contain diffuse aggregates of secreted proteins. Constitutive and regulated secretion differ in that constitutive vesicles are continuously released after protein synthesis, whereas regulated granules are stored and released upon appropriate stimuli [21]. The mechanism underlying protein sorting to one of the two pathways is still poorly defined; it is generally envisaged that sorting into the regulated pathway is controlled by selective protein aggregation (also referred to as condensation) [22, 23]. There are two classical models, not mutually exclusive, for regulated granule formation: sorting for entry and sorting by retention. According to the first, proteins are sorted to regulated SGs by specific interactions with membrane receptors and by binding proteins that form insoluble aggregates in the regulated granules [24]. These aggregates prevent proteins from entering constitutive vesicles, which represent a default pathway. In the latter model, a set of different proteins are thought to enter the forming vesicle; regulated secretory proteins (RSPs) are retained passively on the basis of their inter-molecular interactions and structure, yet other proteins are actively removed during granule maturation [23]. Intra-granular conditions, such as low pH and high Ca^{2+} concentrations, together with protein aggregation, promote retention of RSPs in the regulated SGs. Such a mechanism is believed to drive granule biogenesis in pancreatic β cells, where the presence of ions, such as zinc, further favours Ins condensation [25]. It has been suggested that the sorting mechanism (for entry or by retention) might depend on the aggregation tendency of the protein and on the relative rate of protein synthesis and vesicle formation [26].

Regulated vesicles from mammalian secretory cells contain proteins, such as chromogranin A (CgA), chromogranin B (CgB), secretogranin II (SgII), carboxypeptidase E (CPE) and several glycoproteins, capable of forming aggregates in

the ionic milieu of the TGN [27, 28]. For this reason, the aforementioned proteins may act as 'helper' proteins that favour RSPs condensation [24, 29]. This process could be the basis for sorting into regulated vesicles. CgA, CgB and CPE [30-33] may also act as 'sorting receptors', because of an N-terminal disulfide loop structure that might interact with soluble proteins and sort them into SGs. Furthermore, it was suggested that a small fraction of proteins such as CgB [34], proconvertase 2 (PC2) [35], and CPE [36], might bind to the granule membrane through lipid microdomains (rafts) [37].

Another mechanism in the sorting of RSPs into regulated granules may be dependent on their processing by proconvertases (PCs), since the RSPs aggregates are more efficiently retained in the secretory pathway after processing [38, 39].

In summary, according to the prevailing hypotheses, secretory proteins that do not associate with helper proteins, and/or cannot form aggregates, are not retained in the regulated SG and would be sorted into constitutive transport vesicles. However, constitutive secretion is not just a default pathway; indeed,the targeting of its vesicles is regulated, as exemplified by the constitutive protein trafficking to the apical or basolateral membrane in epithelial cells [40, 41], and to the axonal or the somato-dendritic region in neurons [42].

The regulated vesicles that exit the TGN are called immature secretory granules (ISGs), and are the first compartment of the regulated secretory pathway to acquire competence for stimulated release [43, 44]. During maturation, ISGs of some cell types may undergo homotypic fusion and removal of missorted material [43], modifying enzymes [45] and the 'immature' SNARE machinery [38, 46] through clathrin-coated vesicles ('sorting by exit' [47]) that are conveyed to the endosomal compartment.

Ins granule biogenesis - Ins is synthesised as a pre-prohormone (pre-proinsulin) containing an N-terminal signal sequence for ER targeting and a single polypeptide

chain contained amino acid sequences corresponding to the A and B chains of Ins and C-peptide. While progressing through the ER after cleavage of the signal sequence, proinsulin (proIns) undergoes post-translational modifications consisting of inter- and intra-molecular disulfide bonds formation (within the A chain and between the A and B chain). Further along the secretory pathway, commencing within the ISGs [48], proIns is processed into mature Ins upon cleavage at the B chain/C-peptide and C-peptide/A chain junctions by PC1/3 and PC2 [49, 50] and by CPE/CPH [51]. ProIns is not able to aggregate beyond hexamerisation [25, 52], however it can enter forming granules along with other soluble proteins [53]. After processing Ins can form multimeric, highly condensed structures (crystals) [54, 55], the formation of which is favoured by the presence of Zn^{2+}. The Zn^{2+}-Ins crystals are efficiently retained in the secretory granules. Condensation has been proposed to prevent Ins from escaping from maturing granules into budding constitutive-like vesicles [39, 45, 56]. The constitutive-like secretory pathway or post-granular secretory pathway [57, 58] has been proposed as a preferential route for a fraction of newly synthesised C-peptide, Ins and proIns, that is removed from maturing granules [44, 57]. Constitutive-like vesicles are conveyed to the endosomal system and secreted [59]. Therefore, this putative pathway might represent an alternative removal mechanism [60], that leads to refinement of granule composition during maturation.

The complexity of secretory granules - Endocrine and neuroendocrine cells can store in secretory granules a mixture of hormones, peptides, amino acids, amines and nucleotides [61, 62]. It has been generally postulated that when co-packaged in the same SGs [63, 64], peptides are also co-released [65, 66], while distinct SGs can be independently regulated [67]. In pancreatic β cells, granules store other secretory proteins beside Ins, including some members of the granins family [68, 69], IAPP (islet amyloid polypeptide), CART (cocaine- and amphetamine-regulated transcript) and PANDER (pancreatic-

derived factor) [70-72]. Contradicting the idea that co-packaged peptides are co-released, some proteins, such as C-peptide and nucleotides in β cells [54, 73, 74], that are not tightly associated with the granule core but are rather distributed in the clear halo, can be ready releasable as compared to proteins in the core. This is also the case for neurotransmitters in PC12 cells [75]. To make the picture more complex, the differential sorting of peptides into distinct subpopulations of SGs has been reported in different cellular systems [76-79]. Well documented examples for such intracellular sorting are the three peptides derived from the processing of the egg lying hormone precursor of Aplysia, which are stored into three different types of SGs [77, 80], and the two hormones of neurohypophysial neurons, galanin and vasopressin, which are stored both separately in two distinct SGs and together in a mixed SG [67]. Also, the endopeptidases responsible for prohormone processing are differentially packaged and transported [81-83].

Chromogranins - Granins are a family of acidic, sulphated, calcium-binding proteins generally believed to be co-stored with peptide hormones and catecholaminergic neurotransmitters in the SGs of most neuroendocrine cells [30]. The chromogranin (Cg)/secretogranin (Sg) family comprises predominantly CgA, CgB and SgII. Other members are less widely expressed [84]. Even when co-stored and co-released with hormones and neurotransmitters, their synthesis can be independently regulated [79, 85, 86]. Chromogranins undergo tissue-specific processing [87] by endoproteases and their products are released by regulated secretion [88]. Several products of granin processing have been identified in different cell types [89-92]. The granin family is widely distributed in endocrine/neuroendocrine and neuronal cell types [93-95]. For this reason these proteins are commonly used as neuroendocrine cell markers. In addition, they are also diagnostic markers for the development of endocrine or neuroendocrine tumors [96, 97]. The general role of granins and processing products in different cell types has not been completely

elucidated. Beside the already discussed role in sorting and packaging of secretory proteins [29, 98, 99], CgA and CgB have been proposed also to act as Ca^{2+} accumulators in the SGs of neuroendocrine cells [100, 101], due to their Ca^{2+}-binding properties. Processing products derived from CgA, CgB and SgII elicit autocrine, paracrine and endocrine effects on several organs [102-104], often of an inhibitory nature [105]. For instance, the CgA-derived peptide pancreastatin [106] plays an inhibitory role on Ins secretion [107, 108]. Other CgA processed products play a role in cell adhesion [109, 110]. By converse, very little is known about the processing and function of CgB.

1.3 Molecular mechanisms of regulated secretion

The molecular mechanisms of regulated secretion are shared by neurons and neuroendocrine cells, despite their different embryonic origin [62]. The general model of regulated secretion comprises three steps: 'docking' of secretory vesicles to the plasma membrane, triggered by interactions between v- and t-SNAREs; an ATP-dependent stage leading to partial fusion, referred to as 'priming', that renders vesicles competent to Ca^{2+}-triggered exocytosis; vesicle content release by opening of a fusion pore [111, 112]. The kinetics of regulated exocytosis can vary among different cell types [62]. An important difference between neuronal and neuroendocrine cells is that in the latter the secretion by SGs is slower (60 milliseconds to 30 seconds) and sustained, because there are less vesicles docked at the plasma membrane, and their mobilisation and priming is enhanced by Ca^{2+} [113], whereas synaptic transmission mediated by vesicle fusion in neurons is very rapid (0.1 to 6 milliseconds) [62, 114]. The molecular machinery involved in fusion events is composed of four families of proteins: SNARE, NSF, sec1/munc18-like and Rab proteins [111, 115]. The SNARE proteins specific for regulated exocytosis are

the t-SNAREs syntaxin (Stx) 1 or 3 and SNAP-2, and the v-SNARE synaptobrevin 1 or 2, also known as vesicle-associated membrane proteins (VAMP) [116]. The model of regulated exocytosis, that represents a variation of the common mechanism previously described for vesicle fusion during protein trafficking, describes the interaction between Rab3a and its effector Munc-18, that is normally bound to Stx1 and prevents it from binding to SNAP-25 and VAMP. Upon stimulation of regulated exocytosis, some conformational changes occur that lead to the formation of a 'core complex' between Stx1, SNAP-25 and the VAMP proteins. After vesicle fusion, the core complex interacts with SNAPs and NSF and is disassembled upon ATP hydrolysis [18, 62] (see Fig. 3 below).

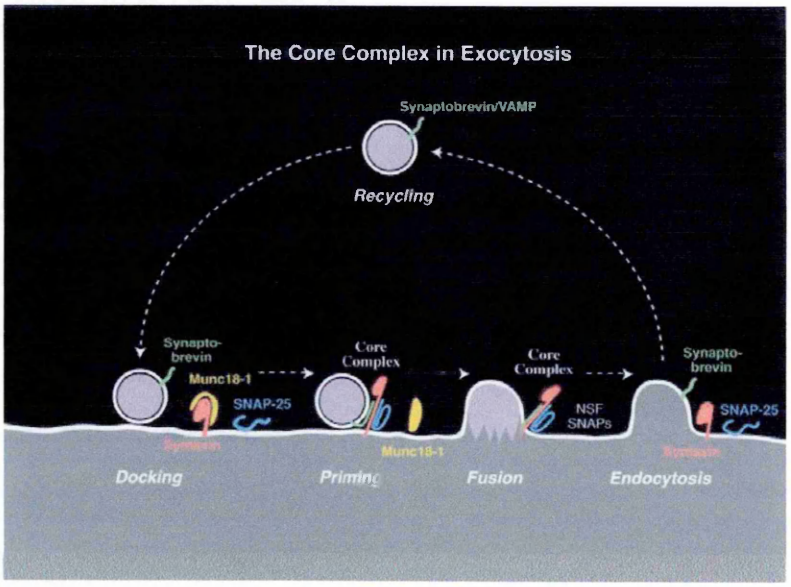

Fig. 3 – Schematic model of the exocytotic steps and of the core complex assembly/disassembly cycle. See text for details. Gerber and Sudhof, Diabetes 2002.

Two other regulatory proteins, the Rab3-interacting molecule (Rim) [117] and Munc-13 [118], act at a post-docking step and regulate vesicle priming. Another family of proteins that directly interact with the core complex to regulate exocytosis, is that of the putative

Ca^{2+} sensor synaptotagmins [119]. Situated on the membrane of secretory vesicles and on the plasma membrane, upon Ca^{2+} binding [120] synaptotagmins can bind to Stx1 [121] and SNAP-25 [122], inducing a conformational change that allows for vesicle fusion. However, their exact role is not yet completely clear [18, 123].

Conformational changes in SNAREs are also modulated through phosphorylation by Ca^{2+}/calmodulin kinase II (CaMKII), casein kinase II (CasKII)[120, 124, 125] and the Ca^{2+}/phospholipid-dependent protein kinase (PKC) [126-128].

Models of granule fusion – Two classical models of exo-/endocytosis have been formulated [129-131]. In the first model, the so-called 'complete fusion', the granule lipid bilayer is integrated into the plasma membrane and its membrane is retrieved by conventional clathrin-mediated endocytosis. In the second type, referred to as 'kiss-and-run', the granule content is released through a fusion pore, that may open transiently and reversibly, so that it may close before complete emptying of the granule interior and without mixing of the granule membrane with the plasma membrane. A third type of exo-/endocytosis has been postulated, in which a large opening between the granule lumen and the extracellular space is formed, but no alteration of the granule structure occurs. Granules undergoing this type of exocytosis are retrieved in less than 10 seconds. This model is referred to as 'semifusion', and has been observed in different β cell lines [132, 133], where it has been estimated that it accounts for 90% of the release events.

1.4 Ins secretion

Ins secretion is a biphasic process, consisting in a sharp rise during the first few minutes (first phase), followed by a slower and much larger sustained Ins release (second phase), which lasts for at least 1 h [134]. The first phase accounts for the β cell's ability to respond rapidly to glucose [135]. The capability of pancreatic β cells to adapt Ins secretion to the actual glucose concentrations arises from the features of their glucose metabolism. β cells express the glucose transporter Glut2 [136]. Once transported inside, glucose is phosphorylated by glucokinase (GK) and converted into glucose-6-phosphate, which can enter into the glycolytic pathway. GK can be envisaged as a glucose sensor, because it couples an increase in glucose concentration to an increase in the metabolic flux [137, 138].

The events initiated by nutrient stimulation and leading to Ins release are referred to as 'stimulus-secretion coupling' [139]. The first product of glycolysis is pyruvate, which enters mitochondria and is metabolised through the tricarboxylic acid (TCA) cycle; substrate oxidation generates reducing equivalents that are transferred to the mitochondrial ETC (electron transport chain). The energy stored in the ETC as proton gradient generates the mitochondrial membrane potential ($\Delta\psi_m$), which represents the driving force for ATP synthesis by the ATP synthase complex (see section 2.1). ATP is translocated to the cytosol by the adenine nucleotide translocator, thus increasing the intracellular ATP:ADP ratio [140]. ATP binds to a subunit of the ATP-sensitive K^+ (K_{ATP}) channels on the plasma membrane, namely the pore-forming subunit Kir 6.2, leading to the closure of the channel [141]. This event leads to membrane depolarisation and gating of voltage-sensitive Ca^{2+} channels [142, 143]. The subsequent increase in cytosolic Ca^{2+} activates Ins granule exocytosis [144-147]. The events described above lie in the so-called

'triggering' pathway of Ins release, where Ca^{2+} is the main trigger of Ins secretion (Fig. 4).

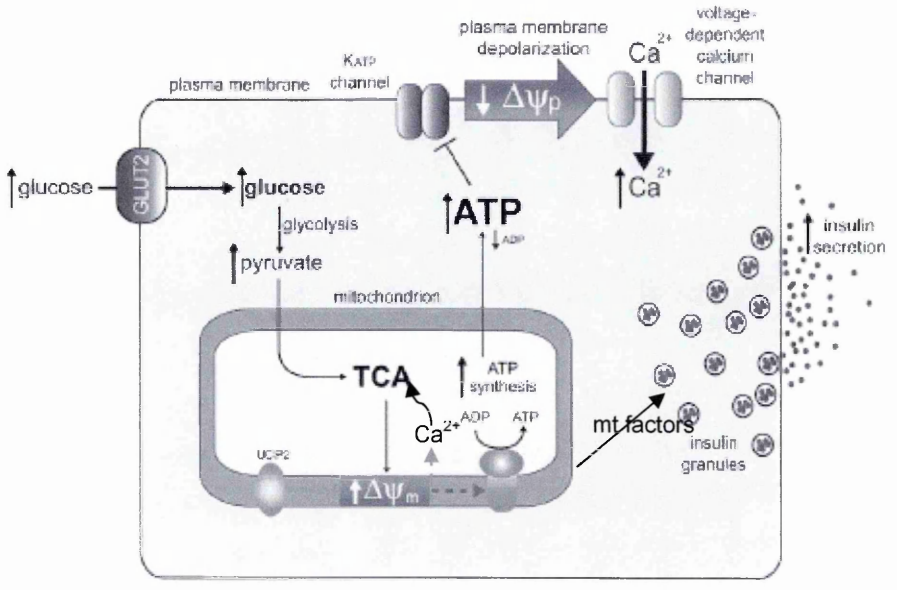

Fig. 4 - Schematic model of the stimulus-secretion coupling in β cells. Glut2: glucose transporter 2; mt-factor(s): mitochondrial metabolites; TCA: tricarboxylic acid cycle; $\Delta\Psi_m$: mitochondrial membrane potential; $\Delta\Psi_p$: plasma membrane potential; UCP2: uncoupling protein-2. Modified from Green et al, Diabetes 2004.

Ca^{2+} elevation directly triggers Ins exocytosis [139, 148] and activates the intracellular signalling pathways that trigger and/or potentiate its release. Beside the triggering pathway, there is a glucose-induced 'amplifying' pathway, which is activated along with glucose metabolism and enhances Ins release (see below). The intracellular messengers activated by both the triggering and the amplifying pathway and their effectors have not been completely identified, however the following signalling pathways are clearly implicated in Ins secretion stimulated either by nutrients, or by neurotransmitters and hormones: PCK, CaMKII, nucleotide-dependent protein kinase (PKA). PKC is regulated by diacyl glycerol (DAG), which is generated either by *de*

novo synthesis [149] or by phospholipid hydrolysis upon phospholipase C (PLC) activation [150]. PKC acts at distal steps of the exocytosis through indirect or direct effects (Munc-18 phosphorylation [127]). The other product of phospholipid hydrolysis, inositol trisphosphate (IP3), mobilises intracellular Ca^{2+}-stores by binding to its receptors on the ER membrane [151], thus further elevating Ca^{2+} levels. Ca^{2+} elevation activates CaMKII [152, 153], associated with Ins SG [154], which is implicated in final secretory steps such as granule fusion and mobilisation [155, 156]. Glucose stimulation also induces an increase in cAMP levels by activating adenylate cyclase, which in turn leads to enhanced activity of PKA [153, 157]. PKA appears to be involved in distal exocytotic steps [158].

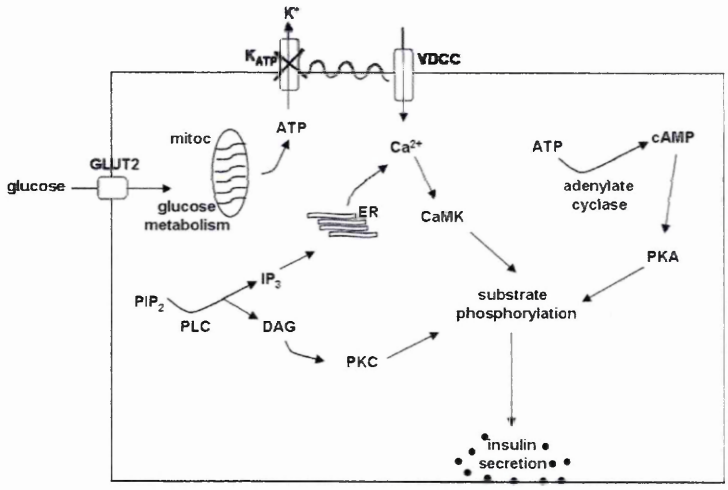

Fig. 5 – Schematic model of the intracellular pathways involved in Ins secretion. VDCC: voltage-dependent calcium channel; PIP_2: phosphatidyl inositol bisphosphate; for the other abbreviations see the text. Personal elaboration of the statements presented in the Introduction section.

The K_{ATP}-dependent mechanism (triggering pathway) only accounts for the first phase of Ins secretion, whereas it seems clear that the second phase response is not mediated by Ca^{2+} elevation [159]. The glucose-induced amplifying pathway accounts for the second phase of Ins secretion. This amplifying pathway comprises two components: a Ca^{2+}-

dependent, K_{ATP}-independent pathway [160-162] and a Ca^{2+}-independent, K_{ATP}-independent one [139, 163]. The latter involves the PKC- and cAMP-mediated signalling [164, 165], while the former is related to coupling factors generated through nutrient metabolism [140, 147, 166]. Anaplerosis, defined as the refilling of TCA cycle intermediates, and cataplerosis, i.e. the efflux of TCA intermediates and their metabolites from the mitochondrion to the cytosol also play a role in Ins secretion [167, 168], possibly via the K_{ATP}-independent pathway [166], involving either malonyl-CoA [169], glutamate [170] or ATP/GTP [171] as coupling factors.

Granule pools in pancreatic β cells - The biphasic nature of Ins secretion may be explained with the existence of distinct pools of Ins granules [139, 172]. Like in other secretory cell types, pancreatic β cell granules exist in at least two distinct pools: the docked or 'ready-releasable' pool (RRP), from which they are promptly and rapidly exocytosed, and the 'reserve' pool, that becomes releasable after a recruitment step. Within the docked population there are two subsets: one of 'immediately releasable' primed granules, and another one of 'ready releasable' unprimed granules [173, 174]. It has been estimated that β cell contains on average 10,000-12,000 granules in the reserve pool, while only 10% of the total number is in the docked state, and the 0,2-1% (50-100 granules) is immediately releasable [133, 175]. This small pool of granules is envisaged to account for the rapid exocytotic burst of the first phase Ins secretion [176, 177]. The second phase requires the refilling of the emptied pool with granules already docked at the plasma membrane. The metabolic requirements of the two phases of Ins secretion (Ca^{2+}-dependency and energy dependency, respectively) are mirrored by the properties of the granules pools [112, 158].

To make the picture more complex, a third granule pool has been described according to its electrophysiological properties, named 'highly calcium-sensitive' pool (HCSP) [178,

[179], that is very small but is markedly increased in response to global Ca^{2+} elevations. On the same line, a small (around 10%) subset of the reserve pool, capable of fast, long-distance movements [180], has been shown to be differently regulated by Ca^{2+} as compared to the majority of granules in the reserve pool (namely, they appear to be regulated by different Ca^{2+} pools: the fast granules respond to Ca^{2+} elevations mediated by Ca^{2+} influx through voltage-gated Ca^{2+} channels, while the slow granules are regulated by Ca^{2+} efflux from the ER). This pool has been suggested to act as an intermediate pool that enables refilling of the RRP during the second phase Ins secretion [181], but a conclusive correlation between this SG pool and its content has not been drawn.

From β cell physiology to pathology – The molecular mechanisms underlying neurosecretion, from protein synthesis and granule biogenesis to the final steps of exocytosis, are tightly regulated. The picture is even more complex in pancreatic β cells, where the unique correlation between stimulation of Ins secretion and metabolism leads to a biphasic release. According to what has been presented in the previous section, several crucial steps can be envisaged in pancreatic β cell function, such as Ins processing and folding, mitochondrial nutrient metabolism, Ca^{2+} homeostasis, intracellular signalling.

In the next sections we will describe two major perturbations of cell homeostasis, the oxidative stress and the ER stress that play a crucial role in cell dysfunction and have been correlated to pathological conditions of pancreatic β cells, such as hyperglycemia and diabetes.

2. *Oxidative stress*

2.1 Role and generation of ROS

Redox homeostasis - Oxidative stress is defined as a serious imbalance between the production of reactive species and antioxidant defences [182], leading to potential tissue damage. Reactive species, either deriving from oxygen (ROS) and nitrogen (RNS), are highly reactive molecules. These include superoxide ($^{\cdot}O_2^-$), hydroxyl radical ($^{\cdot}OH$), hydrogen peroxide (H_2O_2) and nitric oxide ($^{\cdot}NO$). The concentration of reactive species is maintained at low levels by antioxidants, compounds capable of competing with other substrates, thus delaying or inhibiting their oxidation. Endogenous antioxidants include superoxide dismutase (SOD), catalase, ascorbate, glutathione, and less specific compounds, such as free amino acids and proteins, whose scavenging activity is related to oxidation-induced proteolysis [183].

At moderate concentrations ROS may act as regulatory mediators in physiological processes, for instance regulation of vascular tone or signal transduction from membrane receptors. However, most reactive species play an important role in signalling processes implicated in protective responses against oxidative stress, that re-establish the balance between ROS production and scavenging activity, i.e. the so-called redox homeostasis. When ROS production is significantly and persistently increased, the system can still reach an equilibrium, associated with higher ROS concentrations and different patterns of gene expression, which does not necessarily lead to a pathological condition. This occurs for example in the process of aging. Pathological conditions develop in a situation of chronically increased ROS levels [184].

Several endogenous sources of ROS can be envisaged in all cell types and in particular in secretory cells: mitochondria, NADP(H) oxidase and the secretory pathway itself.

Mitochondria - The largest production of ROS takes place in the mitochondria: their generation is directly linked to the mitochondrial activity, which is therefore tightly regulated by substrate availability, Ca^{2+} uptake [185] and feed-back inhibition through NADH [186], ATP and citrate [184]. During mitochondrial respiration, molecular oxygen is consumed for the complete metabolism of glucose and other substrates, leading to the production of ATP. Substrate oxidation along the TCA cycle leads to reduction of the carriers NAD^+ and FADH, which in turn provide electrons to the ETC on the inner mitochondrial membrane. The ETC is formed by four inner membrane-associated enzyme complexes, cytochrome *c* (cyt c) and the mobile electron carrier ubiquinone (Fig. 6) [187]. The electron flow through the ETC generates an electrochemical gradient ($\Delta\mu_{H+}$) across the inner mitochondrial membrane that is used to drive the extrusion of protons from the mitochondrial matrix [185, 186]. The $\Delta\psi_m$ is created by the ETC and is negative inside. ATP synthase (complex V) in the mitochondrial membrane uses the energy stored in the $\Delta\mu_{H+}$ to catalyse the production of ATP from ADP. Although the mitochondrial ETC is very efficient, it is intrinsically prone to some electron leakage through side reactions between each electron carrier and molecular oxygen [188]. Such side reactions generate $\cdot O_2^-$ [189, 190], which dismutates to H_2O_2, that if not detoxified can be converted to $\cdot OH$ [191]. It has been estimated that during oxidative phosphorylation up to 4% of the oxygen consumed gives rise to ROS. The outer mitochondrial membrane is also a source of H_2O_2 through the enzyme monoamine oxidase [188].

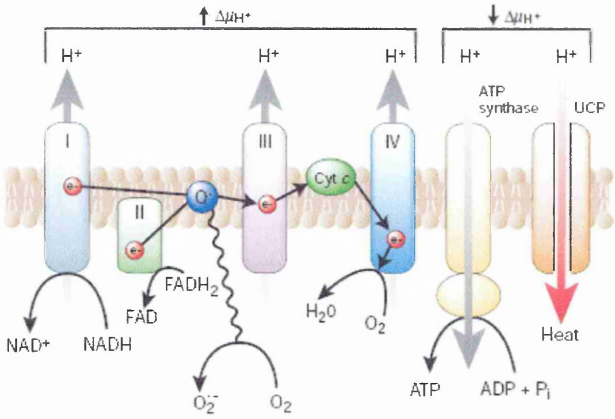

Fig. 6 – Schematic representation of the mitochondrial respiratory chain. Cyt c: cytochrome c; I-IV: complexes of the ETC; $\Delta\mu_{H+}$: proton electrochemical gradient. Brownlee, Nature 2001.

NAD(P)H oxidase - Another relevant source of ROS, which has not been intensively investigated in pancreatic β cells [192, 193], is the NAD(P)H oxidase [184, 194]. Initially characterised in macrophages and neutrophils [195], NAD(P)H oxidase is a heme-containing protein complex, comprising a plasma membrane-bound cytochrome *b*558 complex and three cytosolic components. Its assembly and activation occurs upon translocation of the cytosolic components to the cytochrome *b*558 complex [196, 197]. The NAD(P)H oxidase isoforms of non-phagocytic cells produce O_2^- at a low, but sustained rate [196]. NAD(P)H oxidase activity is tightly regulated by the cytosolic signalling molcule rac [198, 199] and its regulatory proteins Tiam-1 (T-lymphoma invasion and metastasis 1) [200] and RICS (Rho GAP involved in the ß-catenin-N-cadherin and NMDA receptor signalling; NMDA = N-Methyl-D-aspartate) [201]. Other regulatory proteins of the NAD(P)H oxidase components are PKC [200, 202-204] and CaMKII [200, 201]. Upon stress conditions, such as hyperinsulinemia, hyperglycemia and fatty acids (FA) exposure, NAD(P)H oxidase activity is up-regulated [205].

The secretory pathway - Another physiological source of ROS and possible cause of oxidative stress is the protein folding process that occurs in the ER [206, 207]. The formation of disulfide bonds, catalysed by the protein disulfide isomerase (PDI) [208, 209], is essential for the folding and stability of many secretory proteins, including Ins. The disulfide formation is a redox-dependent process, driven by a protein relay [210, 211] that involves PDI and Ero1 [212], a FAD-dependent enzyme. Ero1 oxidises PDI, which in turn oxidises disulfide bonds in folding proteins. Ero1 can then couple its re-oxidation to the reduction of molecular oxygen: as a result, its activity may generate ROS [206, 207, 211]. The balance between oxidised and reduced equivalents in the ER is maintained by the transport of oxidised glutathione from the cytosol into the ER lumen [210, 213]. A summarising model is depicted in Fig.7.

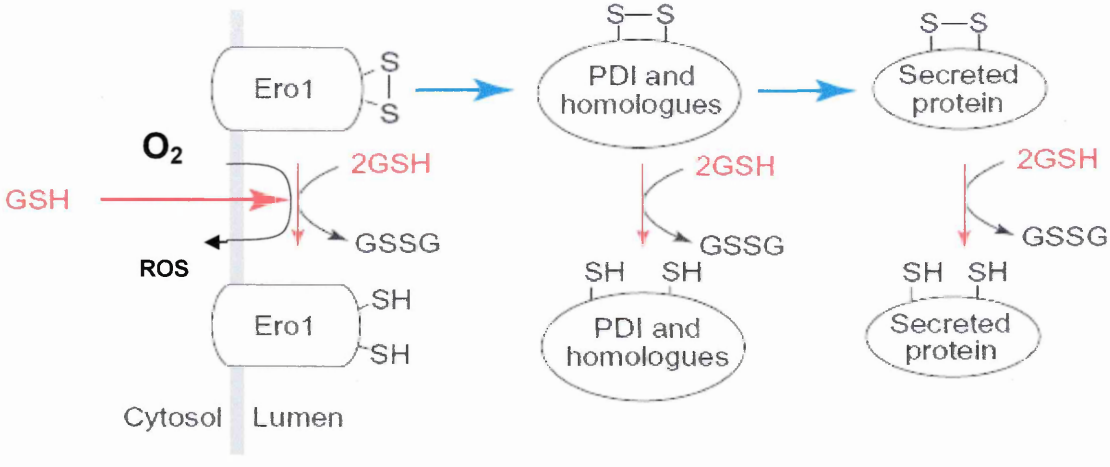

Fig. 7 – Schematic model of the protein relay implicated in disulfide bound formation. GSH: oxidised glutathione; GSSG: reduced glutathione. Modified from Frand et al, Cell Biology 2000.

Considering that up to 80-90% of proteins synthesised in secretory cells may be destined for secretion, it has been estimated that Ero1-mediated oxidation could account for a high fraction of cellular ROS produced during protein synthesis [206].

2.2 Oxidative stress

Upon a strong, persistent perturbation of the redox homeostasis the cells activate the so-called oxidative stress response. Excessive levels of ROS may be generated either by increased stimulation of NAD(P)H oxidases or by other mechanisms (i.e. mitochondria). At high concentrations, ROS and RNS directly oxidise and damage DNA, proteins and lipids. In particular, due to its close proximity to the mitochondrial inner membrane, the mitochondrial (mt)-DNA is a target of ROS attack [185, 186] and some mutations can be induced, whose accumulation leads to mitochondrial dysfunction. ROS and RNS can also indirectly damage tissues by activating a number of cellular stress-sensitive pathways, which may lead to changes in gene expression, perturbation of the intracellular Ca^{2+} homeostasis, activation of endonucleases and eventually apoptosis [214]. High and sustained levels of ROS have been implicated in the pathogenesis of cancer, diabetes mellitus, atherosclerosis and other diseases [184].

Uncoupling proteins – A protective role against oxidative stress may be played by the so-called 'uncoupling' proteins (UCPs), which in certain cell types account for an inducible proton leak from the mitochondrial ETC [215]. This mechanism is distinct from a basal proton leak, present in all cell types, that dissipates a part of the energy stored in the proton gradient. Upon uncoupling, the energy of the electrochemical gradient is not used for ATP synthesis, but results in heat production. Three UCPs, namely UCP1, UCP2 and UCP3, have been identified [216]. UCP-1 or thermogenin, that is typical of

brown adipose tissue (BAT), is involved in thermoregulation in newborns and hibernating animals [217]. UCP2 mRNA has been found in many tissues [218], although the protein is not expressed in all. UCP3 is restricted to BAT and skeletal muscle [219]. Beside the uncoupling function of UCP2 and UCP3, there is some evidence for a role as anion transporters (for free FA for example) [220]. Both these functions may play an important role in protecting cells from oxidative stress. In conditions of high substrate availability but limited oxidising capacity, for instance, electrons exit the ETC and generate ROS. An uncoupling activity, causing a faster electron flow and lowering $\Delta\psi_m$, would decrease ROS formation. Besides, as anion carriers, UCP2 and UCP3 might transport $\cdot O_2^-$ and therefore protect mitochondria from ROS. Upon oxidative stress UCP2 mRNA and protein expression increases [218]: this appears to be a rapid response to oxidative stress. Moreover, UCPs are activated by $\cdot O_2^-$ [221]. Thus, UCP2 and UCP3 have been suggested to play a role in decreasing the $\Delta\Psi_m$ and consequently the production of $\cdot O_2^-$ in oxidative stress conditions.

2.3 Mitochondria and oxidative stress

Mitochondria are an important target of the oxidative stress-induced damage, that causes a decrease in ATP production, a perturbation of Ca^{2+} homeostasis, and the induction of mitochondrial permeability (defined as the opening of a 'megapore' in the mitochondrial inner membrane) which leads to the breakdown of the $\Delta\Psi_m$ [186]. All these events may lead to cell death [222].

Mitochondria may alter their shape to adapt to new environments. In normal conditions their shape is dynamic [223] and they can undergo fusion and fission events. When cells require a large amount of ATP, mitochondria become granular and separated, thus increasing their surface area. When less ATP is required they form filamentous structures and decrease their surface area [224]. Under unfavourable conditions mitochondria undergo two types of structural changes: a simple swelling or the formation of megamitochondria (MG). Mitochondria become two to three times larger in size by simple swelling, whereas beyond those extents they can be classified as MG. MG formation can be envisaged as an adaptive process. They may generate less amounts of ROS because of lower respiration rates and oxygen consumption, and the decrease of ATP production induces growth arrest. If mitochondria succeed in suppressing intracellular ROS levels, they can return to normal structure and functionality. However, upon chronic oxidative conditions, MG become swollen, the $\Delta\psi_m$ is lowered, intracellular ATP levels decrease and several pro-apoptotic proteins, including cytochrome c, are released from the mitochondria because of the membrane permeability increase, leading to activation of caspases and induction of apoptosis [224, 225].

Alterations of the protein machinery implicated in fusion and fission and mitochondrial morphology (i.e., swollen or fragmented mitochondria) are associated with some human diseases [226, 227], including type 2 diabetes [228, 229].

Calcium and mitochondria. It is widely accepted that mitochondria play an important role in the intracellular Ca^{2+} homeostasis: oxidative metabolism and ATP production [185], ER-mitochondria Ca^{2+} signalling, apoptosis [230, 231], and possibly every signalling pathway, are associated with mitochondrial Ca^{2+} uptake. Ca^{2+} flux into the mitochondria represents only a small fraction of the cytoplasmic Ca^{2+} flux during Ca^{2+} redistribution

in the cytoplasm [232]. Nevertheless, the contribution of mitochondrial Ca^{2+} flux is functionally very relevant.

The $\Delta\psi_m$ is the driving force for mitochondrial Ca^{2+} influx, and must be tightly regulated [230]. In resting conditions the mitochondrial Ca^{2+} content is low; Ca^{2+} uptake is mediated by specific transporters, and since there is no counter-ion for Ca^{2+}, the mitochondrial membrane becomes depolarized [233]. The subsequent increased rate of ATP production is thought to restore $\Delta\psi_m$. There are two mechanisms for Ca^{2+} entry in mitochondria which are still undefined at the molecular level: a 'uniporter' [234, 235] and a 'rapid uptake mode' (RaM) [236], which responds to small, rapid Ca^{2+} concentration changes [236]. There are also two distinct mechanisms of Ca^{2+} efflux: a Na^+-dependent and a Na^+-independent transport systems [237]. In addition, Ca^{2+} might be released from mitochondria through the permeability transition pore (PTP), a channel of unknown identity [238, 239], the opening of which is enhanced by a reduction of the $\Delta\psi_m$, elevated matrix $[Ca^{2+}]$ and increased matrix pH.

Mitochondria can form networks or clusters connected with intermitochondrial junctions. The mitochondrial network is an electrically continuous system that facilitates energy delivery and may organise antioxidant defence [240]. Mitochondrial Ca^{2+} uptake takes place at preferential sites associated with the ER, and it diffuses along the network during maximal stimulation [231].

Mitochondria and ER - In several cell types a close apposition of mitochondria with ER can be observed [241]. Subdomains of the sarco/endoplasmic reticulum (SR/ER) are in close contact with mitochondria (Fig. 8): in these discrete areas there is a concentration of Ca^{2+} release sites (IP3-gated channels [242] or ryanodine receptors [243]), which are next to mitochondrial Ca^{2+} uptake sites [238]. This apposition between ER and mitochondria is dynamically regulated by Ca^{2+} [244]. The functional association of ER and mitochondria is

involved in intracellular Ca^{2+} homeostasis and in the induction of apoptosis. Concerning the former, in pancreatic β cells a perturbation of mitochondrial functionality leads to emptying of the ER Ca^{2+} stores and impairment of Ins secretion [245]. With respect to the latter, mitochondrial Ca^{2+} overload in a situation of high ER Ca^{2+} release (induced for example by C2 ceramide) activates the apoptotic pathway, induces mitochondria swelling and rupture of the mitochondrial network [246].

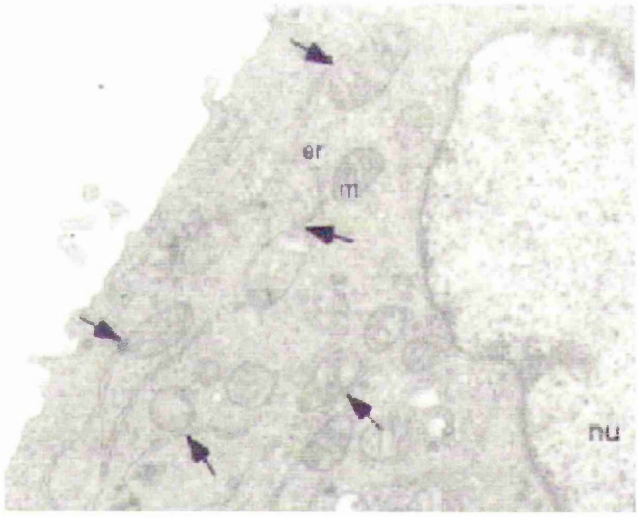

Fig. 8 – Apposition between ER and mitochondria. Electron microscopy image illustrating (arrows) the close apposition of mitochondria (m) and endoplasmic reticulum (er). nu: nucleus. Detail from Hajnoczky et al, Journal of Physiology 2000.

2.4 Oxidative stress and β cells

Formation of ROS and RNS has been associated with β cell dysfunction and/or cell death in both type 1 [184, 247, 248] and type 2 diabetes [249-251]. In addition, ROS-induced stress pathways are responsible for the secondary complications associated with diabetes [247, 252, 253]. B cells have lower antioxidant defences as compared to other tissues and are therefore particularly sensitive to the oxidative stress-induced damages.

As previously illustrated (section 1.4), mitochondrial metabolism is crucial in Ins secretion [146, 254], and mitochondria are both a source of free radicals and their targets. Thus, oxidative stress and ROS-induced mitochondrial dysfunctions lead to impaired Ins secretion [191, 255]. Another possible direct target of ROS in β cells might be glucokinase [191] that is inactivated by oxidation [256].

Once diabetes is overt, chronic hyperglycemia leads to a vicious cycle of continuous perturbation of β cell function, by impairing glucose-induced Ins secretion and Ins gene expression [257] and causing chronic oxidative stress [258, 259]. During chronic hyperglycemia, β cells activate an antioxidant compensatory response that may lead to adaptation and survival [260], however in some cases they fail to trigger the compensatory response [261]. Besides high glucose, chronically elevated levels of FA, which are also essential β cell fuels in normal conditions, lead to impairment of Ins secretion [262] and Ins gene expression [263] and to ROS production, for instance by increasing mitochondrial uncoupling [264].

Ins secretion as a possible source of ROS - B cells are not only a target of oxidative stress: they may also be envisaged as a source of ROS. It has been postulated that oxidative stress in pancreatic β cells may be tightly linked to glucose-stimulated Ins secretion (GSIS) [265]. According to this hypothesis, three players are implicated in ROS generation: increased glycolytic flux, ATP:ADP ratio and intracellular Ca^{2+} concentrations.

Glucokinase stimulates a steep increase of the glycolytic flux and a strong enhancement in the production of reducing equivalents [266]. In addition, increased FA oxidation could further increase the production of reducing equivalents.

Upon increase of the glycolytic flux, the increased $\Delta\psi_m$ induces a reduced state of the carriers along the ETC, thus increasing ROS production [190]. The value of $\Delta\psi_m$ also

depends on the ATP production rate and, in particular, on free ADP concentration, that has been shown to decrease dramatically upon glucose stimulation [267]. A decrease in free ADP concentration leads to decreased ATP production, which in turn increases $\Delta\psi_m$ and, subsequently, ROS production.

The third player of β cells ROS production would be the elevation of intracellular Ca^{2+} levels. Ca^{2+} accumulation in mitochondria is believed to stimulate mitochondrial generation of ROS [268].

ROS production may therefore be a fast event tightly coupled with glucose metabolism; however, oxidative stress can be observed after days of exposure to Ins secretagogues.

UCP2, oxidative stress and Ins secretion - Uncoupling protein UCP2 is expressed in pancreatic β cells. Its role is still debated, and three main functions have been suggested: negative regulation of Ins secretion, defence against oxidative stress and regulation of fat homeostasis [269, 270].

Both knocking-down [271] and over-expression [269] of UCP2 in pancreatic islets affect ATP levels, $\Delta\psi_m$ and glucose-stimulated Ins secretion [269]. The absence of UCP2 seems to lead to a higher degree of coupling in the mitochondria of β cells and to improved Ins secretion.

As expected because of its function as an uncoupler, the over-expression of UCP2 also enhances the resistance of β cells toward ROS toxicity [272]. As previously discussed UCP2 protein levels are enhanced upon high glucose- and free FA-induced oxidative stress [218, 273, 274]. In addition, mitochondrial $\cdot O_2^-$ activates UCP2-mediated proton leak. However, these protective mechanisms against oxidative stress also decrease the rate of ATP production and the corresponding ATP:ADP ratio, leading to impaired glucose-stimulated Ins secretion, as observed in type 2 diabetes [221, 275].

The third hypothesis related to UCP2 function is the regulation of fat homeostasis. In order to optimise Ins secretion, the lipid content in pancreatic β cells must be carefully regulated [276, 277]. UCP2 gene expression is up-regulated upon stimulation of the peroxisome proliferator-activated receptor γ (PPAR-γ) [278], that binds to non-esterified FA. This supports a role for UCP2 in the intracellular fat homeostasis in β cells, as in other tissues [279]. Indeed, chronic exposure to FA leads to Ins secretion impairment, decrease in $\Delta\psi_m$ and ATP:ADP ratio, and over-expression of UCP2 at the level of both mRNA and protein [274, 280]. This role of UCP2 in fat homeostasis points to a protective role of UCP2 in the framework of fatty acids-induced ROS generation.

3. *ER stress*

3.1 The unfolded protein response

Beside oxidative stress, another stress response has been observed under diabetic conditions in several tissues, including pancreatic β cells, i.e. the so-called ER stress, defined as a perturbation of ER homeostasis [281]. The two stress responses are thought to be correlated [207, 282], in particular with regard to the ER redox balance [206] (see section 2.1), although a causal relation has not been established yet.

As discussed in section 2.1, the ER is the organelle responsible for synthesising secretory and membrane proteins, that are post-translationally modified and folded in its lumen. It is also the major intracellular Ca^{2+}-store. Newly synthesised proteins are folded and assembled in a process facilitated by chaperones within the ER lumen. Chaperone activity [283] and inter-molecular electrostatic interactions [284] largely depend on Ca^{2+} [285]. Proteins in the ER undergo a strict 'quality control' [286], so that partially or incorrectly folded proteins are recognised and bound by chaperones such as BIP [287], calnexin and calreticulin [288]. This ensures their retention in order to complete the folding, and in case of failure they are transported to the cytosol and undergo proteasomal degradation [288]. Upon stressful conditions, such as for instance an overload of misfolded proteins, a perturbed redox balance or an altered Ca^{2+} concentration, the ER fails to export correctly folded proteins and a stress-induced signalling cascade is activated that leads to the so-called 'unfolded protein response' (UPR), aimed at restoring physiological conditions. The UPR is a transcriptional and translational signalling pathway encompassing four distinct responses. Firstly, chaperone expression is induced to enhance ER protein folding capacity, while at the same time the overall

rate of transcription and translation is reduced with a concomitant decrease in the biosynthetic rate [289]. A further response consists of an increased ER-associated degradation (ERAD) of misfolded proteins [290, 291]. Finally, if the previous mechanisms fail to re-establish a physiological situation, the apoptotic pathway is triggered. UPR can also be activated in non-stressed conditions, where it is thought to be involved in the control of nutrient fluctuations [292, 293] (see below). Moreover, some physiological conditions can be mediated by ER stress induction, as exemplified by the differentiation of B cells into plasma cells [294, 295].

BIP - The most important chaperone implicated in ER stress sensing and UPR induction is BIP. This chaperone, which belongs to the heat shock protein (Hsp) family, is an essential component of the translocation machinery that is responsible for bringing the newly synthesised peptides into the ER lumen; it also plays a role in retrograde transport across the ER membrane of aberrant proteins destined for proteasomal degradation [296]. Most importantly, BIP binds to unfolded proteins [287]. It exists in two forms, as a monomer and as an oligomer. In the monomeric form, BIP associates with unfolded proteins [297], which appear to enhance its conversion from the oligomeric pool into the monomeric active form [298] as well as to enhance BIP synthesis. The increase in the amount of monomeric BIP is the first event of the UPR and represents a mechanism for sensing the accumulation of unfolded proteins in the ER lumen. The unfolded protein signal is then transduced through the ER membrane by three trans-membrane proteins (IRE1, PERK, ATF6; Fig. 9), that in physiological conditions are maintained in an inactive state by BIP binding [299, 300]. Upon stress induction, in order to face the increased need of protein folding, BIP dissociates from the three transducers, thus allowing their activation. In its unbound form, IRE1 (inositol requiring 1/ERN1 [ER to nucleus signalling 1]) dimerises and can bind other proteins along the ER stress signal

transduction pathway [301]. PERK (double-stranded RNA-activated protein kinase [PKR]-like endoplasmic reticulum kinase/PEK [pancreatic eukaryotic initiation factor 2α (eIF2α) kinase) can sensor and transduce the ER stress signal with a common mechanism, i.e. by stable dimerisation [302]. ATF6 (activating transcription factor 6) is translocated from the ER membrane to the GC upon stress sensing, by way of two independent signal sequences that are unmasked after dissociation of BIP [303, 304].

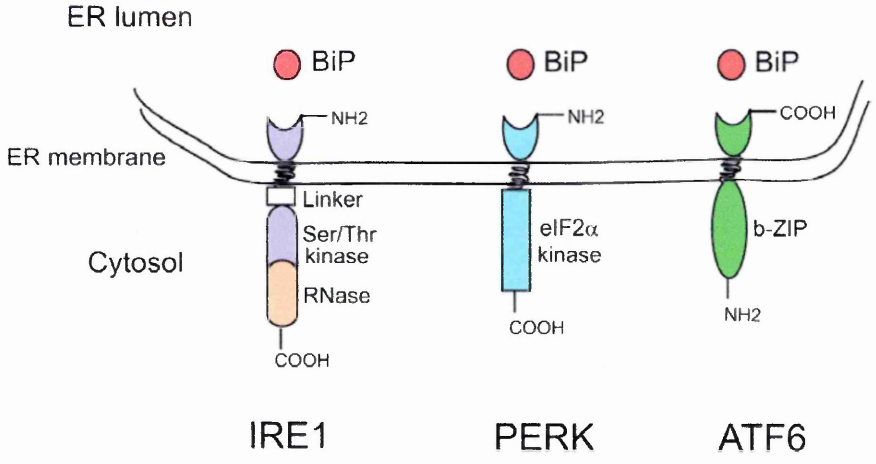

Fig. 9 – Schematic model of the interaction between the ER stress sensor BIP and the three trans-membrane signal transducers IRE1, PERK and ATF6. See text for details. Zhang and Kaufmann, Journal of Cell Biology 2004.

The UPR activated by unfolded proteins signal transduction consists of a signal transduction cascade that involves different pathways, triggered by IRE1, PERK and ATF6 (Fig. 10).

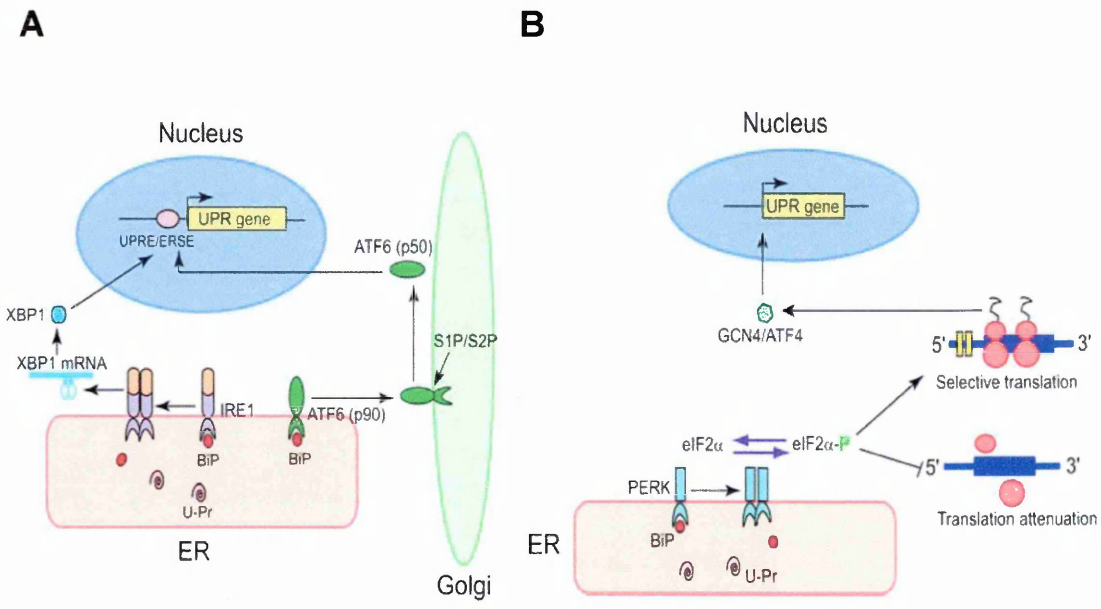

Fig. 10 – Schematic model of the signalling pathways induced by IRE1, ATF6 and PERK. A: IRE1 and ATF6 pathways; B: PERK pathway. See text for details. Zhang and Kaufmann, Journal of Cell Biology 2004.

IRE1 - IRE1 shows kinase [305] and endoribonuclease activity, the latter being induced upon oligomerisation by the former. IRE1 endoribonuclease activity induces splicing of a small intron from the transcription factor XBP-1 (X-box binding protein) mRNA. While the unspliced form of XBP-1 is degraded by the proteasome, the spliced form accumulates and shows an enhanced transcriptional activity [294]. The target of XBP-1 is a subset of genes encoding for ER chaperones [306], that are bound by XBP-1 in the so-called 'UPRE' (unfolded protein response element) or in the 'ERSE-II' (ER stress response element II) on their promoters [307]. These target genes include Herp, the most highly inducible gene under ER stress [308], and EDEM (ER degradation-enhancing α-mannosidase-like protein), a protein complex implicated in the ER quality control that interacts with misfolded proteins and accelerates their degradation via ERAD [309].

PERK – PERK is a kinase whose mRNA is predominantly expressed in the pancreas, and the protein only in pancreatic islets [310]. Its oligomerisation, which occurs upon dissociation of BIP, induces phosphorylation of its substrates, the transcription factors eIF2α [310] and Nrf [311]. The latter is implicated in the survival response. Upon activation and nuclear translocation, Nrf binds to the 'ARE' (antioxidant response element) of its target genes, that encode detoxifying enzymes [312]. eIF2α normally initiates protein translation by delivering the initiator-tRNA^{Met} to ribosomes. Its phosphorylation by PERK results in the inhibition of translation. Upon such attenuation, only specific mRNAs are translated [313], including ATF4 (Activating Transcription Factor 4) [314], that in turn induces the transcription of genes involved in amino acids metabolism, oxidative stress specific gene expression and ER stress-induced apoptosis. Some targets of ATF4 are CHOP, GADD34 and ATF3: CHOP (C/EBP homologous protein)/GADD153 is a pro-apoptotic factor [307, 315] (see below); GADD34 is responsible for a feed-back loop [316, 317] that removes the eIF2α-induced translational block; ATF3 activates GADD34 and CHOP transcriptional activation, thus coordinating the ATF4 response [318].

ATF6 – Upon translocation to the GC, the basic leucine-zipper transcription factor ATF6 is cleaved by the proteases SP1 and SP2 [319]. The fragment released after cleavage moves into the nucleus [320] and binds to the ERSE [321] and ERSE-II [322] on the promoters of the target genes. ATF6 regulates transcription of many important ER stress genes, including BIP, CHOP, XBP-1 and Herp [322-324].

Coordination of UPR – The different branches of the UPR converge onto common downstream targets, such as CHOP [307, 308, 325, 326]. The interaction among the UPR-induced transcription factors can act as a positive or a negative control on the UPR itself. Importantly, there is a temporal sequence in the UPR [327]. The PERK pathway is quickly activated, and the ATF6 pathway is activated before that of XBP-1, thus

allowing the cell to face the ER stress through an increased protein folding. Only later, if the stress is prolonged, XBP-1 is produced and the refolding is coupled to protein degradation [328].

Apoptosis - When ER functions are severely impaired, the cell must be eliminated by apoptosis. A central pathway in ER stress-induced apoptosis is the activation of caspase-9 upon mitochondrial cytochrome c release, mediated by pro-apoptotic factors such as Bax, Bak and Bad on the mitochondrial membrane. Another major ER stress-specific apoptotic pathway is the activation of caspase-12, triggered by direct interactions of IRE1 and by the massive Ca^{2+} release from the ER, that is mediated by the aforementioned pro-apoptotic factors on the ER membrane. Alternative pro-apoptotic cascades such as ASK1 (a stress-activated MAP3 kinase) [329] and JNK (c-jun N-terminal kinase) [330] are activated by the IRE1 pathway. Ca^{2+} released by ER is rapidly taken up by mitochondria, thus inducing collapse of $\Delta\Psi_m$ and induction of apoptosis [331]. In this picture, the ER stress-induced pro-apoptotic factor CHOP suppresses the expression of the anti-apoptotic factor Bcl-2, thus shifting the balance between anti-apoptotic and pro-apoptotic factors towards the latter [327, 332].

3.2 ER stress and Ins secretion

Pancreatic β cells have a highly developed ER and are subject to a massive protein synthesis and secretion. The expression of IRE1, PERK and BIP in β cells is high compared to other tissues, which might reflect the need for a strict quality control of protein folding. Indeed, malfolding leads to apoptosis [333], as exemplified by the Akita mouse, a spontaneous diabetic model [334] which carries a mutation in the insulin 2 (Ins2)

gene, that disrupts a disulfide bond formation between the A and B chain. This has a strong impact on ER homeostasis and leads to apoptosis through CHOP induction [315, 335]. The Akita mouse model has shed some light on the relevance of ER stress in diabetes and in particular in the decrease in β cell mass that is a feature of both type 1 and type 2 diabetes [336]. The increased Ins demand in conditions, such as obesity or Ins resistance, produces ER overload and may lead to chronic ER stress, with consequent induction of apoptosis.

A central player in pancreatic β cell function is PERK, whose functional alterations lead to type 2 diabetes [292, 337, 338]. PERK is physiologically active at low glucose concentrations [339]. Due to the glucose-dependent translational control of proIns [340], in conditions of low Ins demand proIns translation is attenuated. The PERK-induced eIF2α phosphorylation is implicated in such negative regulation of translation [292, 337], whereas under increased glucose levels the UPR is turned off and proIns translation enabled, at least until an ER overload induces again UPR and translational attenuation. Thus, Ins synthesis appears to be coupled with ER folding capacity through UPR, and PERK plays a crucial role in this regulation, preventing ER stress and ensuring the maintenance of β cell function [338].

AIMS

The aim of the work presented in this thesis was to investigate under physiological and stress conditions Ins- and CgB-contanining secretory granules in β cell models. This aim was pursued by:

1. assessing the intracellular distribution and the secretory behaviour of Ins and CgB in two rat, INS1-E and Rin-5AH, one mouse, β-TC3, β-cell lines and in human purified islets under physiological conditions;
2. reducing the complexity of the Rin-5AH population by subcloning and by drawing correlations between the poor Ins secretory behaviour displayed by RIN-5AH cells, and in particular the Q2 subclone derived thereof, and oxidative stress features such as mitochondrial status;
3. studying the effects of ER stress on Ins and CgB secretion in the INS1-E β-cell model and in Rin-5AH and Q2 cells.

RESULTS

1. Ins and CgB granules in β cell models

The co-existence of different secretory products within the same granule [63, 64], as well as the packaging of secretory proteins in different granules, has been documented in different cellular systems [67, 77, 80] but has so far not been extensively investigated in pancreatic β cells, nor it has been studied with regard to a possible differential control of SGs storing of different secretory products. Besides hormones and neurotransmitters polypeptides belonging to the Cg family are markers of SGs in both neurons and neuroendocrine cells [93-95]. Traditionally, these proteins and their processing products have been considered to be co-stored, and co-secreted along with the hormones and transmitters from the same SG [30, 63, 69]. In pancreatic β cells the main secretory product, Ins, largely co-localises with CgA [68, 69]. While CgA has been characterised in β cells from the point of view of its intracellular localisation, processing and secretion, little is known about the other member of the granin family, CgB.

A series of experiments was undertaken to investigate:

- the sub-cellular localisation of CgB in different β cell models
- whether and to what extent Ins and CgB are co-stored within the same SGs
- how Ins and CgB are distributed with regard to the architecture of the SGs

- whether Ins and CgB are always co-released, or can be discharged independently from each other.

1.1 Dissociation of Ins and CgB in the SGs of various B cell models: immunofluorescence

In order to establish whether Ins, and the granin CgB are stored together or in separate SGs, we investigated a number of well known Ins-secreting cell lines together with isolated human islet cell preparations, by using a battery of antibodies against the two proteins and intracellular organelle markers. First of all we noticed that the confocal analysis (Fig. 1A), even when associated to tridimensional reconstruction, gave unsatisfactory results in terms of granular staining, while enhancing the signal from compact structures, such as the GC. Moreover, the resolution of confocal images at high magnification was not satisfying. We therefore improved the image quality by using the Deltavision™ wide-field microscopy system, which couples the acquisition of optical sections along the z-axis with deconvolution analysis and tridimensional reconstruction (Fig. 1B).

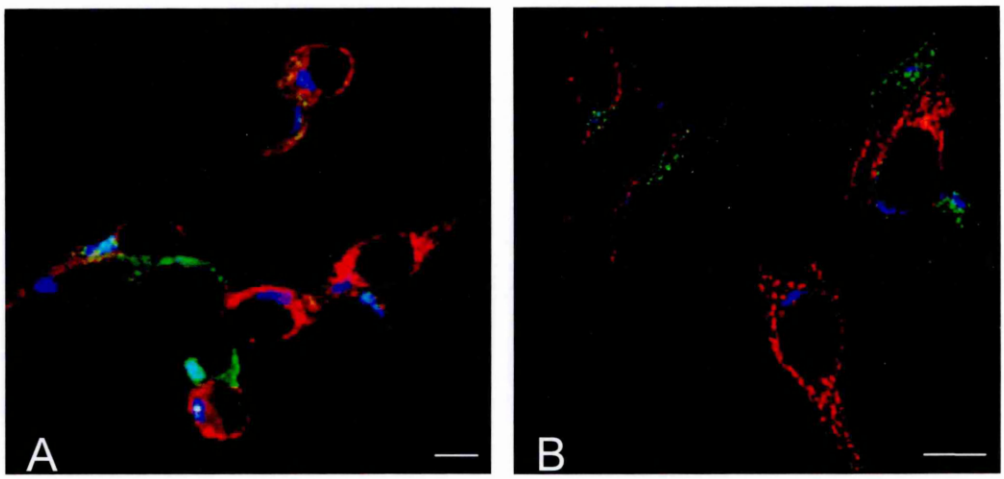

Fig. 1 - Comparison between confocal analysis and wide field acquisition followed by image deconvolution. Immunostaining of INS1-E cells with Ins (red), CgB (green) and TGN38 (blue). Panel A: Confocal image acquired with a Leica TCS-SP2 microscope; Panel B: acquisition with the Deltavision™ system. Scalebar: 6μm.

Fig. 2 shows the results with the various investigated β cell types. In the rat line INS1-E (Fig. 2 A,A'–C,C') a large extent of co-localization between Ins and CgB was observed in the perinuclear area of the TGN labelled by the specific marker, TGN38 (Fig. 2 A,A'), and also in the GC, revealed by the specific marker GM130 (Fig. 2 B,B'). In contrast, many of the discrete dots scattered at the periphery of the cytoplasm, corresponding to SGs, were immunolabelled only for either one of the secretory proteins (Fig. 2 A,A'-B,B'). The considerable dissociation at the level of SGs was confirmed also when, instead of Ins, we compared the distribution of CgB with that of a specific β-SG marker, the single span membrane protein IA-2/ICA-512 (Fig. 2 C,C'). A strong co-localisation of Ins and IA-2/ICA-512 was also observed in β-TC3 cells (Fig. 2L). Also CgA, the granin most often investigated in β cells, largely co-localised with Ins in INS1-E cells (Fig. 2I).

In the other two Ins-secreting lines investigated, the rat RIN-5AH (Fig. 2 D,D'–F,F') and the mouse β-TC3 insulinoma (Fig. 2G), the dissociation between Ins and CgB at the level of SGs appeared even larger than in INS1-E cells. Similar results were obtained in preparations of isolated human islet cells (Fig. 2 H,H'), where CgB was expressed not only in the Ins-positive β cells, but also in other cells that we did not investigate for endocrine function.

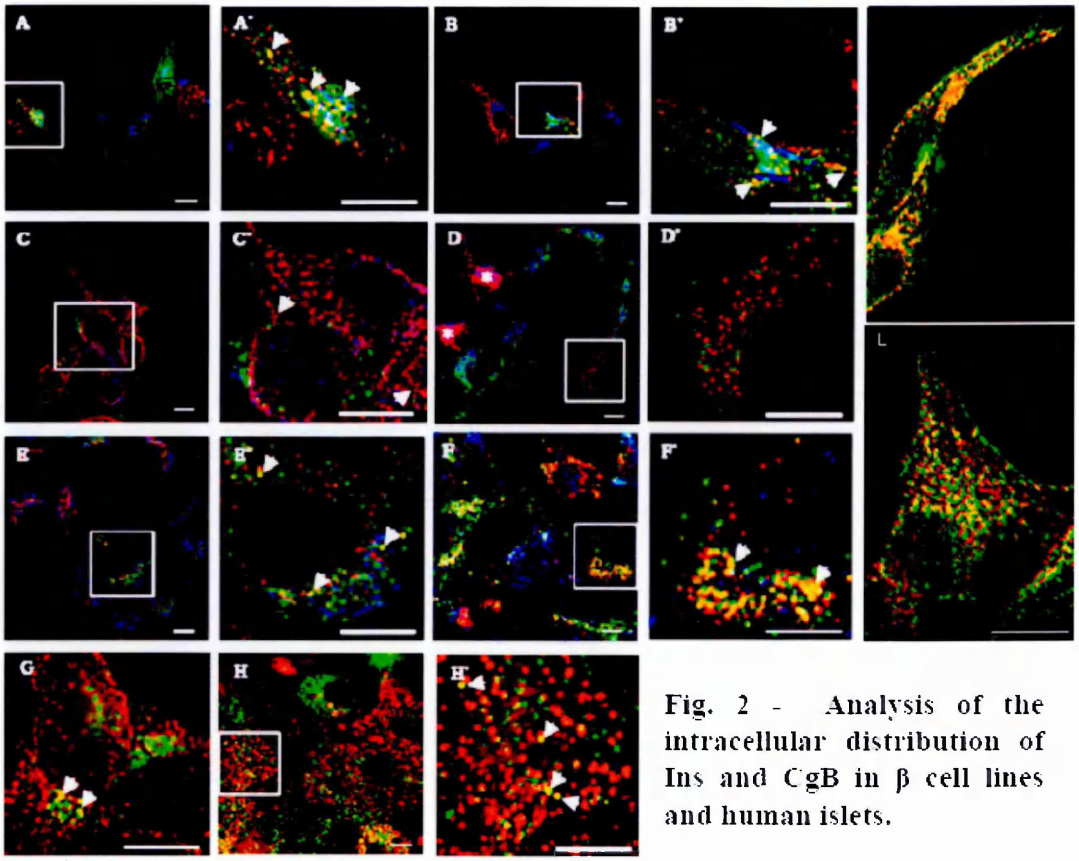

Fig. 2 - Analysis of the intracellular distribution of Ins and CgB in β cell lines and human islets.

Deconvolution of immunofluorescence images of different β cell models, INS1-E (panels A – C and I), Rin-5AH (panels D – F), β-TC3 (panel G and L) and isolated human islets (panels H). Cells were stained with anti-Ins (red), anti-CgB (green) and a third marker (blue). Panels A, B, C, D, E, F and H show overviews of the cell populations. The enlargements of the contoured areas are shown in panels A', B', C', D', E', F' and H'. Clear co-localisation of Ins and CgB is evident in the TGN (TGN38; A, A' and D, asterisks) and in the GC (GM130; B, B' and E, E'); the SG marker IA-2 (blue, panels C, C' and F, F') largely co-localises with Ins (purple) and not with CgB (Fig. 1C and C') in INS1-E cells. In Rin-5AH cells IA-2 appears mostly localised to the GC/TGN area, where it co-localises with Ins and CgB (panels F and F'). Arrows indicate SGs positive for both Ins and CgB (yellow). Islet cells immunopositive for CgB but not for Ins represent non-β cells (panel H). Panel I shows INS1-E cells stained for Ins (red) and chromogranin A (CgA). A nearly complete co-localisation of the two markers is evident in the GC-TGN area and in the peripheral granules (yellow). Panel L shows β-TC3 cells stained for Ins (red) and IA-2/ICA512. Also in this case the co-localisation between the two markers is large. Panel A was obtained by combining two microscopic fields from the same coverslip. Scale bar: 6 μm.

1.2 Ultrastructural immunohystochemistry of Ins and CgB

The properties of the SGs in INS1-E cells were further investigated at the ultrastructural level. In conventional Epon-embedded cell preparations heterogeneity of the SGs was evident, with coexistence of two populations differing from each other in terms of electron density of their internal core (Fig. 3 A,B). At the immunoelectron microscopy level, however, this difference was no longer visible. The SGs positive for both Ins and CgB and those positive for either one of the proteins appeared in fact very similar to each other (Fig. 3 C-H).

1.3 The intra-granular distribution of CgB is a dynamic feature

The next question was whether in INS1-E the dissociation of Ins and CgB is stable or may change depending on the functional state of the cells. For this task we counted the SGs at random in at least 25 cell sections of ultrastructurally immunolabelled cells, collected after 65 min incubation in resting conditions (KRH containing 2.8 mM glucose) or in the same conditions with addition of 5 μM ionomycin (iono) during the last 5 minutes and assigned them to one of the following 3 categories: Ins^+/CgB^-, Ins^-/CgB^+ and Ins^+/CgB^+. In resting cells, over half (66%) of the SGs were positive for Ins alone, 27% were mixed and 7% were positive for CgB alone. Ins appeared always localised in the granule core, whereas the distribution of CgB varied. In resting cells the granin appeared more concentrated in the core (~60%, Fig. 3E and 4A) than at its periphery and in the clear halo between the core and the membrane (Fig. 3 D,E,G,H and Fig. 4A). Five minutes stimulation with iono failed to induce any change of Ins distribution but induced a significant change of that of CgB. The labelling of the CgB

core dropped to ~30% in favour of the periphery/halo, which approached 70% (Fig. 4B). Interestingly an intra-SG distribution of CgB similar to that of the iono-stimulated cells was found in the cells kept until fixation in the culture medium (Fig. 4C), which contains 11 mM glucose and therefore induces some stimulation in the cells.

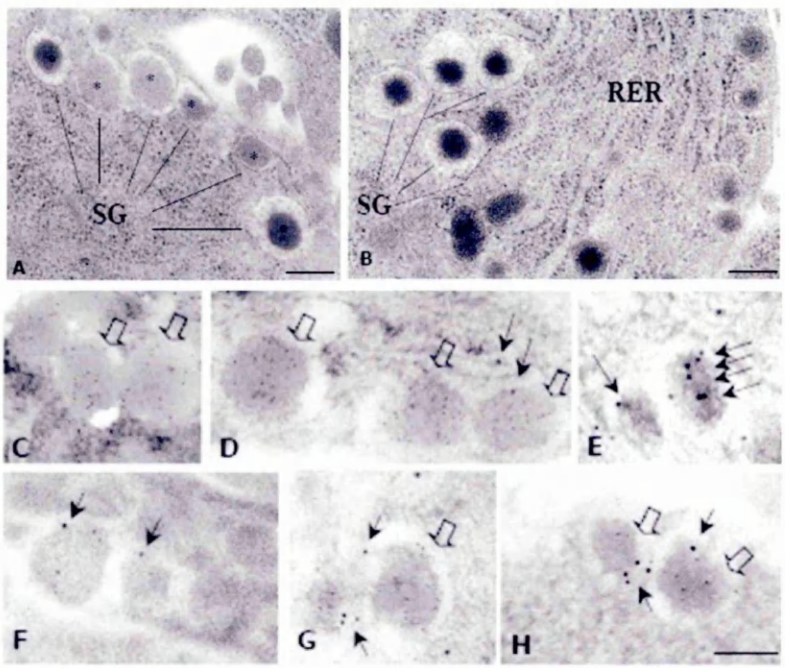

Fig. 3 - Conventional and immunoelectron microscopy of INS1-E cells immunostained for Ins and CgB. Panels A and B show the morphology of different types of SG observed by conventional EM: with (solid line) and without (dashed line) halo; with dense (°) and light (*) core. The two dense structures on the left lower side in panel B could be lysosomes. Panels C-H (scale bars as in H) show different types of SGs as revealed by immunolabelling: double-positive for Ins (6 nm colloidal gold particles) and for CgB (12 nm colloidal gold particles; D, F, G, H); positive for Ins only (C) or for CgB only (E). SGs with different intragranular CgB localisations: in the halo+periphery (D, E, F, G and H); in the core (G) and in the entire granule (E). Black and open arrows point to some gold particles representing CgB and Ins, respectively. Scalebars: 0.1 μm.

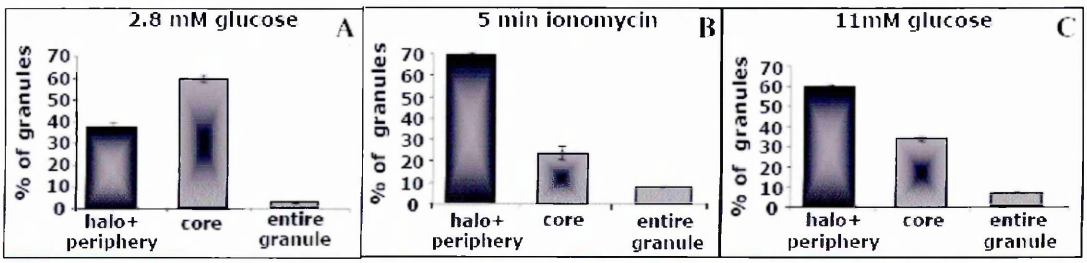

Fig. 4 – Intra-granular distribution of CgB in INS1-E cells under different conditions. Three populations of SGs are illustrated, with CgB labelled in the halo+periphery of the core, in the core only, or in both (entire granule). In B the ionomycin concentration was 5 μM. Granules counted for each condition were 89 (A), 90 (B) and 165 (C).

1.4 Ins and CgB release upon maximal stimulation

Next the secretory behaviour of Ins and CgB under different conditions of stimulation was investigated in INS1-E cells, which are well characterised in terms of secretory activity [341]. To do this, we had to solve a technical problem connected to the evaluation of CgB release. While several ELISA and RIA kits for the detection of rat Ins are commercially available, in the case of rat CgB no such kits exist, and it was not even possible to devise our own because of the low immunoprecipitation efficiency shown by several anti-CgB antibodies available to us. Thus we decided to take advantage of the high specificity observed in Western Blot of a monoclonal anti-CgB antibody raised in our laboratory (CIRO; Fig. 5). We used this antibody to quantitate CgB in supernatants of cells and in aliquots of cell lysates. This method allowed us to concentrate in a single spot the entire supernatant volume (500 µl) of each sample replica.

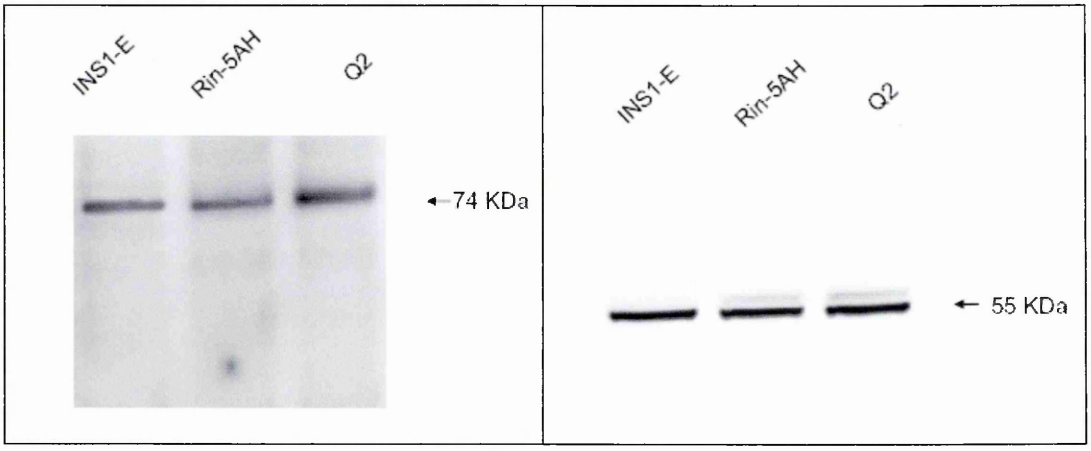

Fig. 5 - Specificity of the anti-CgB antibody CIRO. Immunoblotting of INS1-E, Rin-5AH cells and a sub-clone derived there-from, Q2. Left panel: the blot was incubated with the monoclonal anti-CgB antibody CIRO. Right panel: the blot was incubated with a monoclonal anti-tubulin antibody.

In order to elicit a maximal release, we used a mixture of secretagogues (referred to as secretagogue mix, SM) containing 16,7 mM glucose, 1 mM IBMX, 0.1 μM PMA and 10 μM forskolin. Cells were incubated in the presence of SM for 3, 5 and 20 minutes and the protein release was compared to that of cells kept in non-stimulating medium (2.8 mM glucose). The results, expressed as percentage (%) of the total Ins and CgB content released and as ratio of the % of Ins and CgB released, are presented in Fig. 6A. The release of both proteins increased gradually at the different time points (Fig. 6A) and in parallel as it is also shown in Fig. 6B by the Ins/CgB ratio of nearly 1.1 ± 0.26 at 5 minutes and 0.99 ± 0.11 at 20 minutes.

The effects of SM were then dissected by applying its components separately from each other for 20 minutes. As shown in Fig. 6B, the Ins/CgB ratio upon forskolin stimulation resembled that obtained with SM (0.84 ± 0.3). A lower Ins/CgB ratio (0.6 ± 0.12) was observed, by converse, with PMA (Fig. 6B), because this secretagogue induced a proportionally larger release of CgB than Ins compared to forskolin. A recalculation of the release data induced by forskolin and PMA in terms of ratio between the two secretagogues (Fig. 6C) revealed that the first is more than 2-fold effective than the second in terms of Ins whereas in terms of CgB the difference is of only 1.5-fold.

Ins and CgB release was also evaluated upon high glucose (27 mM) stimulation. This condition mobilised the two proteins in a similar way following both 5 and 20 minutes incubation (not shown).

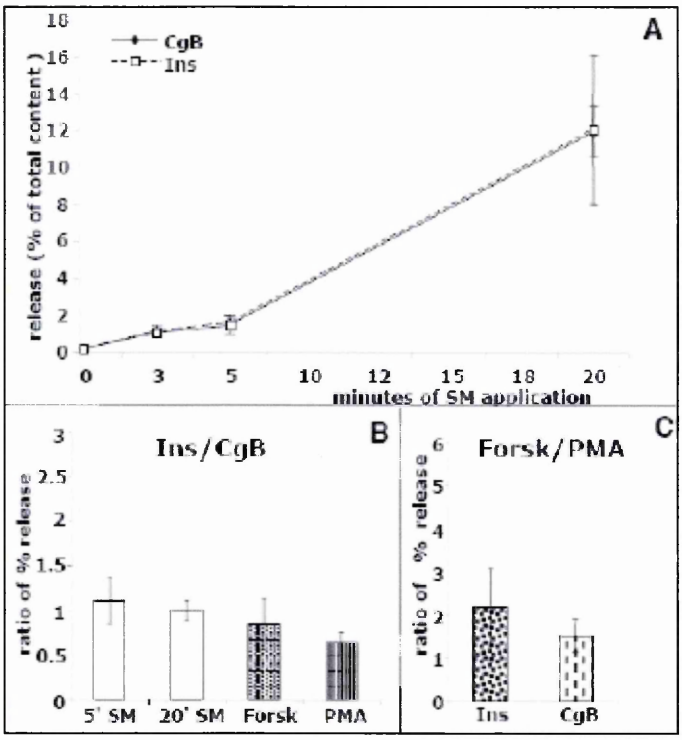

Fig. 6 - Ins and CgB secretion induced by different secretagogues. Panel A: Time-course of Ins (dashed line) and CgB (solid line) releases upon stimulation with SM (3. 5, 20 minutes). Panel B: ratio of Ins versus CgB percentage (%) release, 5 and 20 minutes following stimulation with SM, forskolin and PMA. Panel C: Ratio of forskolin- vs PMA-induced Ins and CgB percentage (%) release.

1.5 Dissociation of Ins and CgB release

The release of Ins and CgB was also investigated upon stimulation with the ionophore iono, that induces intracellular Ca^{2+} increase. Keeping in mind the preferential mobilisation of CgB to the periphery and halo of SGs observed at the ultrastructural level following iono incubation, we asked whether it was possible to detect any dissociation in the release of the two proteins.

Indeed, a clear dissociation between Ins and CgB release emerged from the dose-dependent responses to iono. CgB release was significant already after 5 minutes of 0.1 μM iono and increased progressively at higher concentrations (Fig. 7A) reaching a plateau, which was however much lower (~1/10) than that induced by SM, at 1 μM iono. Ins release was still inappreciable at 1 μM iono; i.e. at the concentration already maximal for CgB. Ins was released at the two highest concentrations (5 and 10 μM), however at a lower extent than CgB. The differential effect of iono on CgB secretion was confirmed after 30 minutes incubation (Fig. 7B). In order to demonstrate that the effect of iono on CgB release was Ca^{2+}-dependent, we incubated the cells in the presence of the Ca^{2+} chelator BAPTA and in Ca^{2+}-free medium. In these conditions the release of both Ins and CgB was strongly reduced, although not completely blocked (not shown).

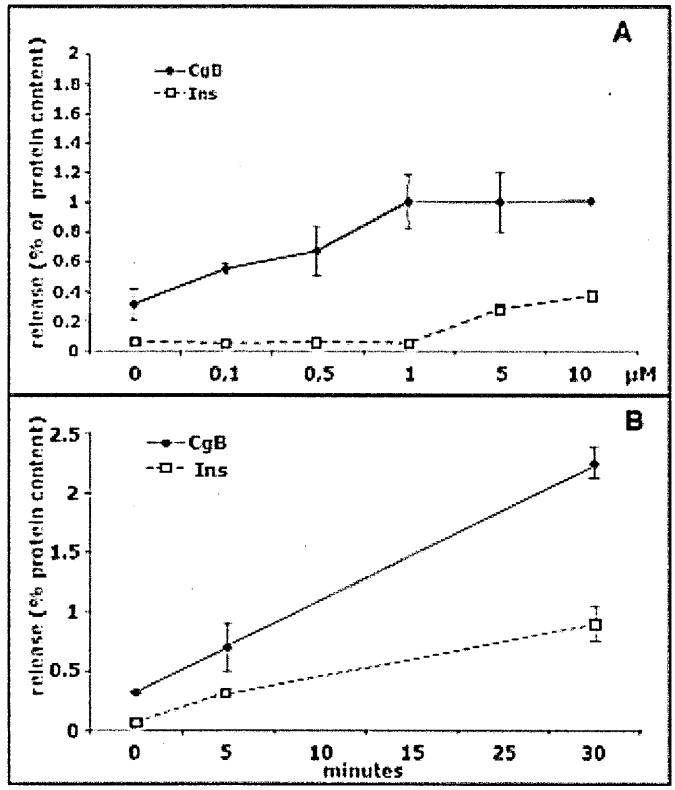

Fig. 7 - Dissociation between Ins and CgB release. Panel A: concentration-dependence of Ins (dashed line) and CgB (solid line) release induced by 5 minutes of ionomycin stimulation. Panel B: time-course of Ins and CgB release induced by ionomycin (10 µM).

1. 6 Heterogeneity of Ins and CgB granules in Rin-5AH cells

The radiation-induced rat Ins-secreting insulinoma Rin-m parental line [342, 343] and its sub-clone Rin-5AH [344], have been widely characterised for their secretory behaviour [345]. As compared to primary β cells or to a good Ins-secreting model such as INS1-E cells RIN-5AH cells show an Ins content which is ~300-fold lower than that of INS1-E (see Fig. 14) despite the less significant difference at the mRNA level (see Fig. 26 A-B). Rin-5AH cells show a poorer secretion index (S.I.: stimulated/basal release) upon

exposure to high glucose concentrations [346] as compared to control clones and to primary β cells. This behaviour has been previously correlated to a low expression of Glut-2 [347, 348] and to some defects in Ca^{2+} mobilisation [349] and in nutrient-induced Ins release, which so far have been however poorly investigated.

In order to investigate the secretory behaviour of Rin-5AH in more depth we started to characterise these cells in terms of their heterogeneity. Immunofluorescence staining for Ins and CgB showed that Rin-5AH are highly heterogeneous with regard to the expression and the relative content of the two proteins. Four phenotypes (Fig. 8), differently represented among the population, could be identified, which were positive for only one of the two SG markers (Ins^-/CgB^+, 27%; Ins^+/CgB^-, 7%), or showed double positive (Ins^+/CgB^+, 62%) or double negative cells (Ins^-/CgB^-, 4%). In the double positive cells, as already shown in the section 1 of the Results, Ins and CgB co-localised largely in the GC and TGN (Fig. 2D-E), and only a partial co-localisation could be detected in the SG compartment (Fig. 2D'-E'). This observation led us to the following questions: 1) Is the dissociation of Ins and CgB expression in Rin-5AH cells linked to a particular state of the cells, i.e. highly proliferation or stress? 2) Could this represent an opportunity to dissect the different subpopulations and to characterise their secretory behaviour? 3) Does CgB play a role in β cell secretion? In order to address these questions we isolated sub-clones representative of the four subpopulations.

1.6.1 Rin-5AH sub-cloning

Sub-cloning of the Rin-5AH cell line was performed by limiting dilution, i.e. by plating cells at a very low density (0.5 cells/well). The first sub-cloning round (384 well at 0.5 cell/well) yielded 25 clones, that were characterised by immunostaining for Ins and CgB. None of them was representative of the Ins^-/CgB^- subpopulation. We chose two clones, displaying the following characteristics: clone D that was Ins^+/CgB^-, although some cells appeared Ins^-/CgB^-; the clone Q, that was Ins^+/CgB^+ but showed an atypical accumulation of Ins in the Golgi.

A second sub-cloning round was performed on the D and Q clones and the 30 Q and 32 D sub-clones were rescreened by means of immunofluorescence staining for Ins and CgB. Among the second sub-cloning round we chose the D1 clone, showing low signals of both CgB and Ins proteins (Fig. 9 A-C), the D2 clone positive for Ins and with barely detectable levels of CgB (Fig. 9 D-F); the Q2 (Fig. 9 G-I) and Q6 (Fig. 9 L-N) clones, with prominent Ins and CgB signals accumulated in the GC and few SG at the cell periphery.

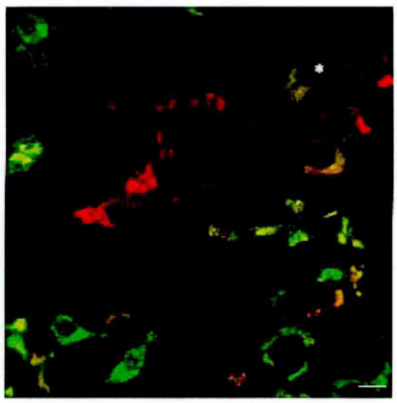

Fig. 8 – Characterisation of Ins and CgB expression in Rin-5AH cells by confocal analysis. Note the high heterogeneity of staining for Ins (red) and CgB (green) in the cell population. The asterisk indicates a cell devoid of both markers. Scalebar: 6 µm.

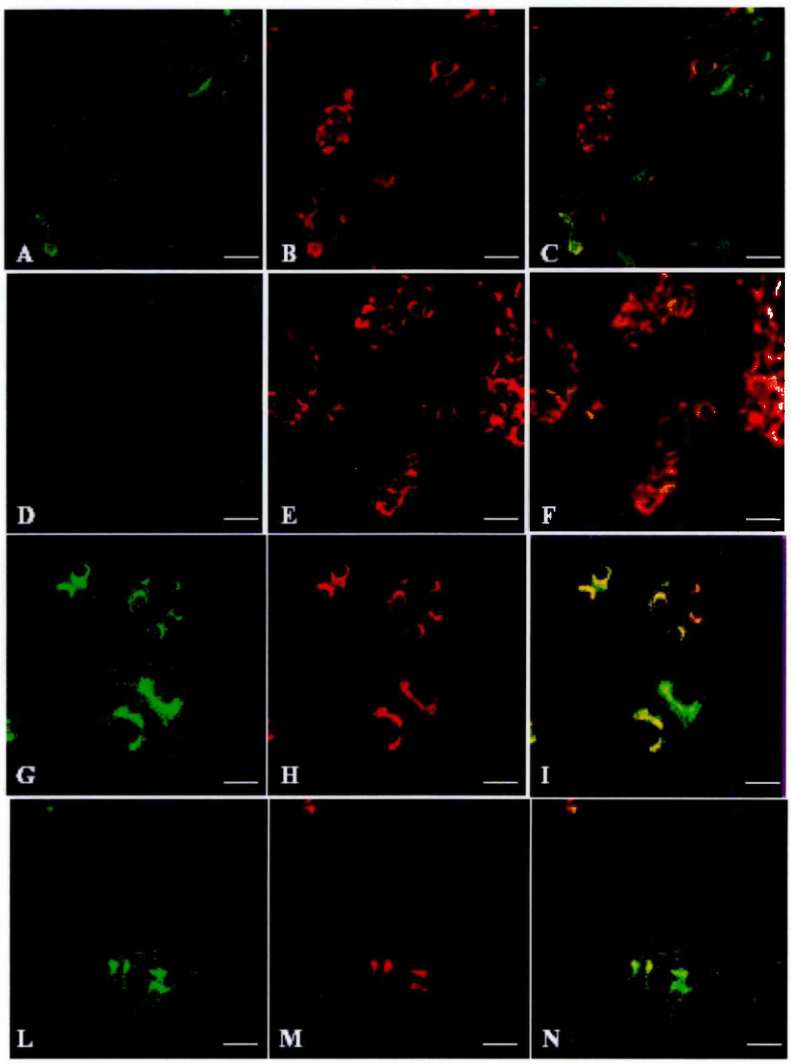

Fig. 9 – Confocal analysis of Ins and CgB expression in four Rin-5AH sub-clones. Confocal images of D1 (A-C), D2 (D-F), Q2 (G-I) and Q6 (L-N) sub-clones derived from Rin-5AH cells. A, D, G, L: Ins staining (red); B, E, H, M: CgB staining (green). C, F, I, N: overlay of the Ins and CgB staining. Yellow indicates co-localisation. The images clearly show the poor Ins and CgB content in D1, the very low CgB expression in D2, the high content of both Ins and CgB in Q2 and Q6, where Ins is mostly accumulated in the GC. Scalebar: 6 µm.

1.6.2 Secretory behaviour of Rin-5AH cells and sub-clones

Rin-5AH cells and the four selected sub-clones were analysed for their Ins and CgB content by RIA and immunoblotting, respectively. We confirmed the features observed by immunofluorescence, i.e. the low Ins content of D1, the nearly undetectable CgB levels in D2, and a high expression of both proteins in Q2 and Q6 (Fig. 10).

Ins release upon various stimuli - The secretory behaviour of the four sub-clones was investigated by application of different secretagogues. Regulated secretion was triggered by high KCl and high glucose (KCl/gluc) or by the SM cocktail.

Released Ins was represented as % of total Ins (Fig. 11). In the Rin-5AH population the KCl/gluc stimulus yielded only a 3-fold release, whereas the SM-induced release was about 6-fold over basal (Fig. 11A). The S.I of Rin-5AH cells is low compared to better Ins secreting cell models, such as INS1-E, which have a S.I. as high as 40 (Fig. 14C). Ins secretion in Rin-5AH parental cells could be enhanced by stimulation with 100 μM tolbutamide, which causes the closure of the K_{ATP} channels thus depolarising the plasma membrane. Tolbutamide, in synergy with either glucose or SM, enhanced Ins release 2.1- and 2.5-fold, respectively (not shown).

In contrast to parental cells, the D1 sub-clone showed only a little, if any, stimulated release (1.5-fold) with both KCl/gluc and SM (1.25-fold) (Fig. 11B). The D2 sub-clone (Fig. 11C) displayed a modest stimulated release (3.2-fold with KCl/gluc and 2.5-fold with SM, respectively). The Q2 sub-clone showed a release pattern resembling the parental population, despite the large Ins accumulation in the GC (Fig.11D) and the low number of SG, however its extent was lower upon SM stimulation (2.3-fold; Fig. 11D). Q6 cells (Fig.11E) showed a lower regulated Ins release as compared to Q2 cells, despite the higher Ins content.

A

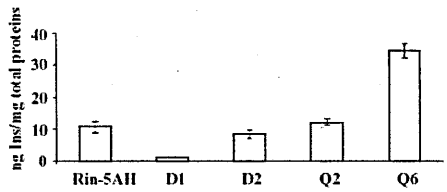

B

	D1	D2	Q2	Q6
CgB content (% of Rin-5AH cells)	87%	n.d.	117%	227%

Fig. 10 – Ins (A) and CgB (B) content in parental Rin-5AH cells and in the four sub-clones. Ins was measured by RIA; the bars represent the average of three independent experiments. CgB content, measured by Western Blot quantitation and normalisation to tubulin levels, is expressed as percentage of the content in Rin-5AH cells (one representative experiment).

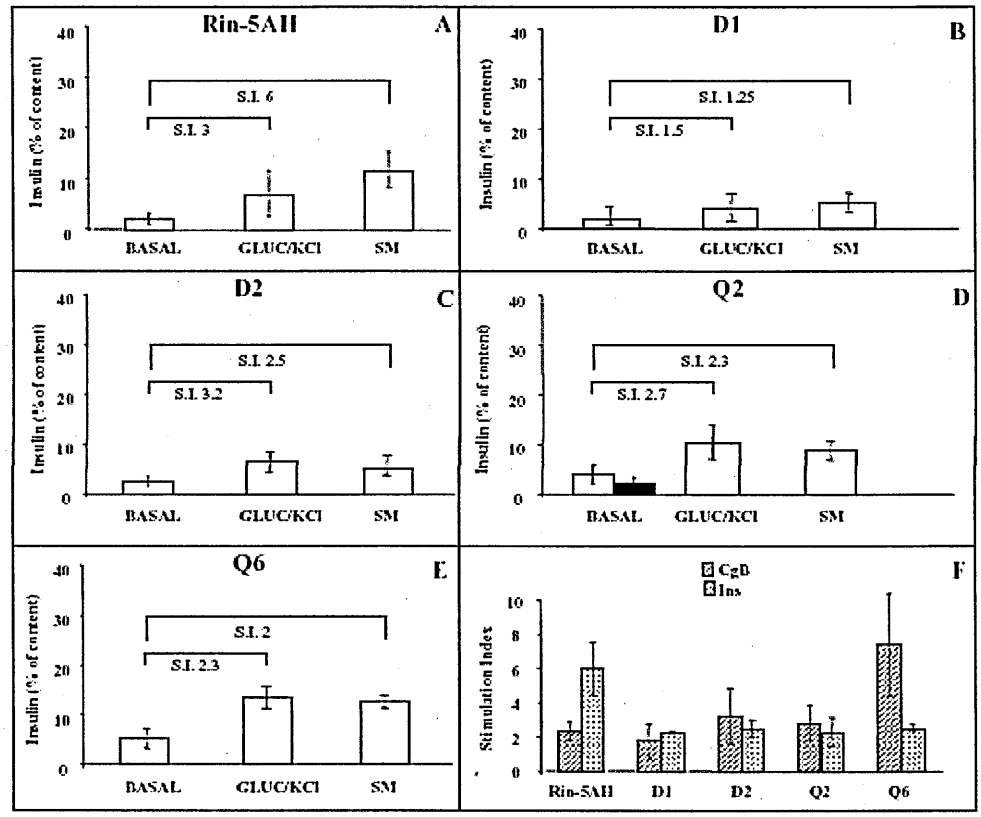

Fig. 11 – Secretory behaviour of Rin-5AH cells and sub-clones. The secretory behaviour of Ins in response to gluc/KCl and to the SM is reported. A: Rin-5AH cells; B: D1 sub-clone; C: D2 sub-clone; D: Q2 sub-clone; E: Q6 sub-clone. In panel D the closed bar represents the basal release after 1 hr incubation with CHX. S.I.: secretion index. F: Ins and CgB secretion upon SM stimulation in the five cell types analysed. The CgB release of D2 sub-clone is discussed in the text. The results are expressed as S.I. All the experiments in Fig. 11 were performed three times with triplicate samples and the average of results is represented.

Regulated versus constitutive Ins secretion - Having observed a low SI for Ins in the Rin-5AH derived sub-clones, and particularly in the case of Q2 cells a high value of basal Ins secretion, we investigated the contribution of the constitutive secretory pathway in Ins release of Rin-5AH and derived subclones.

To evaluate this for the different sub-clones, parallel experiments were carried out where cells were kept for 1 hour in the presence of the protein synthesis inhibitor cycloheximide (CHX), and then stimulated for release in the presence of CHX. This procedure, which allows for the release of proteins from the constitutive pathway without altering the SGs accumulating within cells in the absence of a stimulus triggering regulated release, has been previously used to discriminate *bona fide* regulated secretion from constitutive one [98]. Following 1 hour CHX treatment the release pattern of Rin-5AH cells and all clones, but one, namely Q2, did not change, indicating the prevalence of a regulated release pathway in the parental population. Interestingly, the basal Ins release of Q2 cells decreased following CHX treatment, suggesting that in these cells a fraction of Ins is released by a constitutive pathway. (Fig. 11D; black bar).

Basal Ins release from Q6 cells was higher than in the other sub-clones, but it was not affected by CHX, thus excluding the contribution of constitutive secretion and suggesting that Ins SGs in these cells may have a 'disregulated' discharge.

CgB release – CgB release was measured in Rin-5AH cells and sub-clones under basal condition and following application of SM. As previously described this was performed by a dot blot method and the SI of CgB was compared to that of Ins in the different clones (Fig.11F). Following maximal stimulation with SM, parental Rin-5AH cells as

well as D1, D2 and Q2 sub-clones displayed similar CgB SI (Fig. 11F). The Q6 sub-clone instead showed a higher efficiency of CgB release. The secretory behaviour of CgB was independent of the protein content (compare Fig. 10B with Fig. 11F). Compared to the Ins release, that of CgB appeared not parallel in the different sub-clones. In particular, sub-clones Q2 and Q6, which have the highest levels of CgB, showed different SI for it (Fig 11F) with respect to Ins, Q6 displaying a S.I. lower than the parental population despite the highest CgB content. The CgB S.I. in the D2 sub-clone, apparently comparable to that of parental population and other sub-clones, can be explained by the method of data normalisation. In fact, expressing the protein release as % of the total content in the case of the D2 sub-clone, whose CgB content is very low, leads to over-estimate the S.I. In terms of optical density (OD) measured at the densitometer, CgB released in the media was not significantly higher than in control cells, whereas in the other cell types CgB levels in the media were much higher (not shown).

1.6.3 Biochemical characterisation of regulated secretory markers

Since regulated secretion relies on a complex molecular machinery, we asked about the expression of some pivotal proteins involved in this process. The four Rin-5AH sub-clones were investigated by immunoblotting for their levels of the granule luminal protein CgA, for dopamine-β-hydroxylase (DBH) and for proteins involved in regulated exocytosis: VAMP2/synaptobrevin2, SNAP-23 and SNAP-25, Munc 18-1, synaptotagmin I, syntaxin 1 (Stx) and synaptophysin I (SYP). Among the sub-clones only D2 showed reduced levels of VAMP2 and SYP (Table 1). The levels of the other

proteins analysed were similar in all the sub-clones as compared to parental cells. From these data it is not possible to draw a correlation between the expression of the exocytotic molecular machinery proteins and the poor secretory performance of Rin-5AH sub-clones.

	Rin-5AH	D1	D2	Q2	Q6
Synaptotagmin I	+	+	+/-	+	+
Munc-18	+	+	+	+	+
DBH	+	+	+	+	+
Stx I	+	+	+	+	+
SNAP-25	+	+	+	+	+
SNAP-23	+	+	+	+	+
CgA	+	+	+/-	+	+
VAMP2	+	+/-	+/-	+	+
SYP	+	+	+/-	+	+

Table 1 – Western Blot analysis of proteins involved in regulated secretion in Rin-5AH cells and in the various sub-clones. The markers of regulated secretion reported in the table were investigated. + indicates presence; - indicates absence; +/- indicates a low expression

1.6.4 Dissection of the Ins secretory pathway in RIN-5AH and sub-clones

We decided to investigate two key steps of the Ins secretion pathway in Rin-5AH cells and sub-clones: the intracellular Ca^{2+} mobilisation and the mitochondrial ATP production upon secretagogue stimulation.

Ca^{2+} mobilisation – We measured the overall intracellular Ca^{2+} mobilisation in Rin-5AH cells and in the four sub-clones by loading adherent cells with the Ca^{2+} indicator

Fura2/AM, followed by population analysis at the fluorometer. Fura2/AM emits at two different wavelengths, depending on whether it binds (340 nm) or not to Ca^{2+} (380 nm). Thus, an increase in the whole free Ca^{2+} concentration leads to an increase in the bound signal (340 nm) and to a parallel decrease of the unbound signal (380 nm), which allows for a ratiometric measurement of Ca^{2+} mobilisation (expressed as 340nm/380nm ratio). The results of the fluorometric analysis of one representative experiment are expressed as % increase over basal in Fig. 12. The Ca^{2+} mobilisation induced by carbachol (cch) was used as a positive control for the analysis. The comparison of SM- and cch-induced Ca^{2+} mobilisation showed that D1 and D2 sub-clones respond similarly, whereas Rin-5AH cells and Q2 sub-clone mobilised more Ca^{2+} upon cch and Q6 displayed the opposite behaviour. From these data we conclude that Rin-5AH cells and the four clones derived therefrom are competent for Ca^{2+} mobilisation; however, the extent of such mobilisation is independent of their secretory efficiency (compare Fig. 12 with Fig. 11F).

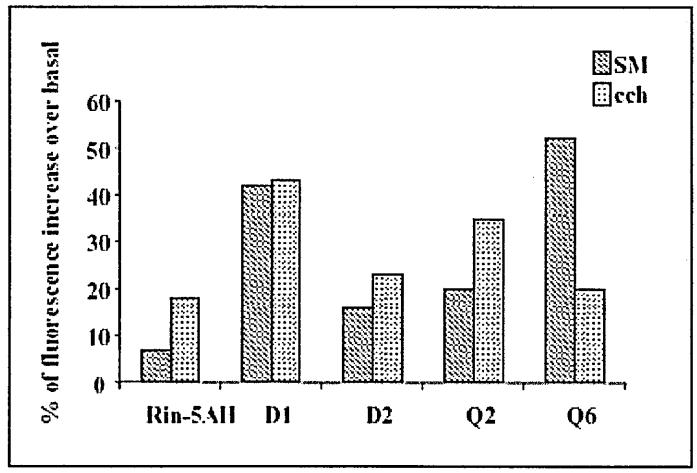

Fig. 12 - Fluorometric analysis of intracellular Ca^{2+} mobilisation. The cell populations were stimulated with carbachol (cch, black lines) or SM (blue lines). On the Y-axis the % of Fura-2/AM fluorescence increase over basal is represented. The figure shows the results of one representative experiment carried on the cell populations.

ATP production – Mitochondrial nutrient metabolism is coupled to ATP synthesis by the ETC and driven by the $\Delta\Psi_m$. ATP production starts as soon as 2 minutes following stimulation of Ins secretion and lasts few more minutes [255]. We measured the total intracellular ATP level 4 minutes following stimulation by means of a luminescent assay that detects ATP and ADP in cell lysates. While Rin-5AH cells produced ATP upon stimulation of Ins secretion, the four sub-clones appeared unable to produce ATP, rather the overall ATP levels decreased following stimulation. ADP levels (not shown) decreased in parental cells, whereas in the four sub-clones they increased, leading to the ATP:ADP ratio shown in Fig. 13. The average increase of the ATP:ADP ratio over basal, obtained from three independent experiments, is reported. Since the detection method employed was not quantitative, we can not conclude that the apparently higher ATP levels observed at basal conditions in the four sub-clones compared to Rin-5AH cells are a *bona fide* observation.

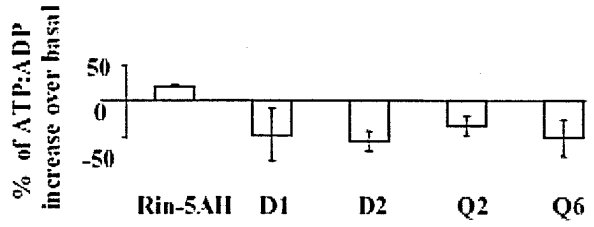

Fig. 13 - ATP levels measured in cell lysates under basal and stimulated conditions. The changes in ATP:ADP ratio upon SM application in parental Rin-5AH cells and sub-clones are expressed as % of luminescence over basal. Only parental cells are able to increase the ATP:ADP ratio upon stimulation, whereas the four sub-clones display a decrease of ATP:ADP.

2. *Molecular mechanisms of the impaired Ins secretion in RIN-5AH cells*

The sub-cloning strategy described in the previous section led us to consider Rin-5AH cells and the sub-clones derived therefrom as a valuable tool to investigate novel mechanisms underlying their low efficiency of Ins secretion. Despite their low S.I., Rin cells have been used by many research groups as a β cell model to study the regulation of Ins secretion [350-353]. Instead, their poor secretory behaviour was never correlated to a pathological state of β cells, and the molecular mechanisms underlying the latter have not been investigated in depth. We decided to look into the mechanism(s) responsible for the impairment of Ins secretion in Rin-5AH cells and as a more homogeneous model, the previously described Q2 sub-clone. We selected this sub-clone because as compared to the Rin-5AH parental population it showed a higher CgB content but a similar S.I., and a lower Ins S.I. despite the comparable protein content. In addition, a fraction of its basal Ins release could be ascribed to constitutive secretion (paragraph 1.6.2 of Results). As a reference model of good-functioning β cell we used the previously described INS1-E cell line.

2.1 Comparison of Ins content and S.I. in INS1-E and Rin-5AH insulinomas

The rat insulinoma cell line INS1-E, as compared to Rin-5AH and the Q2 sub-clone derived therof, greatly differs in the Ins content and in the secretory efficiency. Ins contents measured by both RIA and ELISA (Fig. 14A) showed what was already known from the literature, but never analysed comparatively, i.e. that Rin-5AH and Q2 cells have approximately 300 times less Ins than INS1-E cells. The secretory behaviour of the three cell types, upon stimulation of Ins secretion for 20 minutes with SM, is

represented in Fig. 14B expressed as percentage of total content and in Fig. 14C as S.I. INS1-E release around 12% of their Ins content upon stimulation, whereas the basal release is as low as 0.2%; Rin-5AH and Q2, despite a 300-fold lower Ins content than INS1-E cells, show a similar % of stimulated release (14% and 9.6%, respectively), however their basal release is significantly higher (3.7% and 4.1%, respectively). In terms of S.I. (Fig. 14C), INS1-E are very efficient (S.I.=40), whereas Rin-5AH and Q2 cells respond 10- to 20-fold less (S.I.=4 for Rin-5AH and S.I.=2 for Q2).

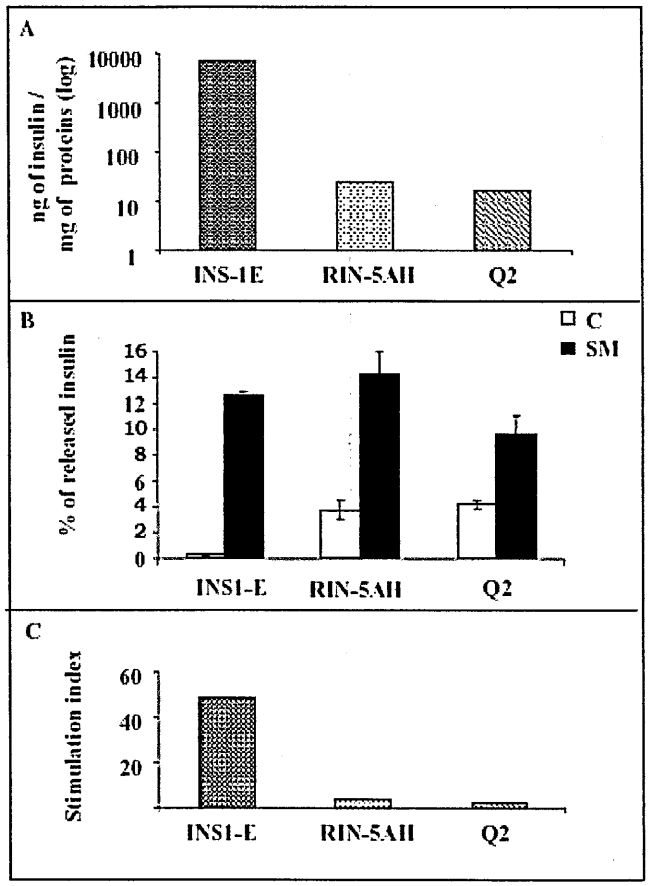

Fig. 14 – Ins content and secretory behaviour of INS1-E, Rin-5AH and Q2 sub-clone derived therefrom. A: Ins concentration is indicated as ng Ins/mg total protein content. The Y-axis reports values on a logarithmic scale. B: Ins release of INS1-E, Rin-5AH and Q2 cells. Open bars: basal conditions (C); closed bars: SM stimulation. The results were expressed as % of released Ins/total content. C: Ins secretion expressed as stimulation index, i.e. stimulated/basal.

2.2 Comparison of cytosolic Ca^{2+}-mobilisation and ATP production in Rin-5AH and Q2 with INS1-E

2.2.1 Cytosolic Ca^{2+} measurements

The stimulation of Ins secretion determines a net Ca^{2+} influx through the voltage-gated Ca^{2+}-channels, accompanied by a mobilisation of Ca^{2+} from intracellular stores, such as ER and mitochondria. The intracellular Ca^{2+} homeostasis, i.e. the equilibrium between free and bound cytosolic Ca^{2+} and sequestered Ca^{2+}, is maintained by the cross-talk between ER and mitochondria. We investigated whether a defect in Ca^{2+} mobilisation correlated with the poor secretory phenotype of Rin-5AH and Q2 cells as compared to INS1-E. The overall Ca^{2+} mobilisation was detected by single-cell imaging of Fura2/AM-labelled cells at the fluorescence microscope. For each cell type about 50 cells for each coverslip were analysed. The resulting traces were averaged and represented in Fig. 15. Upon stimulation with SM INS1-E cells show a sharp Ca^{2+} peak with mean height of ratio 340nm/380nm of 0.5 (Fig. 15A). The extent of Ca^{2+} mobilisation in Rin-5AH was variable (not shown) and lower than that in INS1-E; Q2 cells (Fig. 15B) showed a much smaller peak as compared to INS1-E.

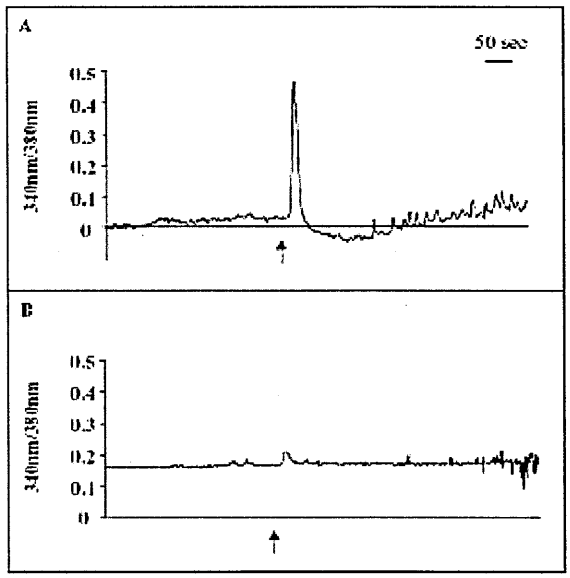

Fig. 15 – Ca2+ mobilisation measured by single cell imaging. Fura2/AM fluorescence measured in INS1-E (A) and Q2 (B) cells was normalised by calculating the dF/F ratio (see text). The graphs depict the average of several cells (14 for INS1-E and 8 for Q2). The arrows indicate SM administration. Scalebar: 50 seconds.

2.2.2 ATP production

We measured ATP production in INS1-E, Rin-5AH and Q2 cells in unstimulated conditions and 4 minutes following application of SM. INS1-E cells showed an increase in the ATP:ADP ratio of 26% upon stimulation as compared to the basal condition, which was set as 100%. Rin-5AH showed a smaller increase of the ATP:ADP ratio (19%), whereas Q2 cells showed a 35% drop in the ATP:ADP ratio upon stimulation of secretion (Fig. 16A).

An impaired ATP production has been shown in cell models over-expressing the mitochondrial protein UCP2 (see Introduction, section 2.2 and 2.4); we therefore evaluated UCP2 protein levels in the three investigated cell models by Western blotting. The results obtained from the quantitations of two independent experiments have been normalised to tubulin levels and averages are shown in Fig. 16B. Q2 cells express a higher (~2.6-fold) amount of UCP2 as compared to both INS1-E and Rin-5AH. We

conclude therefore that one of the possible causes of the lower ATP production in Q2 cells is the over-expression of UCP2.

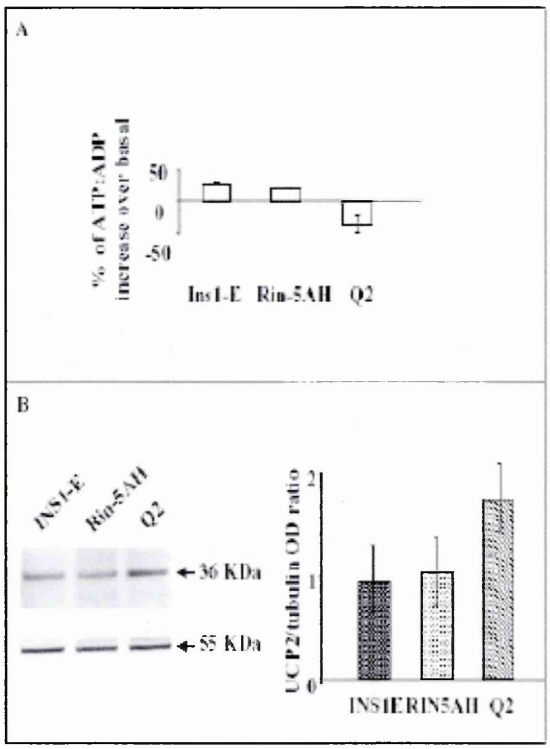

Fig. 16 – ATP and UCP2 levels in the three cell models investigated. A: ATP levels were measured in cell lysates of INS1-E, Rin-5AH and Q2 cells following incubation at resting conditions (C; open bars) or with SM (closed bars). B: UCP2 levels in INS1-E, Rin-5AH and Q2 cells. Left: one representative Western Blot is shown. Upper part: the blot was incubated with a polyclonal anti-UCP2 antibody; lower part: the same blot was incubated with a monoclonal anti-tubulin antibody. Right: The OD of UCP2 were normalised with tubulin levels. The graph represents the average of two experiment.

2.3 Mitochondrial membrane potential

Since Rin-5AH cells appear to have an intermediate phenotype between INS1-E and Q2 cells both in terms of ATP production and Ca^{2+} mobilisation upon secretion stimulation, we decided to focus our attention on the comparison between INS1-E and Q2 for the following studies. The impaired production of ATP upon stimulation of secretion in the Q2 sub-clone, in combination with the observed lower cytosolic Ca^{2+} mobilisation led us to hypothesise that these cells might have an impairment of mitochondrial function. To evaluate this hypothesis the $\Delta\psi_m$ was measured by the fluorescent dye TMRM, which emits fluorescence proportionally to the $\Delta\psi_m$. When analysed under the

fluorescence microscope Q2 cells (Fig. 17E) showed a very low $\Delta\psi_m$ as compared to INS1-E (Fig. 17A). The fluorescence intensity was analysed in the population of INS1-E (160 cells) and Q2 (100 cells), using for each cell type the data of three independent experiments. The arbitrary fluorescence intensities of single cells from the different populations were grouped into four intervals: 1 (a.u. 0-4,999), 2 (a.u. 5,000-9,999), 3 (a.u. 10,000-14,500) and 4 (a.u. above 15,000). INS1-E cells showed a population distribution with the majority of cells (92.5%) falling into fluorescence intervals 2 and 3 and a residual 7.5% in interval 4 (Fig. 17B), whereas Q2 showed the majority of cells (93.1%) falling in intervals 1 and 2 and residual 5.9% and 1% in intervals 3 and 4, respectively (Fig. 17F).

2.4 Mitochondrial morphology

Mitochondrial dysfunctions are often associated to an altered morphology. Therefore the mitochondrial morphology was analysed *in vivo* by staining cells with the appropriate concentration of MitoTracker (25 nM for INS1-E, 50 nM for Q2) and observed under the Deltavision system. The acquired images were subjected to deconvolution and three-dimensional reconstruction, as already described. INS1-E cells showed a filamentous-like mitochondrial morphology (Fig. 17C), which is consistent to previous observations [255]. In contrast, in Q2 cells (Fig. 17G) mitochondria appeared highly fragmented and swollen. We confirmed the latter observation by conventional electron microscopy, where in INS1-E (Fig. 17D) mitochondria appeared tubular, whereas in Q2 cells (Fig. 17H) they are swollen and round-shaped.

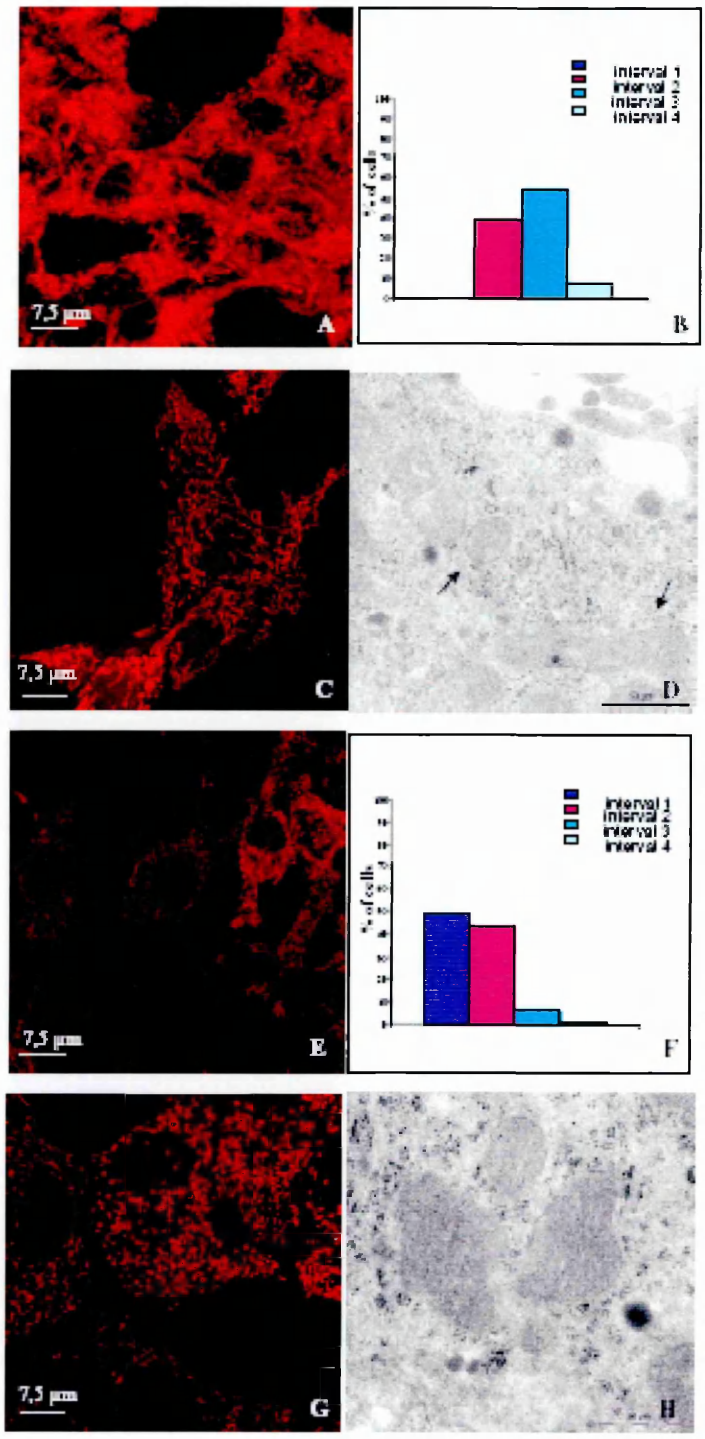

Fig. 17 – Analysis of mitochondrial potential and mitochondrial morphology. A-D: INS1-E cells; E-H: Q2 cells. A, E: confocal images following TMRM staining to measure mitochondrial potential ($\Delta\psi m$). Q2 (E) cells show lower $\Delta\psi m$ than INS1-E (A). B, F: distribution of $\Delta\psi m$ in the two cell types. The values of $\Delta\psi m$, expressed as arbitrary units of fluorescence, were ascribed to 4 ranges (see text). Most cells in the INS1-E cell line (B) displayed high $\Delta\psi m$, whereas in the Q2 sub-clone (F) most cells lied in the lowest intervals of $\Delta\psi m$. C, G: morphological analysis of mitochondria following mitotracker staining and *in vivo* observation. Images were acquired at the Deltavision system and analysed by deconvolution and 3D reconstruction. Q2 cells (G) showed fragmented, round-shaped mitochondria as compared to INS1-E (C). D, H: electron microscopy characterisation of mitochondria. INS1-E (D) displayed filamentous mitochondria (arrows). In Q2 cells (H) all mitochondria were swollen and larger than in the other cell type.

2.5 *Functional analysis of $\Delta\Psi_m$*

The observations obtained so far showed that Q2 cells have an impaired ATP production upon stimulation of secretion and a distinctly lower $\Delta\psi_m$ than INS1-E. Both these two features have been observed in cells exposed to an oxidative stress condition [255]. Under this condition mitochondria of β cells are not able anymore to increase their $\Delta\psi_m$ upon stimulation of Ins secretion. We investigated this issue by loading the cells with TMRM and performed a time-lapse recording at the confocal microscope under basal condition and upon SM application. The $\Delta\psi_m$ values, originally indicated by arbitrary units of fluorescence, were normalised by calculating the dF/F ratio (Fig. 18A-B). The mean increase of TMRM fluorescence over basal in INS1-E and Q2 cells is also represented in Fig. 18C. While in INS1-E cells (Fig.18A) there is a marked increase of $\Delta\psi_m$ short after SM administration, in Q2 cells (Fig.18B) instead the increase has a different kinetic and is smaller. In the set of experiments presented here we used SM as stimulus, however we obtained similar results also by administration of high glucose (27 mM; not shown). At the end of the experiment we added the mitochondrial uncoupler FCCP, which decreases TMRM fluorescence. The decrease of fluorescence induced by FCCP obtained from 3 independent experiments was measured and plotted in Fig.18D. It is known that the higher the $\Delta\psi_m$, the larger and faster its decrease upon uncoupling. The TMRM fluorescence of INS1-E cells falls steeply in the first 100 seconds of uncoupling, whereas the decrease in Q2 cells appears slower and less pronounced.

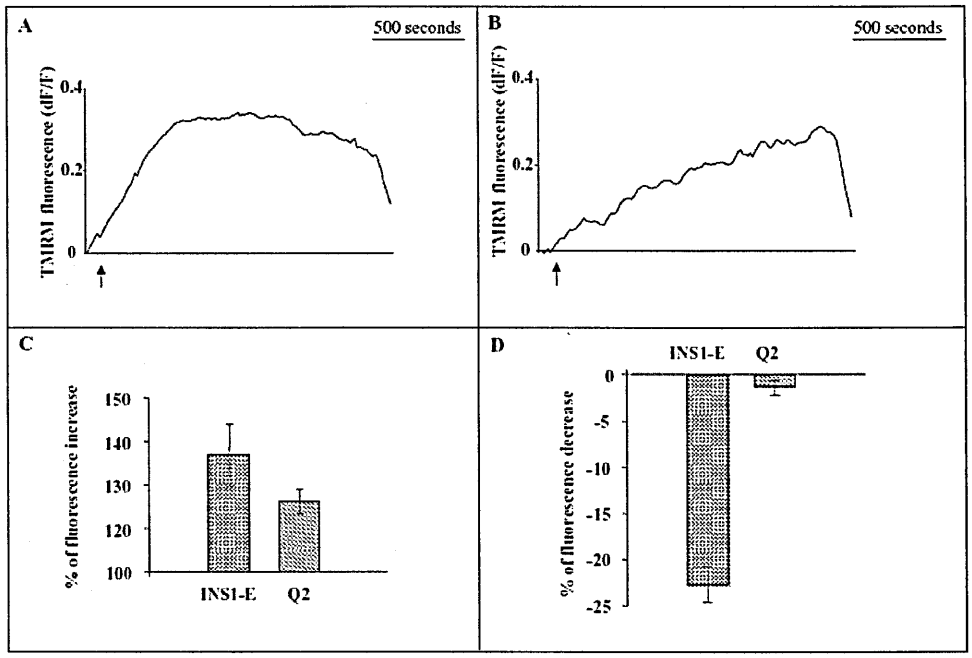

Fig. 18 – A, B: Functional analysis of $\Delta\psi_m$ by TMRM staining and time-lapse recording. A: INS1-E cells; B: Q2 cells. The graphs show the average of around 10 cells from one representative experiment. The values of TMRM fluorescence were normalised by calculating the dF/F ratio. SM was added at 60 seconds; FCCP at 1300 seconds. Scalebar: 500 seconds. There is a marked difference between INS1-E and Q2 in the kinetics of the $\Delta\psi_m$ (TMRM fluorescence) increase following stimulation of Ins secretion with SM. C: The $\Delta\psi_m$ increase upon SM stimulation was represented as average of the peak/basal ratios ± s.e.m. D: $\Delta\psi_m$ decrease 100 seconds after application of the mitochondrial uncoupler FCCP. The results, obtained from three independent experiments, were expressed as average of the ratio between fluorescence values at t=0 and t=100 seconds.

2.6 Attempts to rescue the $\Delta\Psi_m$ response in Q2 cells

CGP-37157 treatment - We hypothesised that the poor cytosolic Ca^{2+} mobilisation observed in Q2 cells might account at least partly for the impaired mitochondrial functionality, first of all because of the impaired ATP production and also because the Ca^{2+} cross-talk between ER and mitochondria plays a crucial role in the mitochondrial Ca^{2+} homeostasis and mitochondrial functionality. Several efforts were made in order to

visualise the mitochondrial Ca^{2+} by transfecting cells with aequorin targeted to the mitochondria and, alternatively, by using the indicator Rhod1/AM, that has high affinity for mitochondria. However, Q2 cells showed very low transfection efficiencies, not allowing for a population analysis with aequorin, and Rhod1/AM displayed a low selectivity for mitochondria, especially in INS1-E cells, which resulted in recording fluorescence both from the cytosolic and the mitochondrial compartments. We therefore decided to test the role of Ca^{2+} in the mitochondria indirectly, by blocking the Ca^{2+} export and consequently increasing the Ca^{2+} levels inside the mitochondria. The only system that has been characterised at the molecular level, which is relevant to the mitochondrial Ca^{2+} export, is the Na^{+}-Ca^{2+}-exchanger, that is favoured by the $\Delta\psi_m$ and can be inhibited by the derivatives of diltiazem, such as CGP-37157. We argued that if on one side mitochondrial Ca^{2+} levels in Q2 cells are possibly lower, inhibition of Ca^{2+} export [232] could improve both the $\Delta\psi_m$ response and possibly the secretory behaviour. Since in a good cell model such as INS1-E the effect of CGP-37157 has been already characterised [354] and it is known that upon maximal stimulation (30 mM glucose) there is no further increase of Ins secretion, we performed all the analysis only on Q2 cells. The latter were pre-incubated for 4 minutes with CGP-37157, which was kept during the following 20 minutes incubation in basal conditions. Both the $\Delta\psi_m$ and Ins secretion were measured under these conditions. Upon CGP-37157 addition the $\Delta\psi_m$ of Q2 cells gradually increased and remained sustained over at least 10 minutes (Fig. 19). At the secretory level, this resulted into a ~36% improvement of Ins secretion (not shown). This result was confirmed in three independent experiments, where the % increase of Ins secretion in the cells treated with CGP-37157 was similar; however, due to some variability in the cells, it was not possible to mediate the results.

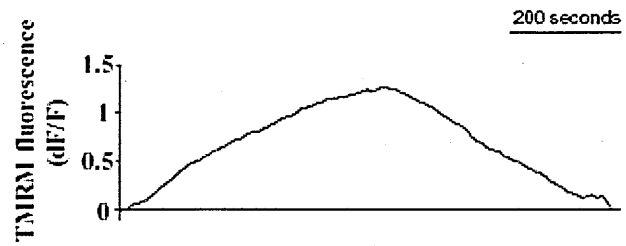

Fig. 19 – Effects of CGP-37157 on $\Delta\psi_m$ and Ins secretion in Q2 cells. Analysis of $\Delta\psi_m$ by TMRM staining and time-lapse recording of cells treated with CGP-37157. The results were normalised and expressed as dF/F. CGP-37157 was added at 30 seconds. Scalebar: 200 seconds. The TMRM fluorescence was monitored for 1000 seconds, until the signal decreased to basal values.

Antioxidant treatment - The data so far obtained all suggest that Q2 cells could be cells in a state of chronic oxidative stress. We decided therefore to treat the cells overnight with ascorbic acid, that is not specific for mitochondria nor especially powerful as an antioxidant, however it clearly acts in ROS scavenging [355]. After incubation, the antioxidant was kept in the medium and measurements of $\Delta\psi_m$ and of Ins secretion at resting and stimulated conditions were performed. While Ins release was not improved by the antioxidant treatment (not shown), we observed some changes in the $\Delta\psi_m$. The mitochondrial response to stimulation remained unchanged (not shown), however the distribution of $\Delta\psi_m$ showed a clear shift, with more cells in the highest ranges of values (Fig. 20). We therefore conclude that an oxidative stress condition may well be at the basis of the phenotype of Q2 cells, and a more specific and powerful antioxidant might be able to rescue to a greater extent the defective secretory behaviour of Q2 cells.

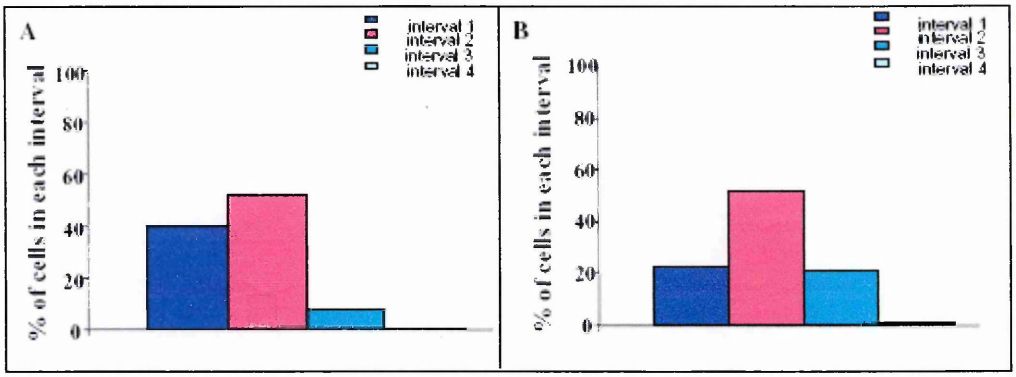

Fig. 20 – Effects of ascorbate on $\Delta\psi_m$ in Q2 cells. Distribution of mitochondrial potential in Q2 cells (A) and in Q2 cells treated overnight with ascorbic acid (B). The $\Delta\psi_m$ intervals are the same than in Fig. 10A. A shift of $\Delta\psi_m$ toward the highest values can be observed.

3. *Ins and CgB secretion under ER stress conditions*

The ER stress has been in recent years more and more implicated in diabetes and β cell dysfunction [333, 337]. A correlation between ER and oxidative stress has been described [281, 282], although it is not clear yet how they are causally linked to each other. The results presented in the previous section suggest that the Q2 cell model appears to bear a state of oxidative stress. Independently of the causative mechanism, we asked whether it might be accompanied by, or make cells more susceptible to, ER stress. In addition, the observed peculiar accumulation of Ins in the Golgi area suggested that the protein might undergo incomplete maturation, thus generating a stressful condition for the cell.

We compared Q2 cells to INS1-E, and addressed the following questions:

- Does a cell model carrying oxidative stress (Q2) appear more sensitive to ER stress induction in terms of cell functionality and apoptosis?
- What is the effect of ER stress at the level of granule proteins other than Ins?

Bona fide ER stress was induced by treatment of cells for 24 hours with thapsigargin (Tg), an inhibitor of the ER Ca^{2+} pump SERCA 2b, which determines an increase in unfolded proteins and thus induces ER stress [356]. This type of treatment represents a maximal stress condition, which is accompanied by apoptotic cell death and by the up-regulation of the expression of several ER stress markers (see Introduction, section 1.3), including:

- BIP, which acts as the upstream regulator of the three ER stress signal transducers IRE1, PERK and ATF6;

- ATF4, whose expression is induced upon PERK activation;

- CHOP, which is induced by both PERK and ATF6 through the ATF4 pathway;

- XBP-1, which upon alternative splicing by IRE1 generates a functional transcription factor. In the case of XBP-1, following quantification of the two splicing forms the ratio of the spliced XBP-1 versus the unspliced was calculated. The alternative splicing was revealed by enzymatic digestion of the PCR product with *Pst I.*

The above markers were analysed by semiquantitative PCR to monitor the induction of ER stress. In addition cell death by apoptosis was assessed by propidium iodide (PI) staining of fixed cells and flow cytometric analysis.

To test the effects of ER stress on Ins secretion and on the regulated secretory granule machinery we chose to analyse a sub-lethal stress condition, in which no significant signs of cell death are detectable in the cell population. In our cell models the sub-lethal stress inducing treatment consisted of 6 hours incubation with 3 μm Tg.

3.1 Expression of ER stress markers in basal conditions

The semiquantitative analysis performed in basal conditions showed that the only markers of ER stress that were differently expressed in INS1-E and Q2 cells are BIP (Fig. 21A) and XBP-1 (Fig. 21B). BIP levels were approximately 4-fold higher in INS1-E as compared to Q2 cells; in contrast, in the latter cell models the spliced product of XBP-1 was 1.6-fold more expressed than in INS1-E cells.

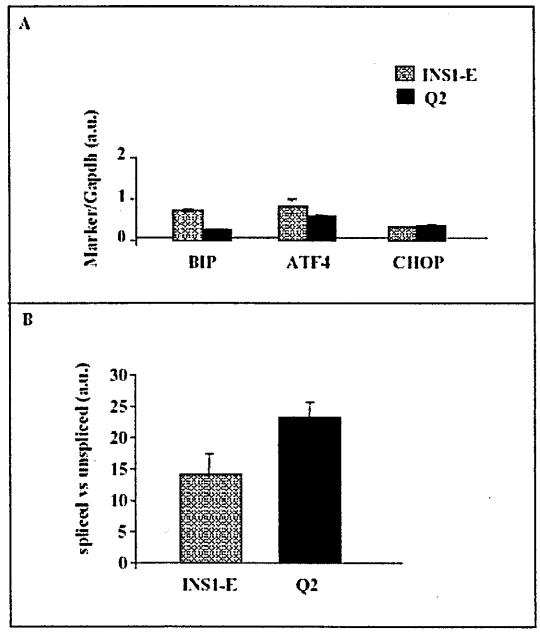

Fig. 21 – Basal levels of ER stress markers in INS1-E and Q2 cells. Semiquantitative PCR analysis of expression levels of some markers of ER stress measured in cells kept at rest. A: Expression levels of BIP, ATF4, CHOP in INS1-E and Q2 cells. INS1-E show higher level of BIP than Q2. B: Under ER stress conditions, XBP-1 mRNA undergoes splicing. Q2 cells display higher levels of the XBP-1 spliced form.

3.2 Maximal induction of ER stress

3.2.1 Expression of ER stress markers

The quantitation of PCR products obtained following semiquantitative amplification were normalised for GAPDH levels in control conditions and upon 24 hours of Tg treatment (Fig. 22). In terms of fold increase, i.e. the ratio between Tg treated and control conditions, BIP mRNA levels (Fig. 22A) increased 4.6-fold in INS1-E and 3.5-fold in Q2 cells. The increase of ATF4 levels (Fig. 22B) is similar in the two cell types (3-fold in INS1-E and 3.3-fold in Q2). Also the induction of CHOP (Fig. 22C), is not significantly different (3.7-fold in INS1-E, 3.9-fold in Q2).

Marked differences were observed with regard to the induction of XBP-1 splicing upon Tg treatment (Fig. 22D). The spliced transcript was induced 9-fold in INS1-E cells, whereas in Q2 cells its increase was lower (4.3-fold).

3.2.2 Expression levels of Ins

Rat cells, as well as mouse cells, transcribe Ins from two non allelic genes, Ins1 and Ins2. Ins1 is the most abundant transcript in INS1-E cells, whereas in Rin-5AH and Q2 cells derived therefrom it is the only transcript detectable [357]. In Tg-treated INS1-E cells the Ins1 mRNA levels decreased 10-fold (Fig. 23 B,C) and the Ins2 was no longer detectable (Fig. 23 A,C). In Q2 cells Tg treatment caused a 6-fold decrease in Ins1 transcript levels (Fig. 23 B,C).

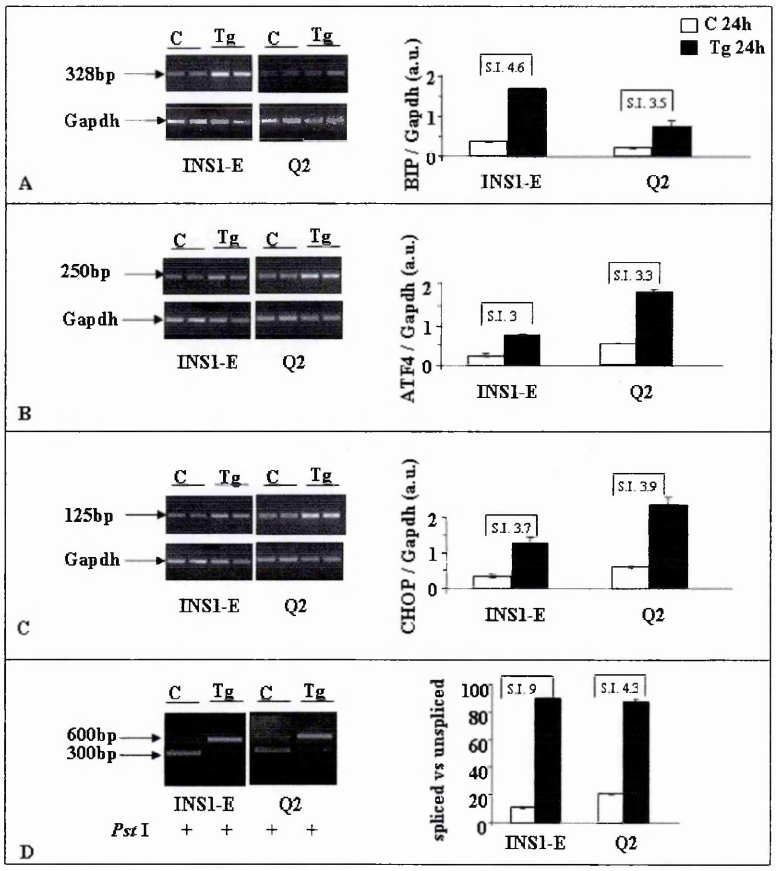

Fig. 22 – Induction of ER stress markers following 24 hours Tg. Expression levels of BIP (A), ATF4 (B), CHOP (C) and of the spliced form of XBP-1 (D) in control INS1-E and Q2 cells and after 24 hours Tg. XBP-1 splicing causes the loss of a *Pst I* restriction site, therefore the PCR product is a 600bp band, whereas the unspliced form gives two bands of 300bp. On the left the PCR panels for each marker are shown; on the right the graphs derived there-from are depicted. Open bars: control conditions (C); closed bars: Tg. The Secretion Index (S.I.) of each marker over basal levels is reported in the graphs. Each experiment was performed three times in duplicate.

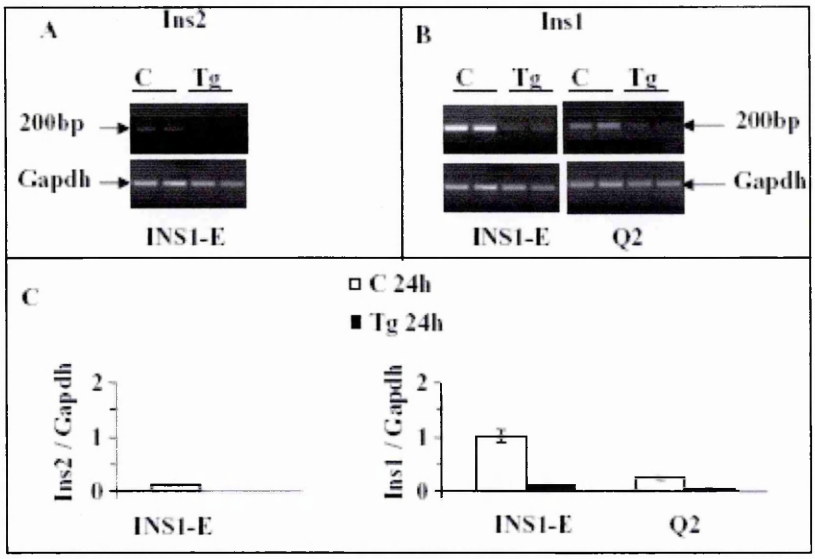

Fig. 23 – Effects of ER stress induction on Ins1 and Ins2 gene. Expression levels of Ins1 (B, C) and Ins2 (A, C) in INS1-E and Q2 cells in control conditions and after 24 hours Tg. Q2, as well as parental cells, express only Ins1. Open bars: control conditions (C); closed bars: Tg.

3.2.3. Cell death by apoptosis

The % of apoptotic cells induced by 24 hours of Tg treatment in INS1-E and Q2 was measured by flow cytometry analysis following PI staining of fixed cells. The results are represented in Fig. 24, where for each cell type the DNA content (DNA) was measured (DNA <2n indicates apoptotic cells; DNA =2n represents the % of cells in G_1 phase; DNA >2n represents actively replicating cells).

In both INS1-E (Fig. 24A) and Q2 cells (Fig. 24B) in control conditions the fraction of apoptotic cells (DNA <2n) was in the range of 10% . Upon 24 hours incubation with Tg, the population of apoptotic cells in the three lines increased about 5-fold, reaching 50% in INS1-E and 40% in Q2 cells. The fraction of cells replicating (i.e., DNA >2n)

was similar in INS1-E (40%) and Q2 (49%) and decreased upon 24 hours of stress induction in both cell models.

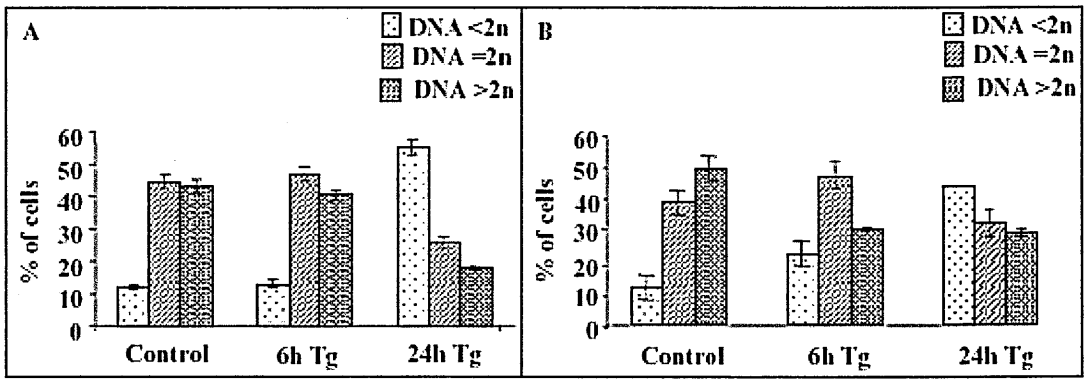

Fig. 24 – Analysis of apoptosis in INS1-E and Q2 cells after 6 and 24 hours incubation with Tg. C: Control conditions. DNA <2n: apoptosis; DNA =2n; G_1 phase; DNA >2n: replication.

3.3 Sub-lethal induction of ER stress

3.3.1 Analysis of induction of apoptosis

Once determined the effects of a massive stress in our cell models, we identified a sub-lethal condition, in which some ER stress markers were induced with no visible cell death. Our aim was to mimic a condition of ER stress, in which to analyse compensatory or detrimental effects on the regulated secretory pathway.

Following 6 hours of Tg treatment there was no significant induction of apoptosis in our reference model (INS1-E cells) as compared to untreated cells (Fig. 24A). Interestingly, under these conditions we observed that Q2 cells appeared more susceptible to apoptosis (the % of apoptotic cells increased from 12.4±3.6 to 24±8.3; Fig. 24B).

Moreover, while in INS1-E cells the fraction of replicating cells was not affected by 6 hours Tg treatment, Q2 cells showed a marked decrease in the size of the population of replicating cells (from 50% in controls to 25% upon 6 hours Tg).

3.3.2 Analysis of ER stress markers expression

The expression analysis of the ER stress markers after 6 hours Tg treatment showed increased levels of BIP mRNA (3-fold) in INS1-E and Q2 cells (Fig.25A). The expression of ATF4 (Fig. 25B) showed no change in INS1-E, whereas in Q2 it was 3-fold higher. CHOP (Fig. 25C) was up-regulated in INS1-E and Q2 to a similar extent (3- and 5-fold, respectively. The increase of XBP-1 splicing was higher in INS1-E cells (5.5-fold) than in Q2 (3.5-fold; Fig. 25D).

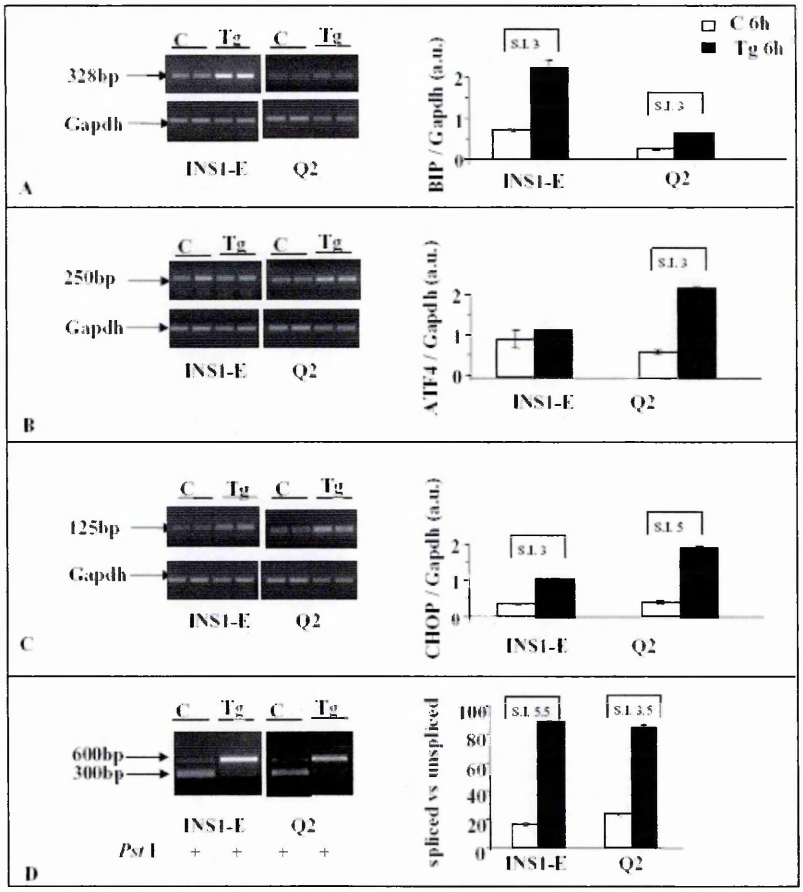

Fig. 25 - Induction of ER stress markers following 6 hours Tg. Expression levels of BIP (A), ATF4 (B), CHOP (C) and of the spliced form of XBP-1 (D) in control INS1-E and Q2 cells and after 6 hours Tg. Open bars: control conditions (C); closed bars: Tg.

Summarising the results of the present section, after 6 hours of Tg treatment the expression of some ER stress markers (BIP, ATF4, CHOP) was similar to that obtained following 24 hours treatment, although some differences were observed: in Q2 cells BIP was already over-expressed following 6 hours of Tg at the same level than after 24 hours; ATF4 was not induced in INS1-E cells after 6 hours of Tg; the spliced XBP-1 form was less induced following 6 hours Tg than after 24 hours, however also in this case in Q2 cells its level did not further increase after 24 hours Tg.

3.3.3 Expression analysis of granule markers upon sub-lethal stress induction

The following granule markers were chosen to be analysed under sub-lethal stress conditions:

- Ins1 and Ins2
- CgA
- CgB
- IA2/ICA 512
- SNAP-25
- SYP.

Ins1 (Fig. 26B) and particularly Ins2 (Fig. 26A) mRNA levels markedly decreased (~30% and ~80% over untreated cells, respectively) in INS1-E cells following 6 hours Tg treatment. In Q2 cells the stress-induced decrease of Ins1 was similar as in INS1-E cells. CgA and CgB levels (Fig. 26 C,D, respectively) did not change in INS1-E cells treated with Tg, whereas in Q2 we could observe a slight increase of CgA and CgB mRNA (around 2- and 1.5-fold, respectively). Similar results were observed in the case of IA-2/ICA 512 (Fig. 27A) and SNAP-25 (Fig. 27C). SYP levels (Fig. 27B) were not affected by Tg treatment.

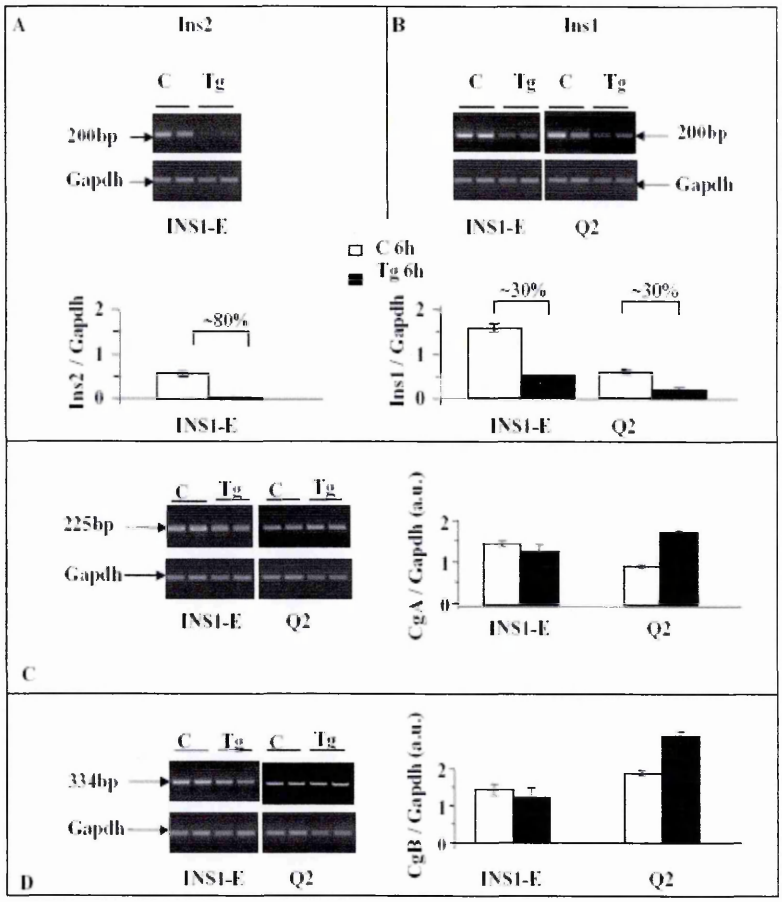

Fig. 26 - Effects of ER stress induction on the mRNA levels of some granule markers I. Expression levels of Ins1 (B) and Ins2 (A), CgA (C) and CgB (D) in control INS1-E and Q2 cells and after 6 hours Tg. Open bars: control conditions (C); closed bars: Tg.

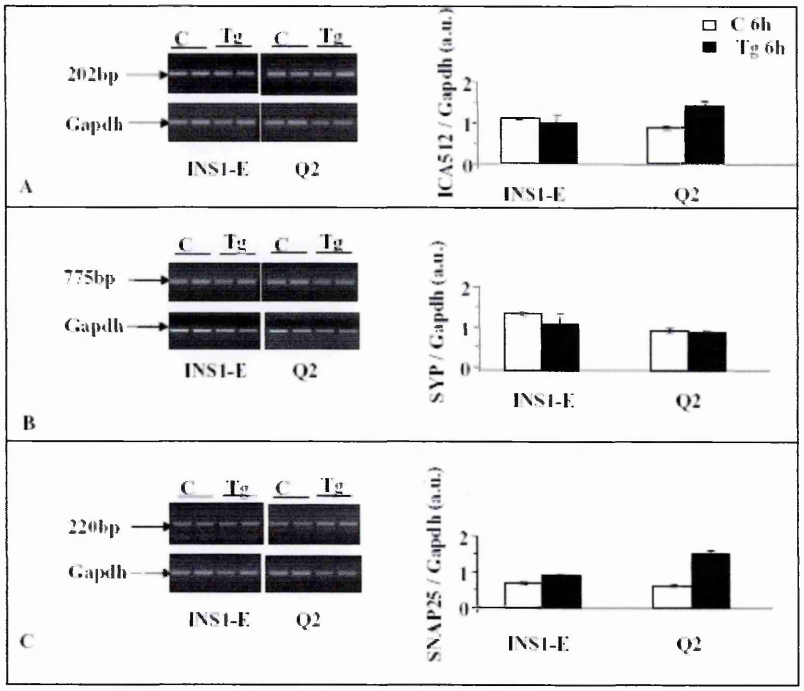

Fig. 27 - Effects of ER stress induction on the mRNA levels of some granule markers II. Expression levels of ICA512/IA-2 (A), SYP (B) and SNAP25 (C) in control INS1-E and Q2 cells and after 6 hours Tg. Open bars: control conditions (C); closed bars: Tg.

3.3.4 Ins and CgB secretion under sub-lethal stress conditions

Ins and CgB release from INS1-E and Q2 cells upon sub-lethal stress conditions was evaluated by stimulation with SM. The results of the Ins secretion assays are represented in Fig. 28. Tg-treated INS1-E cells showed no difference in the stimulated Ins release as compared to control cells, however the basal release of Ins increased 2-fold (Fig. 28A). Tg-treated Q2 cells showed a 2-fold increase of basal Ins release, but also showed a 2-fold decrease of the stimulated release (Fig. 28B). Their S.I. well reflects this change with a 4-fold decrease.

Preliminary analysis of CgB secretion showed no effect of 6 hours Tg treatment in both INS1-E and Q2 cells (not shown).

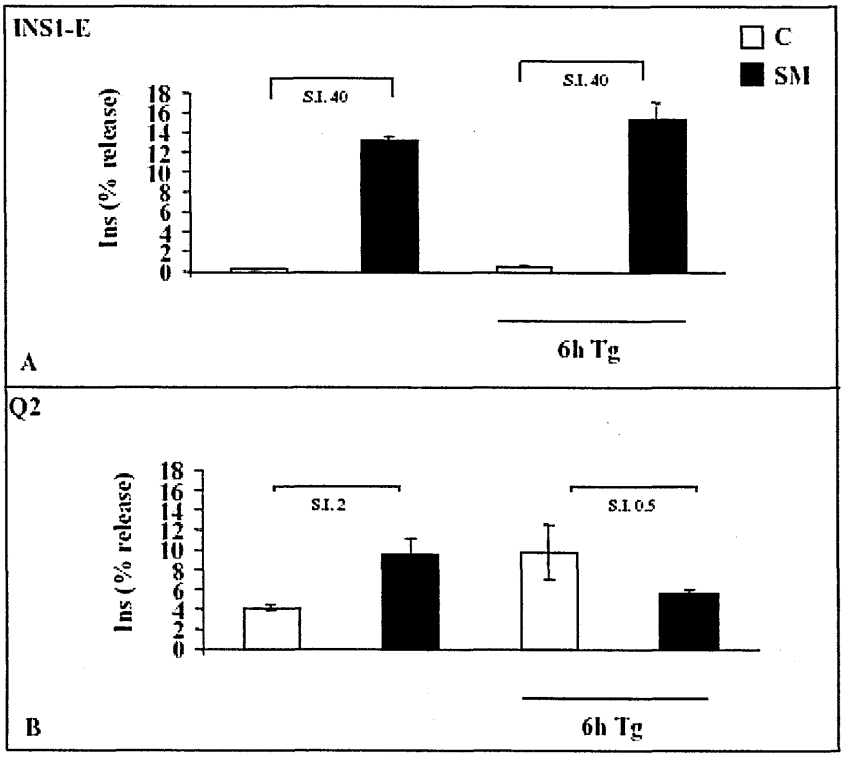

Fig. 28 - Effects of ER stress induction on Ins secretion. Ins secretion was measured in INS1-E (A) and Q2 (B) cells in control conditions and after 6 hours Tg. C (resting conditions): open bars; SM: closed bars. The results are expressed as % of Ins total content and the S.I. is reported in the graphs.

DISCUSSION

1. Ins and CgB granules in β cell models

Multiple secretory proteins are co-expressed by specialized cells and transported along the secretory pathway. Their transport is often envisaged as the flow of a protein mixture from the ER to the GC and then to the SGs, destined to be finally discharged to the extracellular space upon appropriate stimulation [13]. However, in various cell types the secretory proteins flowing out of the Golgi do not remain intermixed but are sorted to different types of SGs, some of which contain single proteins or mixtures of a few [77, 79, 358]. In Ins-secreting cells separate sorting had never been reported previously. The various secretory proteins, including granins, were rather believed to be co-stored and co-released with Ins [68-70]. Our data, obtained in four different Ins-secreting cell types, show that indeed in the GC/TGN area the hormone and CgB are probably intermixed. In the SGs, however, co-storage of Ins and CgB is restricted to only a fraction of the organelles. The other SGs appear in contrast specific for only one of these two secretion products. The discrepancy of our results with respect to the previous conclusions is probably due, at least in part, to the different experimental techniques used. In fact, dissociation between Ins and CgB, which was barely visible in our conventional confocal images, became evident when cells were analysed by the Deltavision™ reconstitution system, and was confirmed by electron microscopy. The multiplicity of

the SGs observed with regard to Ins and CgB may reflect only part of that existing in the Ins-secreting cells. In fact, other secretory proteins are expressed along with Ins in β cells [70-72]. Additional proteins travelling along the secretory pathway might have the tendency to segregate away from Ins and possibly also from CgB, contributing to an even more complex SG pattern. This however does not seem to be the case for the other granin, CgA, that in the SGs of β-TC3 and INS1-E cells largely co-localised with Ins.

In the context of the observed dissociation between Ins- and CgB- containing SGs, an unexpected result revealed by ultrastructural immunocytochemistry was the intra-granular redistribution of CgB from the core to the halo, taking place when INS1-E cells kept at rest were treated for a few minutes with iono. The redistribution to the halo may be typical of stimulated cells since it is present also in INS1-E kept in the culture medium, which contains 11 mM glucose. The change of CgB distribution seems to be specific because it was not accompanied by a redistribution of Ins, which remained confined to the core of SGs. Different results were obtained from the analysis of Ins, CgB and CgA intra-granular distribution in β cells by [359]. CgB was reported to be confined to the granule core in mature β cells, whereas it was observed throughout the granule matrix (halo+core) during ontogeny. Our data, in apparent contradiction to the latter findings, have been however obtained under completely different conditions, i.e. rat cell culture instead of pig pancreatic tissue sections. In addition, the different techniques used for the ultrastructural immunocytochemistry might also account for some discrepancy.

It was previously proposed that granins bind to granule membrane at low pH and high Ca^{2+} [89, 360]. Our findings of a peripheral redistribution of CgB within SGs upon Ca^{2+} mobilisation with iono and elevated extracellular glucose appear to be more in

agreement with a possible binding of CgB to the granule membrane upon Ca^{2+} elevation.

The dynamic redistribution of a secretory protein in the SG lumen upon stimulatory conditions had never been reported so far. Other organelles, such as ER, mitochondria and GC, can modify their internal environment in response to changes of the cytosolic milieu [361]. Some changes, for example accumulation and release of Ca^{2+}, have been reported to occurr in β cell SGs [362, 363], but the experimental evidence and the physiological importance of those findings are still debated. Our results suggest that the iono-induced changes of the cytosolic Ca^{2+} concentration may trigger a partial re-organisation of the granule core determining a prevalent distribution of CgB to the core periphery and halo. The functional significance of this redistribution is not clear, however there might be a correlation between the distribution and the release of secretory proteins. In fact, in SGs of PC12 cells the catecholamines localised preferentially in the halo have been proposed to be ready releasable through the fusion pore [75, 364]. Similar hypotheses have been proposed for the release of C-peptide from Ins-containing SGs [73].

When INS1-E cells were strongly stimulated by SM, we observed a parallel Ins and CgB release, suggesting a concomitant discharge of all SGs. However, with concentrations of iono ≤1 μM only CgB was released, while with larger iono concentrations, and also with PMA, the percentage contribution of CgB exceeded that of Ins. These results strongly suggest that the various SGs are not equally sensitive to the second messengers and signals. In particular, the CgB-rich SGs appear much more sensitive to Ca^{2+} than the Ins-containing granules. A mediator of such differential sensitivity might be PKC, a well known target of PMA which can be also activated by ionomycin-induced Ca^{2+} influx across the plasma membrane [400]. According to this

possibility, CgB might be preferentially released by PKC. Furthermore, PMA mobilises Ca^{2+} along the PLC pathway. An alternative possibility would be that PMA induces in our experimental model a Ca^{2+}-dependent exocytosis of CgB. It was indeed suggested that Ca^{2+} is released locally by PMA stimulation, as well as by ionomycin [399]. Whatever the mechanism, Ca^{2+} appears to be a critical player in the prefential release of CgB induced by ionomycin and PMA.

A differential secretion of CgB raises the question whether CgB is release from a CgB-enriched granule pool or from Ins- and CgB-containing granules. In this framework, an additional process that might contribute to the differential release of Ins and CgB is the redistribution of the latter within SGs occurring upon cell stimulation, however at the moment the role of this process was not precisely evaluated.

2. *Lessons from Rin-5AH cells heterogeneity*

2.1. Dissociation in the expression and secretion of Ins and CgB

While studying the dissociation in the intracellular distribution and secretory behaviour of Ins and CgB in various β-cell models, we observed that Rin-5AH cells appeared heterogeneous with regard to the expression of both proteins. Rin-5AH cells are a clone derived from the radiation-induced rat insulinoma Rin, which is composed of Ins-, glucagon- and somatostatin–secreting cells [365]. Rin-5AH clone has been characterised as a bona fide β cell line because it expresses only Ins [342, 366, 367], and we could also confirm the lack of glucagon expression at both the mRNA and protein level (not shown). Therefore, the heterogeneity of Ins and CgB expression is not due to the presence of cells with different hormonal specificities but rather to a differential

expression of the two proteins. Rin-5AH cells have been traditionally considered to display traits of immature β cells [366], mostly because of their low Ins content as compared to other insulinomas and to primary β cells. We disagree with this interpretation mainly because, when a battery of transcription factors was investigated in Rin-5AH as compared to INS1-E cells, we found no difference in the pattern of expression of these factors implicated in the terminally differentiated β cell phenotype (Table 1 and Fig. 1). We rather hypothesise that the low Ins content and the poor secretory performance of Rin-5AH cells is due to a perturbed secretory function.

	Isl1	PdX1	NeuroD/B2	Nkx2.2	Nkx6.1	Pax6
INS1-E	+	+	+	+	+	+
Rin-5AH	+	+	+	+	+	+
D1	+	+	+	+	+	+
D2	+	+	+	+	+	+
Q2	+	+	+	+	+	+
Q6	+	+	+	+	+	+

Table 1 – Expression analysis of transcription factors involved in the terminal development of β cell phenotype. The expression of the transcription factors reported in the table was analysed in Rin-5AH cells. + indicates presence.

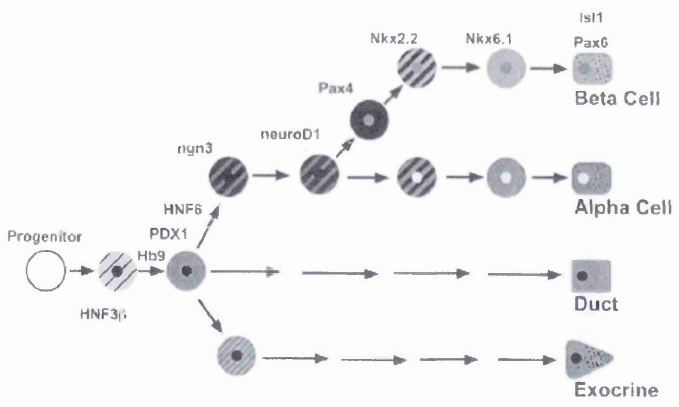

Fig. 1 – A model of the hierarchy of transcription factors involved in pancreas development [368]. PdX-1 marks the territory of the future pancreas. Later it becomes restricted to β and delta cells. Ngn3 expression starts at early stages, increases to a peak and decreases thereafter. It is turned off prior to final differentiation. The expression of NeuroD1, also called B2, can be induced by ngn3. Pax4 is not necessary for the development of early Ins-expressing cells, but is required for their maturation and maintenance. Nkx2.2 protein expression becomes progressively restricted to the alpha, β and PP cells of the mature islet. Nkx2.2 is required for terminal differentiation of β cells and maintenance of Nkx6.1 expression. Nkx6.1 protein is initially broadly expressed and becomes progressively restricted; in the adult pancreas Nkx6.1 is only present in β cells. In newborn mice, Pax6 is expressed in mature alpha, β, delta and PP cells. Isl1 is involved in the early formation of the pancreas. At early stages all the glucagon positive cells express Isl1. Later, Isl1 is detectable in all the islet cells.

2.2 Rin-5AH sub-clones

In an attempt to understand more in depth the phenotype of the four different subpopulations composing Rin-5AH cells we tried to isolate them on the basis of their positivity or negativity for Ins and CgB (Ins^+/CgB^+; Ins^+/CgB^-; Ins^-/CgB^+; Ins^-/CgB^-). Despite the observation of cells devoid of any Ins and CgB signal in the Rin-5AH population it was not possible to isolate such a sub-clone, possibly because the Ins^-/CgB^- cells reflect a transient functional state of some cells.

The investigation of the secretory behaviour of Rin-5AH parental cells and the four sub-clones selected gave us some insights into the possible molecular defects underlying the poor secretory behaviour of this cell model.

Responsiveness to the stimulatory treatments varied among the sub-clones, suggesting that they could be useful tools to investigate differences in trans-membrane signalling and/or the processes regulating SG exocytosis. While no significant differences were observed when stimulating cells with KCl/glucose, except for D1 sub-clone, application of the SM yielded variable release not only of Ins, but also of CgB. Two sub-clones appeared particularly interesting, namely D2 and Q2. D2 sub-clone showed normal Ins

content and basal release, however Ins stimulated secretion was lower as compared to parental cells. In addition, this sub-clone displayed very low CgB levels. Indeed, the % CgB release, apparently comparable to parental cells and other sub-clones, was sustained by a low amount of the protein. In fact protein release is measured as the % of the total content of the secreted protein. Intriguingly, D2 cells also displayed a very low VAMP2 and SYP levels. This might reflect either a low granule content, or a defective equipment of the cells in terms of the molecular machinery implicated in regulated exocytosis. In line with this observation is the fact that Ins secretion from D2 cells is lower than that in Rin-5AH parental cells. Taking in account that in other cellular systems the granins, and in particular CgA, have been proposed to play a structural or a sorting role during granule generation [22, 23, 369], it may be interesting to study whether CgB has any role in Ins granules biogenesis and secretion.

Q2 sub-clone attracted our attention because it showed a lower Ins release compared to parental cells, despite a similar content, and a higher CgB content which was not accompanied by a similarly high release. Together with the strong accumulation of both Ins and CgB at the GC/TGN level, these results led us to hypothesise a condition of cellular stress, which induces a functional impairment.

2.2.1 Constitutive secretion of Ins in Rin-5AH cells and sub-clones

Interesting results came from the analysis of constitutive secretion of Ins in Rin-5AH cells and sub-clones. Pre-treatment of the cells for few hours with the inhibitor of protein synthesis CHX in the absence of secretagogues causes, along with block of *de novo* protein synthesis, the release of proteins stored within constitutively released vesicles, while retaining those stored within SGs [370]. When applied to Rin-5AH cells and the four clones derived therefrom, this procedure revealed a considerable decrease

in basal Ins release only in Q2 cells, however with no effect on stimulated one. This result suggests the existence in this sub-clone of a diversion of a fraction of the hormone to a constitutive (or constitutive-like [44]) pathway, which sustains its continuous release independently from stimulation. By contrast, the high basal Ins release of Q6 sub-clone was not modified by cell pre-incubation with CHX, thus excluding in this clone a high constitutive secretion. A possible explanation of our results is the spontaneous exocytosis of SGs occurring at high rate in resting conditions.

A feature of Rin-5AH cells that was noticed in the context of the present study, as compared to other β cell models, is the predominant accumulation of Ins immunoreactivity in the GC/TGN area. One explanation for this may be a slower conversion ability of pro-Ins into Ins, which occurs during granule maturation [39, 371], despite the expression of the responsible enzymes, PC 1/3 and PC2 expression (not shown). We could not investigate the relative proportions and distribution of the hormone and its precursor, since the different antibodies available for this analysis recognise both forms. In addition, a clear GC/TGN accumulation was seen, especially in Q2 and Q6 sub-clones, also for CgB, a granule protein that does not undergo processing in β cells. Thus, the low efficiency of organelle transport along the GC-granule pathway appears to be a general property of Rin-5AH cells, possibly valid also for the other secretory proteins expressed by this line.

2.3 SNAREs machinery

An initial attempt to assess whether the differential expression of proteins involved in the secretory machinery could explain the secretory features of Rin-5AH cells and the sub-clones derived therefrom was performed by the analysis at the protein level of the SNAREs Stx1, VAMP2 and SNAP-25, as well as of the Stx-controlling protein

Munc18-1 and the Ca^{2+} sensor synaptotagmin I. We did not observe any difference in the expression of the aforementioned markers among the cells of the parental line and the sub-clones, except for VAMP2, which appeared significantly less expressed in D2 cells. In the future expression by transfection of VAMP2 in the D2 sub-clone could be useful to investigate the role of this protein in Ins secretion.

Concerning the other neurosecretory markers, they undergo post-translational modifications [128, 372], therefore their expression does not rule out the possibility of a different functional state in the subclones.

Beside dense core secretory granules (DCSGs), pancreatic β cells also contain synaptic-like microvesicles (SLMVs), which cycle between the plasma membrane and the early endosome compartment. SLMVs store [373] and release [374] by regulated exocytosis the neurotransmitter γ-aminobutyric acid (GABA), which has been proposed to play a paracrine [375] and/or an autocrine [376] role in islets physiology. Some characteristics of β cell SLMVs resemble those of the acetylcholine-containing small synaptic vesicles (SSVs) of neuroendocrine cells such as PC12 [62, 377]; for instance, they show much faster kinetics than DCSGs and are released at lower Ca^{2+} concentrations. In pancreatic β cells some proteins involved in the regulated exocytosis, such as VAMP2, are shared by DCSGs and SLMVs [378], whereas others are present on either vesicle type. This is the case for synaptotagmin III, that is only present on SGs [379], and SYP, which is restricted to SLMVs [373, 378, 379]. Taking this in account, we hypothesised that the low content of SYP and VAMP2 in the D2 sub-clone could reflect a reduced number of SLMVs. If this was true, this sub-clone could be an interesting also for investigating the effect of a reduced GABA release on Ins secretion.

3. *Revisiting RIN-5AH cells: a cell model of oxidative stress*

In the effort to identify the possible cause of the secretory behaviour of Rin-5AH cells and sub-clones we found that the latter are unable to synthesise ATP upon stimulation of Ins secretion. Furthermore, the lack of ATP production was accompanied by an increase in ADP levels suggesting also the existence of ATP consuming activities in these cells. This led us to suspect that Rin-5AH cells have a metabolic impairment leading to cellular stress. In order to investigate this issue we focused on the Q2 sub-clone, that displayed a strong accumulation of Ins and CgB in the GC/TGN and a poor secretory behaviour.

3.1 Mitochondrial function

In Q2 cells mitochondria appeared swollen and fragmented, the $\Delta\psi_m$ was lower as compared to INS1-E cells, and its increase upon stimulation of Ins secretion showed a kinetics different from that observed in the latter cells. Low $\Delta\psi_m$ levels can be due to a loss of $\Delta\Psi_m$, caused by a perturbation of the ETC. This affects ATP production, mitochondrial Ca^{2+} influx [230] and the ability of mitochondria to undergo hyperpolarisation upon stimulation of Ins secretion. Ca^{2+} homeostasis is crucial for a correct cell functionality: an impairment of Ca^{2+} handling may affect protein folding in the ER [285], Ca^{2+} cross-talk between ER and mitochondria [230, 231], leading to impaired ATP production [185], and malfunctioning of many intracellular signalling pathways. In the attempt to investigate whether a low mitochondrial [Ca^{2+}] could underlie the defective secretory behaviour of Q2 cells, the latter were treated with CGP-37157, a benzothiazepine inhibitor of the mitochondrial Na^+-Ca^{2+} exchanger, leading to an increased intramitochondrial Ca^{2+} level [232]. The improvement of Ins secretion, albeit

slight, observed in CGP-37157-treated cells suggests that the perturbed Ca^{2+} mobilisation does indeed play a role in the secretory behaviour of Q2. This might reflect an impaired mitochondrial Ca^{2+} influx, due to, or causing, the observed low $\Delta\psi_m$. A more in depth investigation of the mitochondria of Q2 cells will help further elucidate the mechanisms responsible for these defects.

In the framework of a loss of $\Delta\Psi_m$, which affects on one hand mitochondrial ATP production and on the other hand mitochondrial Ca^{2+} influx, we interpreted our finding regarding UCP2 protein levels as a possible link between the two events. UCP2 plays a clear role in decreasing the $\Delta\Psi_m$, by inducing a proton leak from the ETC and subsequently dissipating the electrochemical gradient as heat. The energy stored in the electrochemical gradient is therefore uncoupled from ATP synthesis. As discussed in Sections 2.2 and 2.4 of Introduction, UCP2 over-expression can be regarded as a defensive mechanisms upon oxidative stress, because it can lower $\Delta\psi_m$ by causing a faster electron flow, which would decrease ROS formation [218]. UCP2 was indeed shown to be activated by $\cdot O_2^-$ [221], and proposed to act also as anion carrier [218], thus transporting $\cdot O_2^-$ out of mitochondria and therefore protecting them from ROS. In the case of Q2 cells, a perturbed mitochondrial function, accompanied by higher UCP2 levels as compared to INS1E cells, might underlie a state of oxidative stress. The side effect of such a defensive mechanisms would be inevitably an impairment of Ca^{2+} influx, due to perturbed ATP production. In fact, the $\Delta\psi_m$ is the driving force for mitochondrial Ca^{2+} influx [230]. Upon Ca^{2+} uptake, $\Delta\psi_m$ is depolarised [233] and ATP production is thought to restore it. If UCP2 lowers $\Delta\Psi_m$ and impaires ATP production, mitochondria can not drive any longer Ca^{2+} uptake. This hypothesis would be supported by the effect of CGP-37157 on restoration of $\Delta\psi_m$ and Ins secretion.

Taken together, our findings of mitochondrial morphological and functional alterations led us to hypothesise that Q2 cells undergo oxidative stress causing impaired Ins secretion, accompanied by elevated ROS production [191], as observed in both type 1 [247, 248] and type 2 diabetes [249-251]. ROS are generated by several intracellular sources, among which are mitochondria. Here ROS production occurs during respiration by an electron leakage from the ETC [185, 186, 188]. Mitochondria are also important intracellular targets of ROS. Thus uncontrolled accumulation of ROS can cause perturbation of mitochondrial function by means of alterations in mtDNA, mitochondrial proteins or lipids. Finally, mitochondrial mutations can cause increased production of ROS, which in turn worsen the situation [186]. It will be of great interest to measure ROS levels in Q2 cells, as compared to INS1-E. We predict that ROS levels in Q2 cells are higher. Incubation with ascorbic acid, a mild ROS scavenger, did not yield any improvement of Ins secretion, however we observed a redistribution of the cell population to higher $\Delta\psi_m$, suggesting that a stronger or more targeted antioxidant treatment might be able to significantly improve Ins secretion in Q2 cells [380].

Finally, under chronic oxidative conditions, the $\Delta\psi_m$ is lowered, intracellular ATP is decreased and several pro-apoptotic proteins, among which the cyt c, are released from mitochondria because of the membrane permeability increase, leading to activation of caspases and apoptosis [224, 225]. These aspects are all currently investigated in the Q2 cell model. The cell viability was comparable to that of INS1-E cells, however we cannot rule out the possibility that in Q2 cells early apoptotic pathways are induced, because we have not measured the activation of caspases.

3.2 *Mitochondrial morphology*

Upon glucose up-take and metabolism, liver cells mitochondria undergo morphological changes, such as fragmentation. These changes seem to be required for glucose metabolism and ROS over-production [381]. Round-shaped mitochondria are considered to be more active because of the increased surface area; therefore, when ATP is required, mitochondria are converted from a filamentous meshwork to round-shaped, separate structures [224]. The need of ATP in Q2 cells, which are unable to produce it upon stimulation of Ins secretion, could account for the presence of round-shaped mitochondria. Our findings may be interpreted as a perturbation of a physiological phenomenon. In fact, we found fragmented and swollen mitochondria not only in culture conditions (11 mM glucose: stimulatory), but also at resting conditions (2.8 mM glucose). This might reflect an over-activation of mitochondria, possibly necessary to overcome the low overall mitochondrial functionality. If this were the case, the over-activation of mitochondria should be reflected by high basal ATP levels and oxygen consumption. Indeed we have observed higher basal ATP levels in Q2 cells with respect to Rin-5AH. However this observation is still preliminary and needs further confirmation.

3.3 *Q2 cells as a type 2 diabetes cell model*

The morphological and functional alterations of mitochondria in Q2 cells were similar to those described in β cells of type 2 diabetes patients [228, 229]. This led us to formulate the intriguing hypothesis that the Q2 sub-clone might be a cell model of oxidative stress. The relevance of this possibility is intuitive, since the study of oxidative stress in diabetes is currently being carried out on β cell models by application of agents, such as H_2O_2, which lead to cell death. A cell line, characterised by a chronic oxidative stress,

may mimic the patho-physiological state of β cells in type 2 diabetes patients and could thus be useful for validating therapeutic strategies based on counteracting oxidative stress.

The low Ins content and the impaired Ins release of Rin-5AH and Q2 cells, as compared to a good β cell model such as INS1-E cells, may be regarded as effects of oxidative stress. In particular, a very intriguing parallelism can be observed between the secretory behaviour of Rin-5AH and Q2 cells and the effects of FA-induced oxidative stress. The latter causes an increased basal Ins secretion and a decrease of stimulated release. Nevertheless, cells can still respond to secretagogues, acting directly on K_{ATP} channels, thus by-passing regulation by the ATP source, the mitochondria. In addition, upon FA-induced oxidative stress, ATP levels and $\Delta\psi_m$ are lowered, whereas the expression of UCP-2 is increased [280]. One interesting aspect of further investigation in Q2 cells will be the fatty acids metabolism, which could lead to their accumulation in mitochondria, rather than to their oxidation and elimination. This would cause a chronic oxidative stress and could explain well-known features of Rin-5AH cells and Q2 cells, such as the impaired Ins secretion and Ins gene expression [262, 263]. The same features have been described in β cells undergoing oxidative stress obtained by elevated levels of both glucose [257 258, 259].

4. ER stress in β cell models

Pancreatic β cells are highly engaged in Ins synthesis, processing and regulated secretion. They have a very developed ER, whose folding capacity must counterbalance the protein overload determined by an increase of Ins demand, thus adapting to

physiological stress. Several patho-physiological conditions, such as hypoxia, hyperglycemia, mutations which impair protein folding, can lead to ER stress [382]. In the case of pancreatic β cells, mutations of the Ins2 gene [335] or of proteins implicated in the UPR [337] lead to ER stress and diabetes (see Section 3.2 of Introduction).

Since ER and oxidative stress are both proposed to be induced under patho-physiological conditions [281, 282], we asked whether a cell model bearing oxidative stress is more susceptible to ER stress induction. In this context our finding that INS1-E cells show higher levels of BIP mRNA as compared to the Q2 sub-clone might indicate that INS1-E, while releasing actively Ins, undergo physiological stress and trigger a protective response, whereas this response in Q2 cells is less effective. Moreover, the higher levels of the XBP-1 spliced form in the latter cell model might reflect a higher need for chaperones.

We tested our hypotheses by inducing a sub-lethal ER stress to mimic a chronic ER stress. Under the experimental conditions chosen, i.e. incubation for 6 hours in the presence of 3 μM Tg, our reference cell model (INS1-E) showed no significant increase of apoptosis. By converse, Q2 cells appeared more sensitive to Tg treatment, suggesting that they may be more susceptible to ER stress induction.

An important observation concerns the induction of some stress markers in Q2 cells upon Tg treatment: the expression of ATF4 and, more markedly, of CHOP, was higher in Q2 cells than in INS1-E. By contrast, in INS1-E the treatment induced a higher expression of BIP and of the spliced form of XBP-1. These results could therefore suggest a higher sensitivity of Q2 to ER stress and a faster induction of apoptosis as compared to INS1-E, which appear actively engaged in the UPR. In the future it will be interesting to test this hypothesis by measuring the apoptosis at earlier stages of ER stress (<6 hours Tg treatment) and by assessing the activation of signalling pathways

implicated in apoptosis induction, e.g. those of caspases.

4.1 Effects of ER stress on regulated secretion

ER stress is associated to impaired glucose-induced Ins secretion. It has been proposed that a physiological UPR induction regulates the glucose-depending Ins synthesis, thus coupling supply and demand and preserving ER function [292]. According to this model, at resting glucose concentrations pro-Ins translation is attenuated by the PERK pathway, whereas it is induced at stimulatory glucose levels. Under patho-physiological conditions, such as Ins resistance, the Ins demand increases and the high rate of pro-Ins translation exceeds the folding capacity of the ER. This leads to accumulation of pro-Ins, reduced granule biogenesis and Ins secretion dysfunction [338]. In this context it is intriguing that Q2 cells show features, such as the accumulation of Ins at the level of the GC (suggestive of a defect in protein maturation), a smaller number of granules as compared to INS1-E and a poorly efficient Ins release. Taken together with the apparent lower capacity to overcome ER stress, these results suggest that Q2 cells are more prone to the establishment of ER stress conditions.

Little is known about the effects of ER stress on other components of SGs and of the secretory machinery. It has been shown that upon 24 hours exposure of rat primary β cells to the cytokine IL1β (interleukin 1), SNAP25 and VAMP2 are down-regulated, decreasing the granule docking and exocytosis of the cells [383]. Cytokines cause ER stress [384], therefore the decreased Ins secretion occurring upon ER stress may be due to a lower exocytotic rate.

We investigated the effects of a sub-lethal ER stress on the expression of some proteins of the secretory machinery and on Ins and CgB secretion in INS1-E and Q2 cells. Our analysis showed that in INS1-E cells, while Ins mRNA levels decrease upon stress

induction more markedly than in Q2 cells, the expression levels of CgA, CgB, ICA512/IA-2 and SNAP25 remain unchanged, whereas they slightly increase in Q2 cells. These results might suggest a differential regulation of the mRNA of Ins and some granule proteins, such as CgA, CgB and ICA512. Furthermore, the mRNA levels of SYP remain unchanged upon stress induction in both INS1-E and Q2 cells. This suggests that ER stress affects β cell SGs, but not SLMVs.

We therefore investigated the effect of ER stress on protein secretion with regard to Ins and CgB release. In INS1-E cells the % Ins release upon Tg treatment was similar to that of control cells, despite the decrease of both Ins mRNA and protein. In Q2 cells, where the reduction of Ins mRNA upon stress induction was smaller, we observed an increase of basal Ins release together with a decrease of its stimulated secretion. This suggests that in these cells more Ins is released by constitutive secretion upon stress induction. It would be interesting to evaluate the proportion of Ins constitutively released by pre-incubation with CHX.

In order to evaluate also the CgB release in our cell models following Tg treatment we performed a preliminary experiment. The results showed that CgB secretion was not affected by stress induction, suggesting that the two granule proteins are differently sensitive to ER stress.

The effect of ER stress on Ins and other granule proteins might be due to a different regulation of their transcription or, alternatively, to a different stability of their mRNA. The latter hypothesis would be of great interest, because so far only a mechanism of mRNA stabilisation has been described, which is common to Ins, CgA and CgB [385].

5. *Conclusions*

In the present work we have gained insights into the molecular mechanisms underlying Ins and CgB secretion in pancreatic β cells. Despite their different embryonic origin, β cells share with neurons and other endocrine cells a number of properties and molecular mechanisms, collectively known as neurosecretion competence. Moving from other neuroendocrine systems, where granins such as CgB are often expressed and thought to play a role in secretory granule biogenesis, we investigated the relative distribution of CgB in β cells, demonstrating for the first time a partial dissociation between this protein and Ins at the level of SGs. Our findings of a dynamic intra-granular redistribution of CgB under stimulatory conditions and of a functional dissociation of their regulated release upon Ca^{2+} influx, clearly suggest the possibility that in β cells secretory proteins are differently regulated. The highly heterogeneity of one of our cell models (the Rin-5AH cell line) with regard to Ins and CgB expression further confirmed our hypothesis of a differential regulation of the two proteins and raised questions about the interrelation of either protein with respect to the regulated secretion of the other. In particular, we could isolate a sub-clone, the D2, expressing very low levels of CgB and displaying a poor efficiency of Ins secretion, which represents a useful tool to further investigate the possible role of CgB in Ins release.

After a preliminary characterisation of Rin-5AH cells we concluded that this insulinoma does not display immature traits, as previously proposed, and rather regarded its poor Ins content and secretion as a possible effect of a perturbed secretory function. The Rin-5AH cell line may thus represent a cell model of endogenous stress, rather than of β cell function. The functional alterations observed in the Q2 sub-clone, in particular at the level of mitochondria, led us to hypothesise that Rin-5AH cells bear oxidative stress. It

will be very interesting to characterise the levels of ROS and other markers of oxidative stress in Q2 cells. The intriguing parallelism between our cell model and some features observed in type 2 diabetes patients suggests that Q2 cells might be a useful tool to gain further insights into the correlation between oxidative stress and Ins secretion dysfunction under chronic stress conditions. So far these studies are most often carried on β cell models by induction of oxidative stress, which leads to cell death.

Finally, our observation that a cell model possibly carrying oxidative stress is more susceptible to ER stress induction, as compared to a good β cell model (INS1-E cells), may shed a light on the correlations between oxidative stress, ER stress and Ins secretion dysfunctions. Under diabetic and other patho-physiological conditions both stress may be observed, however very little is known about the causative mechanisms and there is no knowledge about the effects of ER stress on the secretory machinery. We plan to investigate in more detail the regulation of proteins implicated in exocytosis under ER stress, which appears to be independent from that of Ins, as suggested by our preliminary results about mRNA expression and protein secretion.

Chapter 4

MATERIALS AND METHODS

Cell cultures

Cells and growth media

The cell lines used in the present work are: INS1-E [386], kind gift of M. Solimena (University of Technology, Dresden, Germany); RIN-5AH [387]; β-TC3 [388]. Human islets were obtained from post-mortem donors and kindly provided by F. Bertuzzi (San Raffaele Hospital, Milan, Italy).

Cells were grown at 37°C, under a 5% CO2 humidified atmosphere, in RPMI1640 or DMEM (11 mM glucose) media supplemented with 10% fetal clone serum III (Hyclone, Utah, USA), 100 U/ml penicillin/streptomycin and 2 mM ultra-glutamine (Cambrex Bio Science, Italy). The medium for INS1-E cells was supplemented also with 1 mM pyruvate (Cambrex Bio Science, Italy), 10 mM Hepes pH 7.4 and 50 μM β-mercaptoethanol; that for RIN-5AH cells with 1 mM pyruvate. Human islets were grown for 2 days after isolation in RPMI 1640 containing 10% serum.

For all the analyses only early to medium (12-25) passages were used, being RIN-5AH cells little characterised for stability. The same standard was also adopted for INS1E cells, although their stability in long term culture has been well characterised [341].

Subcloning

A subcloning by limited dilution was performed on Rin-5AH cells, plating 0.5 cells/well in a 96 well plate. When the clonal subpopulations were visible at the microscope, they were picked up and transferred to a 6 well plate, then the subclones were expanded for the morphological analysis. All the subclones derived showed a similar grow rate and they were cultivated in the same growth medium.

Subcellular and ultrastructural analysis

Antibodies

The antibodies used for immunofluorescence, Western blotting and immunoelectron microscopy are listed below. The polyclonal antibodies were: a guinea pig polyclonal anti-Ins (DAKO, Italy); two rabbit polyclonal anti-CgB: PE-11 [389] and an antibody generated by [390] (generously provided by P. Rosa, CNR Institute of Neurosciences, Milan, Italy); rabbit polyclonal anti-synaptotagmin I (Synaptic Systems, Goettingen, Germany); goat polyclonal anti-dopamine-β-hydroxylase (Santa Cruz, CA, USA); anti-CgA GE-19 (kind gift of Dr. Andrea Laslop, Innsbruck, Austria); anti-Munc-18 (Synaptic Systems, Goettingen, Germany); anti-UCP2 (Santa Cruz, CA, USA). The mouse monoclonals were: IgG2a anti-CgB, CIRO [391], available in our laboratory; anti-Ins (SIGMA-Aldrich, Italy); anti-TGN38 and anti-GM130 (Transduction Laboratories,

BD Biosciences, San Jose, CA USA); two anti-IA2: mICA512cyto [392] (kindly provided by M. Solimena, University of Technology, Dresden, Germany) and 76F [393], available in our laboratory; anti-CgA LK2H10; monoclonal anti-synaptophysin I (mAb38; Boehringer, Mannheim, Germany); monoclonal anti-syntaxin I (SIGMA-Aldrich, Italy); anti-VAMP-2/synaptobrevin-2 (Synaptic Systems, Goettingen, Germany); anti-tubulin (SIGMA-Aldrich, Italy). Anti-SNAP23 and anti-SNAP25 were kindly provided by M. Matteoli.

The secondary antibodies fluorescein (FITC)- and indodicarbocyanine (CY5)-conjugated goat anti-mouse and goat anti-rabbit, and the rhodamine (TRITC)-conjugated donkey anti-guinea pig were purchased from Jackson ImmunoResearch Europe Ltd. (Soham, UK). The horse-radish peroxidase (HRP)-conjugated anti-rabbit and anti-mouse secondary antibodies were from Biorad (Biorad laboratories, Italy).

Immunofluorescence analysis

The cells were plated at low density on 100 µg/ml poly-L-lysine (SIGMA-Aldrich, Italy)-coated 24 mm coverslips two days before the analysis. The cell monolayers were fixed for 20 min at room temperature (RT) with 3% paraformaldehyde dissolved in PBS pH 7.4, quenched with 15 mM glycine in PBS for 5 min, and washed with PBS. The cells were then permeabilised for 4 min with 0.2% (weight/volume, W/V) Triton X-100 in PBS, washed and the unspecific antibody binding was blocked by incubating with 0.2% (W/V) gelatine in PBS for 10 min. The cells were incubated at RT for 1 hour with the primary antibodies diluted in the following goat serum dilution buffer (GSDB): 0.2% (W/V) gelatine, 16,5% (W/V) Normal Goat Serum (Sigma-Aldrich), 0.3% (W/V) Triton X-100, 20 mM phosphate buffer pH 7.2, 0.45 M NaCl, PBS). The coverslips

were then washed with 0.2% (W/V) gelatine in PBS and incubated at RT for 45 min with the fluorescent conjugated secondary antibodies diluted in GSBD. After extensive wash with 0.2% (W/V) gelatine in PBS and PBS the coverslips were finally mounted in gelvatol and let dry at RT overnight. In the immunofluorescence with human islets, before mounting with gelvatol the coverslips were incubated for 5 min with 1 µg/ml DAPI (2-(4-Amidinophenyl)-6-indolecarbamidine dihydrochloride; SIGMA-Aldrich) to label the nuclei.

Cell were observed under either a confocal microscope (Leica TCS SP2) or a fluorescence microscope (DeltavisionTM, Applied Precision, Issaquah, WA, USA), with a 60x objective at a resolution of 1024x1024. Image deconvolutions and tridimentional cell reconstructions were performed by the DeltavisionTM wide-field microscopy system by z-stack 150 nm optical sections acquisition and processing by the softWoRx® software (Applied Precision, Issaquah, WA, USA). Exported tiff files were assembled into figures with Adobe Photoshop CS v.8 for MacOS X, according to the code of image-manipulation ethics [394].

Electron microscopy

Conventional electron microscopy (EM) was performed in Epon-embedded ultrathin sections of cells fixed with (W/V) glutaraldehyde (2%) and OsO4 (2%), as described in [395]. For immunoelectron microscopy, INS1-E cell pellets were fixed at room temperature in a mixture (W/V) of 4% formaldehyde and 0.2% glutaraldehyde, washed in 100 mM phosphate buffer pH 7.4, dehydrated in ethanol and infiltrated in LR white resin (Polyscience Europe GmBH, Eppelheim, Germany) which was polymerised for 24 hours at 50°C. Embedded samples were cut on an Ultracut microtome (Leica

Microsystems, Wetzlar, Germany), incubated with monoclonal anti-Ins (1:100) and polyclonal anti-CgB (1:100) diluted in phosphate buffer, then washed and reacted with goat anti-mouse and goat anti-rabbit Ig-coated colloidal gold particles (6 and 12 nm, respectively). After extensive washes, the grids were exposed to uranyl acetate and lead citrate and finally examined in a LEO 912AB electron microscope.

Quantification of labelled SGs was performed on printed micrographs (at least 20 for each condition). Labelled granules were counted manually by point counting. Results were expressed as percentages of total granules counted in the different experimental cell groups, both as a whole and depending on their gold particle localization in the two subcompartments, the core and the core periphery/halo.

Protein expression analysis

SDS-PAGE and Western Blotting

The cells monolayers were solubilised on ice in lysis buffer (50 mM Hepes pH 7.5, 150 mM NaCl, 15 mM $MgCl_2$, 1 mM EGTA, 10% glycerol, 1% Triton X-100) supplemented with a proteases inhibitor cocktail (0.5 mM PMSF and CLAPA: 8.25 mM chymostatin, 10.5 mM leupeptin, 8.25 mM antipain, 7.5 mM pepstatin A, 0.75 mM aprotinin; all were purchased from SIGMA-Aldrich, Italy), then kept on ice for at least 30 min and finally centrifuged at 13,000 rpm for 15 min. The supernatants containing the soluble proteins was stored at -80°C. The total protein content was measured by BCA assay (Pierce), then 25 µg of each sample were diluted in a loading buffer (0,125 M Tris-HCl pH 6.8, 5% SDS, 20% glycerol, 2% Bromophenol Blue in ethanol, 5% β-

mercaptoethanol), denatured and separated by SDS-PAGE on acrylamide gels prepared at the suitable percentage. The proteins were then transferred on 0.22 μm nitrocellulose membranes (Schleicher&Schuell Italy) in a Western blot apparatus (Biorad laboratories, Italy) overnight.

Development of nitrocellulose membranes

The nitrocellulose membranes from both Western blotting and dot blots were blocked for 1 hour with a blocking solution (5% non-fat milk in PBS-0.1% tween-20), incubated for 1 hour with the primary antibody diluted in PBS-2% BSA, thoroughly washed with PBS-0.1% tween-20 (T-PBS) and incubated for 1 hour with the appropriate HRP-conjugated secondary antibody (Biorad laboratories, Italy) diluted in the blocking buffer. After extensive wash with blocking buffer and with T-PBS, the membrane was finally developed by ECL system (Amersham, Life Sciences, Italy).

Secretion assays

Pharmacological treatments

Cycloheximide – All the incubations in low glucose KRH (see below) with or without stimuli were performed in the presence of 20 μg/ml cycloheximide (CHX; SIGMA-Aldrich, Italy), in order to inhibit protein synthesis.

CGP-37157 - Upon incubation for 1 hour in low glucose KRH, the cells were pre-treated with 20 μM CGP-37157 (7-Chloro-5-(2-chlorophenyl)-1,5-dihydro-4,1-benzothiazepin-2(3H)-one; Calbiochem, Merck Biosciences, Germany); a specific

inhibitor of the mitochondrial Na^{+}-Ca^{2+} exchanger) for 4 min at 37°C. The cells were then stimulated or not for 20 min with SM in the precence of CGP-37157.

Ascorbic acid - The cells were treated for 20 hours with 250 µM ascorbic acid (SIGMA-Aldrich, Italy) freshly solved in water. The day after a new solution of ascorbic acid was prepared and added during the incubation with low glucose KRH (see below) for 1 hour and the following 20 min of stimulation with SM or resting conditions.

Thapsigargin – The SERCA2b inhibitor thapsigargin (Tg; SIGMA-Aldrich, Italy), dissolved in DMSO, was added at the final concentration of 3 µM to the culture media. Control and treated cells were respectively incubated with DMSO alone or Tg for 6 or 24 hours.

Secretion assays

Each experiment was performed in triplicate and repeated at least three times. Cells, plated three days before the experiment and used at sub-confluence, were incubated at 37°C for 1 hour in modified, low (2.8 mM) glucose Krebs-Ringer bicarbonate buffer (KRH: 4.8 mM KCl, 1.2 mM $MgSO_4$, 10 mM Hepes pH 7.4, 2 mM KH_2PO_4, 8.3 mM $NaHCO_3$, 134 mM NaCl, 2 mM $CaCl_2$). Incubation was then continued for different times in either low glucose KRH alone (controls) or in the presence of various secretagogues (SIGMA-Aldrich, Italy). The stimuli used were a secretagogue mixture (SM: 16.7 mM glucose, 1 mM isobutylmethylxantine (IBMX), 0.1 µM phorbol 12-myristate 13-acetate (PMA), 10 µM forskolin; modified from [396]), used to induce maximal secretion; glucose, PMA or forskolin given individually; or iono (ionomycin) (0.1-10 µM). For the [Ca^{2+}]–free experiments, BAPTA-AM (50 µM) was administered to the cells for 45 minutes prior to secretagogues in [Ca^{2+}]–free KRH additioned with 1 mM EGTA, pH 7.4. In the characterisation of Rin-5AH cells and sub-clones cells were

incubated with a mixture of 50 mM KCl and 27 mM glucose (gluc/KCl), with SM or with 100 μM tolbutamide alone or in the presence of glucose and SM.

Supernatants were collected at the indicated time-points, centrifuged at 2,000 rpm for 2 min at 4°C to remove any detached cells, and stored at -80°C. Cell monolayers were solubilised on ice with lysis buffer containing 50 mM Hepes pH 7.5, 150 mM NaCl, 15 mM $MgCl_2$, 1 mM EGTA, 10% (W/V) glycerol, 1% (W/V) Triton X-100, 0.5 mM PMSF, and the protease inhibitor cocktail described for Western blotting. After lysis at 4°C for 30 minutes the cells were thoroughly homogenised by pushpull through a 26G needle and freeze-thawed 3-fold to ensure complete solubilisation of Ins and cellular proteins. Cell lysates were eventually centrifuged at 13,000 rpm for 15 min at 4°C and the supernatants stored at -80°C.

Ins and CgB assays

Insulin - Ins levels in media and lysates were measured by the rat Insulin ELISA kit (Mercodia AB, Uppsala, Sweden) following the manufacturer's indications. Ins levels in cell lysates and media of RIN-5AH cells and subclones were measured by the Linco rat insulin RIA kit (Linco Research, USA), since being the Ins content of these cells very low the differences among the samples are little appreciated with the ELISA kit, where most samples are in the first part of the standard curve. The RIA kit allows to better distinguish little differences in the Ins content. INS1-E cells were also analysed by RIA when they had to be compared to RIN-5AH cells.

The results were expressed as % of released Ins over total Ins content. In each experiment, the mean % release values were obtained from triplicate wells. Given values ± s.e.m. are averages of three to six experiments.

Chromogranin B - CgB levels were determined by dot-blot assay [397]. Total proteins of cell lysates and the entire volume (600 ul) of supernatants from secretion assays were diluted in 10% (V/V) methanol, 0.5% (W/V) sodium-deoxycholate, 50 mM Tris pH 7.4, and 150 mM NaCl, together with the antiprotease mixture. Samples were then loaded onto a 0.22 μm pore size nitrocellulose membrane (Biorad laboratories, Italy) in a dot-blot apparatus connected to the vacuum. Protein-loaded membranes were air dried at room temperature, then immediately processed as previously described for western blots and finally detected with Western Femto Signal (Pierce Biotechnology Inc., Rockford, IL, USA). Chemiluminescence images were acquired every 30 seconds in a UVP Bioimaging System (UVP, Inc., Upland, Ca, USA) by the dynamic integration mode. Samples to be compared were processed in parallel, in order to acquire the images with identical settings. Dot intensities were integrated with the LabWorks™ Image Acquisition and Analysis software (UVP, Inc., Upland, Ca, USA). Following correction for dilution factors, optical densities (OD) were used to calculate the % released CgB over total CgB ± s.e.m. Dot blots were incubated with a mixture of two anti-CgB antibodies: the rabbit polyclonal anti-CgB PE-11 (working dilution 1:400) and the mouse monoclonal anti-CgB CIRO (working dilution 1:1000).

Ca^{2+} measurements

Ca^{2+} measurements were performed using two different techniques: spectrofluorometric analysis and single-cell imaging.

Fluorometric analysis – Cells were grown on poly-L-lysine-coated coverslips manually cut to fit in a fluorometric cuvette [398]. After incubation for 30' at room temperature with the Ca^{2+} dye Fura-2/AM (Calbiochem, Merck Biosciences, Germany) in KRH (final concentration 5 μM) and washing, the slides were positioned at appropriate angles in the cuvette by a custom-made adapter. The cuvettes, equipped for medium stirring, were placed in a Perkin Elmer LS5 fluorometer. The temperature of the system was set at 37°C. After basal recording, cells were stimulated for 20 minutes with either the previously described SM or 100 μM carbachol (carbamylcholine chloride; SIGMA-Aldrich, Italy). The fluorometer measured the two wavelengths of emission of Fura-2/AM, i.e. 340 nm and 380 nm, corresponding to free and to bound cytosolic Ca^{2+}, respectively. The data were expressed as 340/380 ratio.

Single-cell imaging - The cells were plated on poly-L-lysine-coated 24 mm coverslips as previously described and used after two-three days, when they reached the sub-confluence. Upon incubation in low glucose KRH for 1 hour at 37°C, the cells were loaded with 2.5 μM Fura-2/AM in KRH for 30 min and washed. After placing the coverslips in a thermostatic chamber on the stage of a Zeiss Axiovert 200 inverted microscope, the cells were observed with a 40x objective at resting conditions (KRH) and upon stimulation with the previously described SM for 20 min. The fluorescent signals of the two wavelengths of Fura-2AM (340 and 380 nm) were monitored (0.2 frame/sec) and the ratio between them was calculated by the MetaFluor 5.0 software. The settings for each set of experiments were constant in order to compare the different cell types.

These experiments were carried out in the laboratory of Prof. Rizzuto, University of Ferrara, Italy, that kindly provided his equipment, reagents and knowledge.

ATP detection

Cells were plated in 96 well-optical compatible plates (Corning, Celbio, Italy) two days before the experiment and used when they reached sub-confluence. ATP and ADP levels in cell lysates and media were revealed by the Apoglow kit (Cambrex Bio Science, Italy) according to the manufacturer's protocol. Upon incubation for 1 hour in low glucose KRH, the cells were either stimulated or not with SM and reagents of the ATP detection kit were added 3 min after stimulation start, since the production of ATP upon stimulation of Ins secretion occurs within the first 4 minutes [140] and then the ATP is rapidly consumed for the exocytotic events. The luminescence produced by the reaction of ATP with luciferine and oxygen was measured at the Victor3 luminometer, and the results were expressed in arbitrary units of luminescence.

Analysis of mitochondria

Mitotracker staining

Cells were plated at low density on poly-L-lysine-coated 24 mm coverslips and used two days later. Upon incubation for 1 hour 30 min in low glucose KRH, they were loaded for 30 min at 37°C with a suitable concentration (25 nM and 50 nM for INS1-E and Q2 cells respectively) of Orange Mitotracker (Molecular Probes, Invitrogen Co., USA) diluted in DMEM supplemented with 2.8 mM glucose and 10% FCIII. The coverslips were then washed with KRH solution and placed in a thermostatic chamber on the stage of the DeltavisionTM wide-field microscopy system; the images were acquired with a 100x objective at a resolution of 1024x1024 pixels. Image

deconvolutions, tridimentional cell reconstructions and analysis of the tiff files generated were performed as previously described.

$\Delta\Psi_m$ measurements

The cells were seeded on 24 mm coverslips two-three days before the experiment and used when they reached the sub-confluence. Upon incubation for 1 hour 30 min in low glucose KRH, the cells were loaded with 10 nM TMRM (tetramethylrhodamine methyl ester; Molecular Probes, Invitrogen Co., USA) in low glucose KRH for 30 min at 37°, and then placed in the presence of TMRM in a thermostatic chamber on the stage of a Zeiss Axiovert 200 inverted microscope. The cells were monitored at resting conditions for 2 min and then stimulated for 20 min with the previously described SM. At the end of the stimulation $\Delta\Psi_m$ was uncoupled with 1 μM FCCP (carbonyl-cyanide 4-(trifluoromethoxy)phenylhydrazone; SIGMA-Aldrich, Italy). A single confocal plan of TMRM fluorescence was acquired for each group of cells analysed. Cells were imaged (0.1 frame/sec) by the Zeiss LSM 510 confocal system (Carl Zeiss, Jena, Germany) with a 40x objective at a resolution of 512x512 pixels. TMRM intensity was quantified using the Zeiss LSM and Metamorph 5.0 softwares.

Gene expression analysis

RNA extraction and reverse transcription

The cells were solubilised with Trizol LS Reagent (Invitrogen Co., USA) and the RNA was exctracted with chloroform and precipitated with isopropanol according to the

manufacturer's protocol. The quality and amount of the recovered RNA was evaluated by spectrophotometric measurement ($OD_{\lambda 260}$ and ratio $OD_{\lambda 260}/OD_{\lambda 280}$) and by electrophoresis on agarose-formaldehyde gel. Equal amounts of RNA from all the samples (4 μg) were pretreated with RNase-free DNase (Invitrogen Co., USA) and then reverse transcribed by the SuperScriptIII kit (Invitrogen Co., USA) using a provided Oligo(dT) mix according to the manufacturer's protocol; the cDNA obtained was then analysed by PCR and electrophoresis.

Qualitative and semi-quantitative PCR analysis

The PCR aimed at the gene expression analysis were performed with the Fast Start Taq DNA Polymerase (Roche Applied Science) according to the manufacturer's protocol and adding the provided GC-Rich reagent to templates in order to enhance the efficiency of the amplification of genes particularly rich in guanine and cytosine bases. The PCR were performed at the suitable annealing temperature and at 35 cycles using equal volumes of template.

The semi-quantitative PCR performed to analyse the expression of the markers of ER stress and granules were set up in the following way: Gapdh was used as a housekeeping gene to normalise the quantification in the different sets of samples. The amount of template (10 ng) and enzyme (0.1 μM) GoTaq DNA Polymerase (Promega, Italy) were adjusted in order to perform a non-saturating amplification of the cDNA, and the number of cycles for each gene was decided after performing three PCR of different cycles number, in order to select an amplification condition which was in the linear range, before saturation was reached. The amplified products were loaded on agarose gel, analysed by electrophoresis and imaged with UVP, Inc. (Upland, Ca, Usa)

using the same settings in order to compare the different sets of experiments; the quantification was performed with the Image Quant software (Molecular Dynamics) and the OD obtained for each gene was normalised with that of Gapdh in the same sample.

Primers sequences

The primers sequences were designed either manually or with the Oligo4 software (EMBL, Heidelberg) and their specificity was checked by BLAST alignment (NCBI search tools). The primers used for the expression analysis and the length of the obtained fragments are listed in the table below.

Gene	Forward Primer (5'-3')	Reverse primer (5'-3')	Fragment size
Actin	GGCATCCTGACCCTGAAGT	CGGATGTCAACGTCACACTT	600 bp
GAPDH	GCGATCGCGAAACCCTGGACCACCC	GATATCGAACTTTATTGATGGTATTCGAG	190 bp
CHOP	CCAGCAGAGGTCACAAGCAC	CGCACTGACCACTCTGTTTC	125 bp
UCP 2	CGAAATGCCATTGTCAACTG	CAAGGGAGGTCGTCTGTCAT	100 bp
ATF 4	AGAATGGCTGGCTATGGATG	GCCAATTGGGTTCACTGTCT	250 bp
XBP-1	AAACAGAGTAGCAGCGCAGACTGC	GGATCTCTAAAACTAGAGGCTTGGTG	600 bp
BIP	GAGTTCTTCAATGGCAAGGA	CCAGTCAGATCAAATGTACCC	328 bp
INS I	GTCCTCTGGGAGCCCAAGCCTG	CAAGGTCTGAAGATCCCCGGCCT	200 bp
INSII	TCATCCTCTGGGAGCCCCGC	GGTCTGAAGGTCACCGGCCC	200 bp
SNAP 25	CAACGTGCAACAAAGATGCT	CAATGGGGGTGACTGACTCT	202 bp
CgA	GCCAACAATACCCAATCACC	CTTTAGGCCCAGCCTTCTCT	225 bp
CgB	AAGAGGAGTCAGTGGCCAGA	CTCTGAAGCCCGGTAGTGAG	334 bp
ICA 512	GGGACAGACTTCAGCTCGAC	GCCAAAGACAGGTTCTGCTC	220 bp
ERP-57	TCCCATTAGCAAAGGTGGAC	CACCACCGAGGCATCTTTAT	200 bp
SYP	CTTGCTGCCCATAGTCGC	CCTTCAGGCTGCACCAAGT	775 bp
PdX-1	CCTGCGTGCCTGTACATG	CCACGCGTGAGCTTTGGT	294 bp
Nkx6.1	ATCTTCTGGCCCGGAGTGAT	GCGTGCTTCTTCCTCCACTT	281 bp
Nkx2.2	AGAAAGGTATGGAGGTGACGCC	CGCTCACCAAGTCCACTGCT	260 bp
Pax6	CACAGCGGAGTGAATCAGCT	CTGTCTCGGATTTCCCAAGCA	344 bp
NeuroD/ Beta2	CTTGGCCAAGAACTACATCTGG	CGACTGGTAGGAGTAGGGGTGTA	238 bp
Isl1	TGATGAAGCAACTCCAGCAG	CAGTTGCTGAAAAGCAGGCT	209 bp

Analysis of apoptosis

FACS analysis

In order to evaluate the induction of apoptosis upon Tg treatment, control and treated he cells were analysed by propidium iodide (PI) staining at the flow cytometry (FACSCAN, Becton Dickinson). The cells harvested after detaching with PBS and from the medium were centrifuged, washed and then fixed and permeabilised with chilled 70% ethanol at -20°C for at least 30 min. The pellets were then washed in hypo-osmotic PBS and stained with 1 μg/ml PI (SIGMA-Aldrich, Italy) in the presence of 0.1 mg/ml RNase. The FACS analysis was performed within 2 hours after the staining.

BIBLIOGRAPHY

1. Malosio, M.L., *et al.* (1999) Neurosecretory cells without neurosecretion: evidence of an independently regulated trait of the cell phenotype. *J Physiol* 520 Pt 1, 43-52
2. Liu, Y., and Edwards, R.H. (1997) The role of vesicular transport proteins in synaptic transmission and neural degeneration. *Annu Rev Neurosci* 20, 125-156
3. Suszkiw, J.B., and Whittaker, V.P. (1979) Role of vesicle recycling in vesicular storage and release of acetylcholine in Torpedo electroplaque synapses. *Prog Brain Res* 49, 153-162
4. Mellman, I., and Warren, G. (2000) The road taken: past and future foundations of membrane traffic. *Cell* 100, 99-112
5. Rothman, J.E., and Wieland, F.T. (1996) Protein sorting by transport vesicles. *Science* 272, 227-234
6. Schekman, R., and Orci, L. (1996) Coat proteins and vesicle budding. *Science* 271, 1526-1533
7. Antonny, B., and Schekman, R. (2001) ER export: public transportation by the COPII coach. *Curr Opin Cell Biol* 13, 438-443
8. Duden, R. (2003) ER-to-Golgi transport: COP I and COP II function (Review). *Mol Membr Biol* 20, 197-207
9. Warren, G., and Malhotra, V. (1998) The organisation of the Golgi apparatus. *Curr Opin Cell Biol* 10, 493-498
10. Pelham, H.R. (2001) Traffic through the Golgi apparatus. *J Cell Biol* 155, 1099-1101
11. Mironov, A.A., *et al.* (2001) Small cargo proteins and large aggregates can traverse the Golgi by a common mechanism without leaving the lumen of cisternae. *J Cell Biol* 155, 1225-1238
12. Orci, L., *et al.* (1997) Bidirectional transport by distinct populations of COPI-coated vesicles. *Cell* 90, 335-349
13. Traub, L.M., and Kornfeld, S. (1997) The trans-Golgi network: a late secretory sorting station. *Curr Opin Cell Biol* 9, 527-533
14. Hirschberg, K., *et al.* (1998) Kinetic analysis of secretory protein traffic and characterization of golgi to plasma membrane transport intermediates in living cells. *J Cell Biol* 143, 1485-1503
15. Toomre, D., *et al.* (1999) Dual-color visualization of trans-Golgi network to plasma membrane traffic along microtubules in living cells. *J Cell Sci* 112 (Pt 1), 21-33
16. Polishchuk, R.S., *et al.* (2000) Correlative light-electron microscopy reveals the tubular-saccular ultrastructure of carriers operating between Golgi apparatus and plasma membrane. *J Cell Biol* 148, 45-58
17. Hay, J.C., and Scheller, R.H. (1997) SNAREs and NSF in targeted membrane fusion. *Curr Opin Cell Biol* 9, 505-512

18. Lin, R.C., and Scheller, R.H. (2000) Mechanisms of synaptic vesicle exocytosis. *Annu Rev Cell Dev Biol* 16, 19-49
19. Sutton, R.B., *et al.* (1998) Crystal structure of a SNARE complex involved in synaptic exocytosis at 2.4 A resolution. *Nature* 395, 347-353
20. Rothman, J.E. (1994) Mechanisms of intracellular protein transport. *Nature* 372, 55-63
21. Palade, G. (1975) Intracellular aspects of the process of protein synthesis. *Science* 189, 347-358
22. Tooze, S.A. (1998) Biogenesis of secretory granules in the trans-Golgi network of neuroendocrine and endocrine cells. *Biochim Biophys Acta* 1404, 231-244
23. Arvan, P., and Castle, D. (1998) Sorting and storage during secretory granule biogenesis: looking backward and looking forward. *Biochem J* 332 (Pt 3), 593-610
24. Palmer, D.J., and Christie, D.L. (1992) Identification of molecular aggregates containing glycoproteins III, J, K (carboxypeptidase H), and H (Kex2-related proteases) in the soluble and membrane fractions of adrenal medullary chromaffin granules. *J Biol Chem* 267, 19806-19812
25. Huang, X.F., and Arvan, P. (1995) Intracellular transport of proinsulin in pancreatic beta-cells. Structural maturation probed by disulfide accessibility. *J Biol Chem* 270, 20417-20423
26. Thiele, C., *et al.* (1997) Protein secretion: puzzling receptors. *Curr Biol* 7, R496-500
27. Chanat, E., and Huttner, W.B. (1991) Milieu-induced, selective aggregation of regulated secretory proteins in the trans-Golgi network. *J Cell Biol* 115, 1505-1519
28. Rindler, M.J. (1998) Carboxypeptidase E, a peripheral membrane protein implicated in the targeting of hormones to secretory granules, co-aggregates with granule content proteins at acidic pH. *J Biol Chem* 273, 31180-31185
29. Natori, S., and Huttner, W.B. (1996) Chromogranin B (secretogranin I) promotes sorting to the regulated secretory pathway of processing intermediates derived from a peptide hormone precursor. *Proc Natl Acad Sci U S A* 93, 4431-4436
30. Huttner, W.B., *et al.* (1991) The granin (chromogranin/secretogranin) family. *Trends Biochem Sci* 16, 27-30
31. Chanat, E., *et al.* (1994) The disulfide bond in chromogranin B, which is essential for its sorting to secretory granules, is not required for its aggregation in the trans-Golgi network. *FEBS Lett* 351, 225-230
32. Cool, D.R., *et al.* (1997) Carboxypeptidase E is a regulated secretory pathway sorting receptor: genetic obliteration leads to endocrine disorders in Cpe(fat) mice. *Cell* 88, 73-83
33. Glombik, M.M., *et al.* (1999) The disulfide-bonded loop of chromogranin B mediates membrane binding and directs sorting from the trans-Golgi network to secretory granules. *Embo J* 18, 1059-1070
34. Wang, Y., *et al.* (2000) Cholesterol is required for the formation of regulated and constitutive secretory vesicles from the trans-Golgi network. *Traffic* 1, 952-962
35. Blazquez, M., *et al.* (2000) Involvement of the membrane lipid bilayer in sorting prohormone convertase 2 into the regulated secretory pathway. *Biochem J* 349 Pt 3, 843-852
36. Dhanvantari, S., and Loh, Y.P. (2000) Lipid raft association of carboxypeptidase E is necessary for its function as a regulated secretory pathway sorting receptor. *J Biol Chem* 275, 29887-29893

37. Thiele, C., and Huttner, W.B. (1998) Protein and lipid sorting from the trans-Golgi network to secretory granules-recent developments. *Semin Cell Dev Biol* 9, 511-516
38. Tooze, S.A., *et al.* (2001) Secretory granule biogenesis: rafting to the SNARE. *Trends Cell Biol* 11, 116-122
39. Kuliawat, R., *et al.* (2000) Proinsulin endoproteolysis confers enhanced targeting of processed insulin to the regulated secretory pathway. *Mol Biol Cell* 11, 1959-1972
40. Yoshimori, T., *et al.* (1996) Different biosynthetic transport routes to the plasma membrane in BHK and CHO cells. *J Cell Biol* 133, 247-256
41. Mostov, K.E., *et al.* (2000) Membrane traffic in polarized epithelial cells. *Curr Opin Cell Biol* 12, 483-490
42. Dotti, C.G., and Simons, K. (1990) Polarized sorting of viral glycoproteins to the axon and dendrites of hippocampal neurons in culture. *Cell* 62, 63-72
43. Tooze, S.A. (1991) Biogenesis of secretory granules. Implications arising from the immature secretory granule in the regulated pathway of secretion. *FEBS Lett* 285, 220-224
44. Arvan, P., *et al.* (1991) Protein discharge from immature secretory granules displays both regulated and constitutive characteristics. *J Biol Chem* 266, 14171-14174
45. Klumperman, J., *et al.* (1998) Mannose 6-phosphate receptors are sorted from immature secretory granules via adaptor protein AP-1, clathrin, and syntaxin 6-positive vesicles. *J Cell Biol* 141, 359-371
46. Bock, J.B., *et al.* (1997) Syntaxin 6 functions in trans-Golgi network vesicle trafficking. *Mol Biol Cell* 8, 1261-1271
47. Molinete, M., *et al.* (2001) Role of clathrin in the regulated secretory pathway of pancreatic beta-cells. *J Cell Sci* 114, 3059-3066
48. Huang, X.F., and Arvan, P. (1994) Formation of the insulin-containing secretory granule core occurs within immature beta-granules. *J Biol Chem* 269, 20838-20844
49. Docherty, K., *et al.* (1989) Proinsulin endopeptidase substrate specificities defined by site-directed mutagenesis of proinsulin. *J Biol Chem* 264, 18335-18339
50. Smeekens, S.P., *et al.* (1992) Proinsulin processing by the subtilisin-related proprotein convertases furin, PC2, and PC3. *Proc Natl Acad Sci U S A* 89, 8822-8826
51. Naggert, J.K., *et al.* (1995) Hyperproinsulinaemia in obese fat/fat mice associated with a carboxypeptidase E mutation which reduces enzyme activity. *Nat Genet* 10, 135-142
52. Frank, B.H., and Veros, A.J. (1968) Physical studies on proinsulin-association behavior and conformation in solution. *Biochem Biophys Res Commun* 32, 155-160
53. Kuliawat, R., *et al.* (1997) Differential sorting of lysosomal enzymes out of the regulated secretory pathway in pancreatic beta-cells. *J Cell Biol* 137, 595-608
54. Michael, J., *et al.* (1987) Studies on the molecular organization of rat insulin secretory granules. *J Biol Chem* 262, 16531-16535
55. Kuliawat, R., and Arvan, P. (1994) Distinct molecular mechanisms for protein sorting within immature secretory granules of pancreatic beta-cells. *J Cell Biol* 126, 77-86
56. Colomer, V., *et al.* (1996) Secretory granule content proteins and the luminal domains of granule membrane proteins aggregate in vitro at mildly acidic pH. *J Biol Chem* 271, 48-55
57. Kuliawat, R., and Arvan, P. (1992) Protein targeting via the "constitutive-like" secretory pathway in isolated pancreatic islets: passive sorting in the immature granule compartment. *J Cell Biol* 118, 521-529

58. Arvan, P., and Castle, D. (1992) Protein sorting and secretion granule formation in regulated secretory cells. *Trends Cell Biol* 2, 327-331
59. Feng, L., and Arvan, P. (2003) The trafficking of alpha 1-antitrypsin, a post-Golgi secretory pathway marker, in INS-1 pancreatic beta cells. *J Biol Chem* 278, 31486-31494
60. Arvan, P., and Halban, P.A. (2004) Sorting ourselves out: seeking consensus on trafficking in the beta-cell. *Traffic* 5, 53-61
61. Hutton, J.C. (1994) Insulin secretory granule biogenesis and the proinsulin-processing endopeptidases. *Diabetologia* 37 Suppl 2, S48-56
62. Gerber, S.H., and Sudhof, T.C. (2002) Molecular determinants of regulated exocytosis. *Diabetes* 51 Suppl 1, S3-11
63. Bassetti, M., *et al.* (1990) Co-localization of secretogranins/chromogranins with thyrotropin and luteinizing hormone in secretory granules of cow anterior pituitary. *J Histochem Cytochem* 38, 1353-1363
64. Steiner, H.J., *et al.* (1989) Co-localization of chromogranin A and B, secretogranin II and neuropeptide Y in chromaffin granules of rat adrenal medulla studied by electron microscopic immunocytochemistry. *Histochemistry* 91, 473-477
65. Bondy, C.A., *et al.* (1989) Coexisting peptides in hypothalamic neuroendocrine systems: some functional implications. *Cell Mol Neurobiol* 9, 427-446
66. Merighi, A. (2002) Costorage and coexistence of neuropeptides in the mammalian CNS. *Prog Neurobiol* 66, 161-190
67. Landry, M., *et al.* (2003) Differential routing of coexisting neuropeptides in vasopressin neurons. *Eur J Neurosci* 17, 579-589
68. Lukinius, A., *et al.* (1992) A chromogranin peptide is co-stored with insulin in the human pancreatic islet B-cell granules. *Histochem J* 24, 679-684
69. Hutton, J.C., *et al.* (1988) Immunolocalization of betagranin: a chromogranin A-related protein of the pancreatic B-cell. *Endocrinology* 122, 1014-1020
70. Lukinius, A., *et al.* (1997) Expression of islet amyloid polypeptide in fetal and adult porcine and human pancreatic islet cells. *Endocrinology* 138, 5319-5325
71. Wierup, N., *et al.* (2006) CART regulates islet hormone secretion and is expressed in the beta-cells of type 2 diabetic rats. *Diabetes* 55, 305-311
72. Xu, W., *et al.* (2005) Interferon-gamma-induced regulation of the pancreatic derived cytokine FAM3B in islets and insulin-secreting betaTC3 cells. *Mol Cell Endocrinol* 240, 74-81
73. Michael, D.J., *et al.* (2006) Pancreatic {beta}-Cells Secrete Insulin in Fast- and Slow-Release Forms. *Diabetes* 55, 600-607
74. Obermuller, S., *et al.* (2005) Selective nucleotide-release from dense-core granules in insulin-secreting cells. *J Cell Sci* 118, 4271-4282
75. Sombers, L.A., *et al.* (2004) The effects of vesicular volume on secretion through the fusion pore in exocytotic release from PC12 cells. *J Neurosci* 24, 303-309
76. Fumagalli, G., and Zanini, A. (1985) In cow anterior pituitary, growth hormone and prolactin can be packed in separate granules of the same cell. *J Cell Biol* 100, 2019-2024
77. Fisher, J.M., *et al.* (1988) Multiple neuropeptides derived from a common precursor are differentially packaged and transported. *Cell* 54, 813-822
78. Klumperman, J., Spijker, S., van Minnen, J., Sharp-Baker, H., Smit, A.B., and Geraerts, W.P.M. (1996) Cell Type-Specific Sorting of Neuropeptides: A Mechanism to Modulate Peptide Composition of Large Dense-Core Vesicles. *The Journal of Neuroscience* 16, 7930-7940

79. Hashimoto, S., *et al.* (1987) Sorting of three secretory proteins to distinct secretory granules in acidophilic cells of cow anterior pituitary. *J Cell Biol* 105, 1579-1586
80. Kreiner, T., *et al.* (1986) Localization of Aplysia neurosecretory peptides to multiple populations of dense core vesicles. *J Cell Biol* 102, 769-782
81. Seidah, N.G., and Chretien, M. (1997) Eukaryotic protein processing: endoproteolysis of precursor proteins. *Curr Opin Biotechnol* 8, 602-607
82. Zhou, A., *et al.* (1999) Proteolytic processing in the secretory pathway. *J Biol Chem* 274, 20745-20748
83. Chun, J.Y., *et al.* (1994) The function and differential sorting of a family of aplysia prohormone processing enzymes. *Neuron* 12, 831-844
84. Taupenot, L., *et al.* (2003) The chromogranin-secretogranin family. *N Engl J Med* 348, 1134-1149
85. O'Connor, D.T. (1983) Chromogranin: widespread immunoreactivity in polypeptide hormone producing tissues and in serum. *Regul Pept* 6, 263-280
86. Galindo, E., *et al.* (1991) Chromostatin, a 20-amino acid peptide derived from chromogranin A, inhibits chromaffin cell secretion. *Proc Natl Acad Sci U S A* 88, 1426-1430
87. Winkler, H., and Fischer-Colbrie, R. (1992) The chromogranins A and B: the first 25 years and future perspectives. *Neuroscience* 49, 497-528
88. Doblinger, A., *et al.* (2003) Proteolytic processing of chromogranin A by the prohormone convertase PC2. *Regul Pept* 111, 111-116
89. Natori, S., and Huttner, W.B. (1994) Peptides derived from the granins (chromogranins/secretogranins). *Biochimie* 76, 277-282
90. Dillen, L., *et al.* (1993) Posttranslational processing of proenkephalins and chromogranins/secretogranins. *Neurochem Int* 22, 315-352
91. Eskeland, N.L., *et al.* (1996) Chromogranin A processing and secretion: specific role of endogenous and exogenous prohormone convertases in the regulated secretory pathway. *J Clin Invest* 98, 148-156
92. Laslop, A., *et al.* (1998) Proteolytic processing of chromogranin B and secretogranin II by prohormone convertases. *J Neurochem* 70, 374-383
93. Fischer-Colbrie, R., *et al.* (1987) Chromogranins A, B, and C: widespread constituents of secretory vesicles. *Ann N Y Acad Sci* 493, 120-134
94. Yoshie, S., *et al.* (1987) Immunological characterization of chromogranins A and B and secretogranin II in the bovine pancreatic islet. *Histochemistry* 87, 99-106
95. Schmid, K.W., *et al.* (1989) An immunological study on chromogranin A and B in human endocrine and nervous tissues. *Histochem J* 21, 365-373
96. Colombo, B., *et al.* (2002) Chromogranin A expression in neoplastic cells affects tumor growth and morphogenesis in mouse models. *Cancer Res* 62, 941-946
97. Corti, A., *et al.* (1996) Characterisation of circulating chromogranin A in human cancer patients. *Br J Cancer* 73, 924-932
98. Malosio, M.L., *et al.* (2004) Dense-core granules: a specific hallmark of the neuronal/neurosecretory cell phenotype. *J Cell Sci* 117, 743-749
99. Day, R., and Gorr, S.U. (2002) Secretory granule biogenesis and chromogranin A: master gene, on/off switch or assembly factor? *Trends Endocrinol Metab* 14, 10-13
100. Yoo, S.H. (2000) Coupling of the IP3 receptor/Ca2+ channel with Ca2+ storage proteins chromogranins A and B in secretory granules. *Trends Neurosci* 23, 424-428

101. Yoo, S.H., and Jeon, C.J. (2000) Inositol 1,4,5-trisphosphate receptor/Ca2+ channel modulatory role of chromogranin A, a Ca2+ storage protein of secretory granules. *J Biol Chem* 275, 15067-15073
102. Gonzalez-Yanes, C., and Sanchez-Margalet, V. (2002) Pancreastatin, a chromogranin A-derived peptide, activates protein synthesis signaling cascade in rat adipocytes. *Biochem Biophys Res Commun* 299, 525-531
103. Sanchez-Margalet, V., *et al.* (1996) Pancreastatin: further evidence for its consideration as a regulatory peptide. *J Mol Endocrinol* 16, 1-8
104. O'Connor, D.T., *et al.* (2005) Pancreastatin: multiple actions on human intermediary metabolism in vivo, variation in disease, and naturally occurring functional genetic polymorphism. *J Clin Endocrinol Metab* 90, 5414-5425
105. Karlsson, E. (2001) The role of pancreatic chromogranins in islet physiology. *Curr Mol Med* 1, 727-732
106. Portela-Gomes, G.M., and Stridsberg, M. (2001) Selective processing of chromogranin A in the different islet cells in human pancreas. *J Histochem Cytochem* 49, 483-490
107. Tatemoto, K., *et al.* (1986) Pancreastatin, a novel pancreatic peptide that inhibits insulin secretion. *Nature* 324, 476-478
108. Sanchez-Margalet, V., *et al.* (2000) Pancreastatin. Biological effects and mechanisms of action. *Adv Exp Med Biol* 482, 247-262
109. Gasparri, A., *et al.* (1997) Chromogranin A fragments modulate cell adhesion. Identification and characterization of a pro-adhesive domain. *J Biol Chem* 272, 20835-20843
110. Colombo, B., *et al.* (2002) Cleavage of chromogranin A N-terminal domain by plasmin provides a new mechanism for regulating cell adhesion. *J Biol Chem* 277, 45911-45919
111. Jahn, R., and Sudhof, T.C. (1999) Membrane fusion and exocytosis. *Annu Rev Biochem* 68, 863-911
112. Klenchin, V.A., and Martin, T.F. (2000) Priming in exocytosis: attaining fusion-competence after vesicle docking. *Biochimie* 82, 399-407
113. Heinemann, C., *et al.* (1994) Kinetics of the secretory response in bovine chromaffin cells following flash photolysis of caged Ca2+. *Biophys J* 67, 2546-2557
114. Sabatini, B.L., and Regehr, W.G. (1999) Timing of synaptic transmission. *Annu Rev Physiol* 61, 521-542
115. Waters, M.G., and Hughson, F.M. (2000) Membrane tethering and fusion in the secretory and endocytic pathways. *Traffic* 1, 588-597
116. Sollner, T., *et al.* (1993) SNAP receptors implicated in vesicle targeting and fusion. *Nature* 362, 318-324
117. Koushika, S.P., *et al.* (2001) A post-docking role for active zone protein Rim. *Nat Neurosci* 4, 997-1005
118. Ashery, U., *et al.* (2000) Munc13-1 acts as a priming factor for large dense-core vesicles in bovine chromaffin cells. *Embo J* 19, 3586-3596
119. Sudhof, T.C., and Rizo, J. (1996) Synaptotagmins: C2-domain proteins that regulate membrane traffic. *Neuron* 17, 379-388
120. Davletov, B.A., and Sudhof, T.C. (1993) A single C2 domain from synaptotagmin I is sufficient for high affinity Ca2+/phospholipid binding. *J Biol Chem* 268, 26386-26390
121. Li, C., *et al.* (1995) Ca(2+)-dependent and -independent activities of neural and non-neural synaptotagmins. *Nature* 375, 594-599

122. Schiavo, G., *et al.* (1997) Binding of the synaptic vesicle v-SNARE, synaptotagmin, to the plasma membrane t-SNARE, SNAP-25, can explain docked vesicles at neurotoxin-treated synapses. *Proc Natl Acad Sci U S A* 94, 997-1001
123. Robinson, I.M., *et al.* (2002) Synaptotagmins I and IV promote transmitter release independently of Ca(2+) binding in the C(2)A domain. *Nature* 418, 336-340
124. Nielander, H.B., *et al.* (1995) Phosphorylation of VAMP/synaptobrevin in synaptic vesicles by endogenous protein kinases. *J Neurochem* 65, 1712-1720
125. Verona, M., *et al.* (2000) Changes of synaptotagmin interaction with t-SNARE proteins in vitro after calcium/calmodulin-dependent phosphorylation. *J Neurochem* 74, 209-221
126. Risinger, C., and Bennett, M.K. (1999) Differential phosphorylation of syntaxin and synaptosome-associated protein of 25 kDa (SNAP-25) isoforms. *J Neurochem* 72, 614-624
127. Fujita, Y., *et al.* (1996) Phosphorylation of Munc-18/n-Sec1/rbSec1 by protein kinase C: its implication in regulating the interaction of Munc-18/n-Sec1/rbSec1 with syntaxin. *J Biol Chem* 271, 7265-7268
128. Barclay, J.W., *et al.* (2003) Phosphorylation of Munc18 by protein kinase C regulates the kinetics of exocytosis. *J Biol Chem* 278, 10538-10545
129. Meldolesi, J. (1998) Regulated exocytosis in neurons and neurosecretory cells: structural events and expression competence. *J Physiol Paris* 92, 119-121
130. Galli, T., and Haucke, V. (2001) Cycling of synaptic vesicles: how far? How fast! *Sci STKE* 2001, RE1
131. Jarousse, N., and Kelly, R.B. (2001) Endocytotic mechanisms in synapses. *Curr Opin Cell Biol* 13, 461-469
132. Ohara-Imaizumi, M., *et al.* (2002) Monitoring of exocytosis and endocytosis of insulin secretory granules in the pancreatic beta-cell line MIN6 using pH-sensitive green fluorescent protein (pHluorin) and confocal laser microscopy. *Biochem J* 363, 73-80
133. Rorsman, P., and Renstrom, E. (2003) Insulin granule dynamics in pancreatic beta cells. *Diabetologia* 46, 1029-1045
134. Grodsky, G.M., *et al.* (1969) [Further studies on the dynamic aspects of insulin release in vitro with evidence for a two-compartmental storage system]. *Acta Diabetol Lat* 6 Suppl 1, 554-578
135. Luzi, L., and DeFronzo, R.A. (1989) Effect of loss of first-phase insulin secretion on hepatic glucose production and tissue glucose disposal in humans. *Am J Physiol* 257, E241-246
136. Newgard, C.B., and McGarry, J.D. (1995) Metabolic coupling factors in pancreatic beta-cell signal transduction. *Annu Rev Biochem* 64, 689-719
137. Matschinsky, F.M. (1996) Banting Lecture 1995. A lesson in metabolic regulation inspired by the glucokinase glucose sensor paradigm. *Diabetes* 45, 223-241
138. Matschinsky, F.M., *et al.* (1998) Pancreatic beta-cell glucokinase: closing the gap between theoretical concepts and experimental realities. *Diabetes* 47, 307-315
139. Aizawa, T., *et al.* (1998) Glucose action 'beyond ionic events' in the pancreatic beta cell. *Trends Pharmacol Sci* 19, 496-499
140. Maechler, P., *et al.* (1998) Continuous monitoring of ATP levels in living insulin secreting cells expressing cytosolic firefly luciferase. *FEBS Lett* 422, 328-332
141. Aguilar-Bryan, L., and Bryan, J. (1999) Molecular biology of adenosine triphosphate-sensitive potassium channels. *Endocr Rev* 20, 101-135

142. Horvath, A., *et al.* (1998) Voltage dependent calcium channels in adrenal glomerulosa cells and in insulin producing cells. *Cell Calcium* 23, 33-42
143. Ligon, B., *et al.* (1998) Class A calcium channel variants in pancreatic islets and their role in insulin secretion. *J Biol Chem* 273, 13905-13911
144. Pralong, W.F., *et al.* (1990) Single islet beta-cell stimulation by nutrients: relationship between pyridine nucleotides, cytosolic Ca2+ and secretion. *Embo J* 9, 53-60
145. Duchen, M.R., *et al.* (1993) Substrate-dependent changes in mitochondrial function, intracellular free calcium concentration and membrane channels in pancreatic beta-cells. *Biochem J* 294 (Pt 1), 35-42
146. Maechler, P., *et al.* (1997) Mitochondrial activation directly triggers the exocytosis of insulin in permeabilized pancreatic beta-cells. *Embo J* 16, 3833-3841
147. Kennedy, E.D., *et al.* (1998) Effects of depletion of mitochondrial DNA in metabolism secretion coupling in INS-1 cells. *Diabetes* 47, 374-380
148. Wollheim, C.B., and Sharp, G.W. (1981) Regulation of insulin release by calcium. *Physiol Rev* 61, 914-973
149. Peter-Riesch, B., *et al.* (1988) Glucose and carbachol generate 1,2-diacylglycerols by different mechanisms in pancreatic islets. *J Clin Invest* 81, 1154-1161
150. Biden, T.J., *et al.* (1987) Ca2+-mediated generation of inositol 1,4,5-triphosphate and inositol 1,3,4,5-tetrakisphosphate in pancreatic islets. Studies with K+, glucose, and carbamylcholine. *J Biol Chem* 262, 3567-3571
151. Pozzan, T., *et al.* (1994) Molecular and cellular physiology of intracellular calcium stores. *Physiol Rev* 74, 595-636
152. Wenham, R.M., *et al.* (1994) Glucose activates the multifunctional Ca2+/calmodulin-dependent protein kinase II in isolated rat pancreatic islets. *J Biol Chem* 269, 4947-4952
153. Jones, P.M., and Persaud, S.J. (1998) Protein kinases, protein phosphorylation, and the regulation of insulin secretion from pancreatic beta-cells. *Endocr Rev* 19, 429-461
154. Mohlig, M., *et al.* (1997) Insulinoma cells contain an isoform of Ca2+/calmodulin-dependent protein kinase II delta associated with insulin secretion vesicles. *Endocrinology* 138, 2577-2584
155. Gromada, J., *et al.* (1999) CaM kinase II-dependent mobilization of secretory granules underlies acetylcholine-induced stimulation of exocytosis in mouse pancreatic B-cells. *J Physiol* 518 (Pt 3), 745-759
156. Easom, R.A. (1999) CaM kinase II: a protein kinase with extraordinary talents germane to insulin exocytosis. *Diabetes* 48, 675-684
157. Zawalich, W.S., *et al.* (1975) Factors governing glucose induced elevation of cyclic 3'5' AMP levels in pancreatic islets. *Diabetologia* 11, 231-235
158. Takahashi, N., *et al.* (1999) Post-priming actions of ATP on Ca2+-dependent exocytosis in pancreatic beta cells. *Proc Natl Acad Sci U S A* 96, 760-765
159. Henquin, J.C., *et al.* (2003) Hierarchy of the beta-cell signals controlling insulin secretion. *Eur J Clin Invest* 33, 742-750
160. Sato, Y., *et al.* (1992) Dual functional role of membrane depolarization/Ca2+ influx in rat pancreatic B-cell. *Diabetes* 41, 438-443
161. Gembal, M., *et al.* (1993) Mechanisms by which glucose can control insulin release independently from its action on adenosine triphosphate-sensitive K+ channels in mouse B cells. *J Clin Invest* 91, 871-880

162. Gembal, M., *et al.* (1992) Evidence that glucose can control insulin release independently from its action on ATP-sensitive K+ channels in mouse B cells. *J Clin Invest* 89, 1288-1295
163. Lee, I.S., *et al.* (2003) Protein kinase A- and C-induced insulin release from Ca2+ -insensitive pools. *Cell Signal* 15, 529-537
164. Komatsu, M., *et al.* (1995) Glucose stimulation of insulin release in the absence of extracellular Ca2+ and in the absence of any increase in intracellular Ca2+ in rat pancreatic islets. *Proc Natl Acad Sci U S A* 92, 10728-10732
165. Komatsu, M., *et al.* (1997) Augmentation of insulin release by glucose in the absence of extracellular Ca2+: new insights into stimulus-secretion coupling. *Diabetes* 46, 1928-1938
166. Schuit, F., *et al.* (1997) Metabolic fate of glucose in purified islet cells. Glucose-regulated anaplerosis in beta cells. *J Biol Chem* 272, 18572-18579
167. Farfari, S., *et al.* (2000) Glucose-regulated anaplerosis and cataplerosis in pancreatic beta-cells: possible implication of a pyruvate/citrate shuttle in insulin secretion. *Diabetes* 49, 718-726
168. Flamez, D., *et al.* (2002) Critical role for cataplerosis via citrate in glucose-regulated insulin release. *Diabetes* 51, 2018-2024
169. Prentki, M., and Corkey, B.E. (1996) Are the beta-cell signaling molecules malonyl-CoA and cystolic long-chain acyl-CoA implicated in multiple tissue defects of obesity and NIDDM? *Diabetes* 45, 273-283
170. Maechler, P., and Wollheim, C.B. (1999) Mitochondrial glutamate acts as a messenger in glucose-induced insulin exocytosis. *Nature* 402, 685-689
171. Detimary, P., *et al.* (1996) Concentration dependence and time course of the effects of glucose on adenine and guanine nucleotides in mouse pancreatic islets. *J Biol Chem* 271, 20559-20565
172. Henquin, J.C., *et al.* (2002) Signals and pools underlying biphasic insulin secretion. *Diabetes* 51 Suppl 1, S60-67
173. Proks, P., *et al.* (1996) Ca(2+)- and GTP-dependent exocytosis in mouse pancreatic beta-cells involves both common and distinct steps. *J Physiol* 496 (Pt 1), 255-264
174. Barg, S., *et al.* (2002) A subset of 50 secretory granules in close contact with L-type Ca2+ channels accounts for first-phase insulin secretion in mouse beta-cells. *Diabetes* 51 Suppl 1, S74-82
175. Straub, S.G., and Sharp, G.W. (2002) Glucose-stimulated signaling pathways in biphasic insulin secretion. *Diabetes Metab Res Rev* 18, 451-463
176. Eliasson, L., *et al.* (1997) Rapid ATP-dependent priming of secretory granules precedes Ca(2+)-induced exocytosis in mouse pancreatic B-cells. *J Physiol* 503 (Pt 2), 399-412
177. Daniel, S., *et al.* (1999) Identification of the docked granule pool responsible for the first phase of glucose-stimulated insulin secretion. *Diabetes* 48, 1686-1690
178. Wan, Q.F., *et al.* (2004) Protein kinase activation increases insulin secretion by sensitizing the secretory machinery to Ca2+. *J Gen Physiol* 124, 653-662
179. Yang, Y., and Gillis, K.D. (2004) A highly Ca2+-sensitive pool of granules is regulated by glucose and protein kinases in insulin-secreting INS-1 cells. *J Gen Physiol* 124, 641-651
180. Pouli, A.E., *et al.* (1998) Secretory-granule dynamics visualized in vivo with a phogrin-green fluorescent protein chimaera. *Biochem J* 333 (Pt 1), 193-199

181. Hao, M., *et al.* (2005) Regulation of two insulin granule populations within the reserve pool by distinct calcium sources. *J Cell Sci* 118, 5873-5884
182. Halliwell, B. (1995) Antioxidant characterization. Methodology and mechanism. *Biochem Pharmacol* 49, 1341-1348
183. Davies, K.J. (1987) Protein damage and degradation by oxygen radicals. I. general aspects. *J Biol Chem* 262, 9895-9901
184. Droge, W. (2002) Free radicals in the physiological control of cell function. *Physiol Rev* 82, 47-95
185. Maechler, P., and Wollheim, C.B. (2001) Mitochondrial function in normal and diabetic beta-cells. *Nature* 414, 807-812
186. Scheffler, I.E. (2001) A century of mitochondrial research: achievements and perspectives. *Mitochondrion* 1, 3-31
187. Brownlee, M. (2001) Biochemistry and molecular cell biology of diabetic complications. *Nature* 414, 813-820
188. Cadenas, E., and Davies, K.J. (2000) Mitochondrial free radical generation, oxidative stress, and aging. *Free Radic Biol Med* 29, 222-230
189. Raha, S., and Robinson, B.H. (2000) Mitochondria, oxygen free radicals, disease and ageing. *Trends Biochem Sci* 25, 502-508
190. Turrens, J.F. (2003) Mitochondrial formation of reactive oxygen species. *J Physiol* 552, 335-344
191. Evans, J.L., *et al.* (2002) Oxidative stress and stress-activated signaling pathways: a unifying hypothesis of type 2 diabetes. *Endocr Rev* 23, 599-622
192. Oliveira, H.R., *et al.* (2003) Pancreatic beta-cells express phagocyte-like NAD(P)H oxidase. *Diabetes* 52, 1457-1463
193. Tsubouchi, H., *et al.* (2005) Sulfonylurea as well as elevated glucose levels stimulate reactive oxygen species production in the pancreatic beta-cell line, MIN6-a role of NAD(P)H oxidase in beta-cells. *Biochem Biophys Res Commun* 326, 60-65
194. Takeya, R., and Sumimoto, H. (2003) Molecular mechanism for activation of superoxide-producing NADPH oxidases. *Mol Cells* 16, 271-277
195. Nathan, C.F., and Root, R.K. (1977) Hydrogen peroxide release from mouse peritoneal macrophages: dependence on sequential activation and triggering. *J Exp Med* 146, 1648-1662
196. Griendling, K.K., *et al.* (2000) NAD(P)H oxidase: role in cardiovascular biology and disease. *Circ Res* 86, 494-501
197. Lambeth, J.D., *et al.* (2000) Novel homologs of gp91phox. *Trends Biochem Sci* 25, 459-461
198. Tauber, A.I., *et al.* (1983) Chronic granulomatous disease: a syndrome of phagocyte oxidase deficiencies. *Medicine (Baltimore)* 62, 286-309
199. Leusen, J.H., *et al.* (1996) Interactions between the components of the human NADPH oxidase: intrigues in the phox family. *J Lab Clin Med* 128, 461-476
200. Fleming, I.N., *et al.* (1999) Ca2+/calmodulin-dependent protein kinase II regulates Tiam1 by reversible protein phosphorylation. *J Biol Chem* 274, 12753-12758
201. Okabe, T., *et al.* (2003) RICS, a novel GTPase-activating protein for Cdc42 and Rac1, is involved in the beta-catenin-N-cadherin and N-methyl-D-aspartate receptor signaling. *J Biol Chem* 278, 9920-9927
202. Bouin, A.P., *et al.* (1998) p40(phox) is phosphorylated on threonine 154 and serine 315 during activation of the phagocyte NADPH oxidase. Implication of a protein kinase c-type kinase in the phosphorylation process. *J Biol Chem* 273, 30097-30103

203. Reeves, E.P., *et al.* (1999) Direct interaction between p47phox and protein kinase C: evidence for targeting of protein kinase C by p47phox in neutrophils. *Biochem J* 344 Pt 3, 859-866
204. Regier, D.S., *et al.* (1999) A phosphatidic acid-activated protein kinase and conventional protein kinase C isoforms phosphorylate p22(phox), an NADPH oxidase component. *J Biol Chem* 274, 36601-36608
205. Kuroki, T., *et al.* (2003) Oxidative stress: the lead or supporting actor in the pathogenesis of diabetic complications. *J Am Soc Nephrol* 14, S216-220
206. Tu, B.P., and Weissman, J.S. (2004) Oxidative protein folding in eukaryotes: mechanisms and consequences. *J Cell Biol* 164, 341-346
207. Haynes, C.M., *et al.* (2004) Degradation of misfolded proteins prevents ER-derived oxidative stress and cell death. *Mol Cell* 15, 767-776
208. Goldberger, R.F., *et al.* (1963) Acceleration of reactivation of reduced bovine pancreatic ribonuclease by a microsomal system from rat liver. *J Biol Chem* 238, 628-635
209. Winter, J., *et al.* (2002) Catalytic activity and chaperone function of human protein-disulfide isomerase are required for the efficient refolding of proinsulin. *J Biol Chem* 277, 310-317
210. Frand, A.R., *et al.* (2000) Pathways for protein disulphide bond formation. *Trends Cell Biol* 10, 203-210
211. Tu, B.P., and Weissman, J.S. (2002) The FAD- and O(2)-dependent reaction cycle of Ero1-mediated oxidative protein folding in the endoplasmic reticulum. *Mol Cell* 10, 983-994
212. Tu, B.P., *et al.* (2000) Biochemical basis of oxidative protein folding in the endoplasmic reticulum. *Science* 290, 1571-1574
213. Stevens, F.J., and Argon, Y. (1999) Protein folding in the ER. *Semin Cell Dev Biol* 10, 443-454
214. Trump, B.F., and Berezesky, I.K. (1995) Calcium-mediated cell injury and cell death. *Faseb J* 9, 219-228
215. Harper, J.A., *et al.* (2001) Mitochondrial uncoupling as a target for drug development for the treatment of obesity. *Obes Rev* 2, 255-265
216. Fleury, C., and Sanchis, D. (1999) The mitochondrial uncoupling protein-2: current status. *Int J Biochem Cell Biol* 31, 1261-1278
217. Matthias, A., *et al.* (1999) The bioenergetics of brown fat mitochondria from UCP1-ablated mice. Ucp1 is not involved in fatty acid-induced de-energization ("uncoupling"). *J Biol Chem* 274, 28150-28160
218. Pecqueur, C., *et al.* (2001) Uncoupling protein 2, in vivo distribution, induction upon oxidative stress, and evidence for translational regulation. *J Biol Chem* 276, 8705-8712
219. Sivitz, W.I., *et al.* (1999) Fasting and leptin modulate adipose and muscle uncoupling protein: divergent effects between messenger ribonucleic acid and protein expression. *Endocrinology* 140, 1511-1519
220. Nedergaard, J., and Cannon, B. (2003) The 'novel' 'uncoupling' proteins UCP2 and UCP3: what do they really do? Pros and cons for suggested functions. *Exp Physiol* 88, 65-84
221. Echtay, K.S., *et al.* (2002) Superoxide activates mitochondrial uncoupling proteins. *Nature* 415, 96-99
222. James, A.M., and Murphy, M.P. (2002) How mitochondrial damage affects cell function. *J Biomed Sci* 9, 475-487

223. Bereiter-Hahn, J., and Voth, M. (1994) Dynamics of mitochondria in living cells: shape changes, dislocations, fusion, and fission of mitochondria. *Microsc Res Tech* 27, 198-219
224. Wakabayashi, T. (2002) Megamitochondria formation - physiology and pathology. *J Cell Mol Med* 6, 497-538
225. Gulbins, E., *et al.* (2003) Role of mitochondria in apoptosis. *Exp Physiol* 88, 85-90
226. Delettre, C., *et al.* (2000) Nuclear gene OPA1, encoding a mitochondrial dynamin-related protein, is mutated in dominant optic atrophy. *Nat Genet* 26, 207-210
227. Niemann, A., *et al.* (2005) Ganglioside-induced differentiation associated protein 1 is a regulator of the mitochondrial network: new implications for Charcot-Marie-Tooth disease. *J Cell Biol* 170, 1067-1078
228. Vincent, A.M., *et al.* (2002) Oxidative stress and programmed cell death in diabetic neuropathy. *Ann N Y Acad Sci* 959, 368-383
229. Anello, M., *et al.* (2005) Functional and morphological alterations of mitochondria in pancreatic beta cells from type 2 diabetic patients. *Diabetologia* 48, 282-289
230. Ganitkevich, V.Y. (2003) The role of mitochondria in cytoplasmic Ca2+ cycling. *Exp Physiol* 88, 91-97
231. Bianchi, K., *et al.* (2004) Calcium and mitochondria: mechanisms and functions of a troubled relationship. *Biochim Biophys Acta* 1742, 119-131
232. Brini, M., *et al.* (1999) A calcium signaling defect in the pathogenesis of a mitochondrial DNA inherited oxidative phosphorylation deficiency. *Nat Med* 5, 951-954
233. Duchen, M.R. (2000) Mitochondria and Ca(2+)in cell physiology and pathophysiology. *Cell Calcium* 28, 339-348
234. Thayer, S.A., *et al.* (2002) Modulating Ca2+ clearance from neurons. *Front Biosci* 7, d1255-1279
235. Pozzan, T., and Rizzuto, R. (2000) The renaissance of mitochondrial calcium transport. *Eur J Biochem* 267, 5269-5273
236. Gunter, T.E., and Gunter, K.K. (2001) Uptake of calcium by mitochondria: transport and possible function. *IUBMB Life* 52, 197-204
237. Pfeiffer, D.R., *et al.* (2001) Release of Ca2+ from mitochondria via the saturable mechanisms and the permeability transition. *IUBMB Life* 52, 205-212
238. Rizzuto, R., *et al.* (2000) Mitochondria as all-round players of the calcium game. *J Physiol* 529 Pt 1, 37-47
239. Gunter, T.E., *et al.* (2000) Mitochondrial calcium transport: mechanisms and functions. *Cell Calcium* 28, 285-296
240. Skulachev, V.P. (2001) Mitochondrial filaments and clusters as intracellular power-transmitting cables. *Trends Biochem Sci* 26, 23-29
241. Hajnoczky, G., *et al.* (2000) The machinery of local Ca2+ signalling between sarco-endoplasmic reticulum and mitochondria. *J Physiol* 529 Pt 1, 69-81
242. Kaftan, E.J., *et al.* (2000) Mitochondria shape hormonally induced cytoplasmic calcium oscillations and modulate exocytosis. *J Biol Chem* 275, 25465-25470
243. Pacher, P., *et al.* (2002) Ca2+ marks: miniature calcium signals in single mitochondria driven by ryanodine receptors. *Proc Natl Acad Sci U S A* 99, 2380-2385
244. Wang, H.J., *et al.* (2000) Calcium regulates the association between mitochondria and a smooth subdomain of the endoplasmic reticulum. *J Cell Biol* 150, 1489-1498

245. Maechler, P., *et al.* (1999) Secretagogues modulate the calcium concentration in the endoplasmic reticulum of insulin-secreting cells. Studies in aequorin-expressing intact and permeabilized ins-1 cells. *J Biol Chem* 274, 12583-12592
246. Szabadkai, G., and Rizzuto, R. (2004) Participation of endoplasmic reticulum and mitochondrial calcium handling in apoptosis: more than just neighborhood? *FEBS Lett* 567, 111-115
247. Baynes, J.W. (1991) Role of oxidative stress in development of complications in diabetes. *Diabetes* 40, 405-412
248. Wolff, S.P. (1993) Diabetes mellitus and free radicals. Free radicals, transition metals and oxidative stress in the aetiology of diabetes mellitus and complications. *Br Med Bull* 49, 642-652
249. Rehman, A., *et al.* (1999) Increased oxidative damage to all DNA bases in patients with type II diabetes mellitus. *FEBS Lett* 448, 120-122
250. Shin, C.S., *et al.* (2001) Serum 8-hydroxy-guanine levels are increased in diabetic patients. *Diabetes Care* 24, 733-737
251. Donath, M.Y., *et al.* (2003) Inflammatory mediators and islet beta-cell failure: a link between type 1 and type 2 diabetes. *J Mol Med* 81, 455-470
252. Yan, S.D., *et al.* (1994) Enhanced cellular oxidant stress by the interaction of advanced glycation end products with their receptors/binding proteins. *J Biol Chem* 269, 9889-9897
253. Nishikawa, T., *et al.* (2000) Normalizing mitochondrial superoxide production blocks three pathways of hyperglycaemic damage. *Nature* 404, 787-790
254. Malaisse, W.J. (1997) Physiology, pathology and pharmacology of insulin secretion: recent acquisitions. *Diabetes Metab* 23 Suppl 3, 6-15
255. Maechler, P., *et al.* (1999) Hydrogen peroxide alters mitochondrial activation and insulin secretion in pancreatic beta cells. *J Biol Chem* 274, 27905-27913
256. Lenzen, S., *et al.* (1988) Inhibition of glucokinase by alloxan through interaction with SH groups in the sugar-binding site of the enzyme. *Mol Pharmacol* 34, 395-400
257. Poitout, V., and Robertson, R.P. (2002) Minireview: Secondary beta-cell failure in type 2 diabetes--a convergence of glucotoxicity and lipotoxicity. *Endocrinology* 143, 339-342
258. Matsuoka, T., *et al.* (1997) Glycation-dependent, reactive oxygen species-mediated suppression of the insulin gene promoter activity in HIT cells. *J Clin Invest* 99, 144-150
259. Ihara, Y., *et al.* (1999) Hyperglycemia causes oxidative stress in pancreatic beta-cells of GK rats, a model of type 2 diabetes. *Diabetes* 48, 927-932
260. Laybutt, D.R., *et al.* (2002) Increased expression of antioxidant and antiapoptotic genes in islets that may contribute to beta-cell survival during chronic hyperglycemia. *Diabetes* 51, 413-423
261. Tiedge, M., *et al.* (1997) Relation between antioxidant enzyme gene expression and antioxidative defense status of insulin-producing cells. *Diabetes* 46, 1733-1742
262. McGarry, J.D., and Dobbins, R.L. (1999) Fatty acids, lipotoxicity and insulin secretion. *Diabetologia* 42, 128-138
263. Gremlich, S., *et al.* (1997) Fatty acids decrease IDX-1 expression in rat pancreatic islets and reduce GLUT2, glucokinase, insulin, and somatostatin levels. *J Biol Chem* 272, 30261-30269
264. Carlsson, C., *et al.* (1999) Sodium palmitate induces partial mitochondrial uncoupling and reactive oxygen species in rat pancreatic islets in vitro. *Endocrinology* 140, 3422-3428

265. Fridlyand, L.E., and Philipson, L.H. (2004) Does the glucose-dependent insulin secretion mechanism itself cause oxidative stress in pancreatic beta-cells? *Diabetes* 53, 1942-1948
266. Patterson, G.H., *et al.* (2000) Separation of the glucose-stimulated cytoplasmic and mitochondrial NAD(P)H responses in pancreatic islet beta cells. *Proc Natl Acad Sci U S A* 97, 5203-5207
267. Ronner, P., *et al.* (2001) Effects of glucose and amino acids on free ADP in betaHC9 insulin-secreting cells. *Diabetes* 50, 291-300
268. Starkov, A.A., *et al.* (2002) Regulation of hydrogen peroxide production by brain mitochondria by calcium and Bax. *J Neurochem* 83, 220-228
269. Chan, C.B., *et al.* (2001) Increased uncoupling protein-2 levels in beta-cells are associated with impaired glucose-stimulated insulin secretion: mechanism of action. *Diabetes* 50, 1302-1310
270. Saleh, M.C., *et al.* (2002) Uncoupling protein-2: evidence for its function as a metabolic regulator. *Diabetologia* 45, 174-187
271. Zhang, C.Y., *et al.* (2001) Uncoupling protein-2 negatively regulates insulin secretion and is a major link between obesity, beta cell dysfunction, and type 2 diabetes. *Cell* 105, 745-755
272. Li, L.X., *et al.* (2001) Uncoupling protein-2 participates in cellular defense against oxidative stress in clonal beta-cells. *Biochem Biophys Res Commun* 282, 273-277
273. Brown, J.E., *et al.* (2002) Glucose induces and leptin decreases expression of uncoupling protein-2 mRNA in human islets. *FEBS Lett* 513, 189-192
274. Medvedev, A.V., *et al.* (2002) Regulation of the uncoupling protein-2 gene in INS-1 beta-cells by oleic acid. *J Biol Chem* 277, 42639-42644
275. Krauss, S., *et al.* (2003) Superoxide-mediated activation of uncoupling protein 2 causes pancreatic beta cell dysfunction. *J Clin Invest* 112, 1831-1842
276. Koyama, K., *et al.* (1997) beta-cell function in normal rats made chronically hyperleptinemic by adenovirus-leptin gene therapy. *Diabetes* 46, 1276-1280
277. Lee, Y., *et al.* (1997) Increased lipogenic capacity of the islets of obese rats: a role in the pathogenesis of NIDDM. *Diabetes* 46, 408-413
278. Shimabukuro, M., *et al.* (1997) Induction of uncoupling protein-2 mRNA by troglitazone in the pancreatic islets of Zucker diabetic fatty rats. *Biochem Biophys Res Commun* 237, 359-361
279. Viguerie-Bascands, N., *et al.* (1999) Increase in uncoupling protein-2 mRNA expression by BRL49653 and bromopalmitate in human adipocytes. *Biochem Biophys Res Commun* 256, 138-141
280. Lameloise, N., *et al.* (2001) Uncoupling protein 2: a possible link between fatty acid excess and impaired glucose-induced insulin secretion? *Diabetes* 50, 803-809
281. Kaneto, H., *et al.* (2005) Role of oxidative stress, endoplasmic reticulum stress, and c-Jun N-terminal kinase in pancreatic beta-cell dysfunction and insulin resistance. *Int J Biochem Cell Biol* 37, 1595-1608
282. Nardai, G., *et al.* (2003) Reduction of the endoplasmic reticulum accompanies the oxidative damage of diabetes mellitus. *Biofactors* 17, 259-267
283. Suzuki, C.K., *et al.* (1991) Regulating the retention of T-cell receptor alpha chain variants within the endoplasmic reticulum: Ca(2+)-dependent association with BiP. *J Cell Biol* 114, 189-205
284. Webb, S.E., and Miller, A.L. (2003) Calcium signalling during embryonic development. *Nat Rev Mol Cell Biol* 4, 539-551

285. Lodish, H.F., *et al.* (1992) Calcium is required for folding of newly made subunits of the asialoglycoprotein receptor within the endoplasmic reticulum. *J Biol Chem* 267, 12753-12760
286. Hurtley, S.M., *et al.* (1989) Interactions of misfolded influenza virus hemagglutinin with binding protein (BiP). *J Cell Biol* 108, 2117-2126
287. Flynn, G.C., *et al.* (1991) Peptide-binding specificity of the molecular chaperone BiP. *Nature* 353, 726-730
288. Zhang, J.X., *et al.* (1997) Quality control in the secretory pathway: the role of calreticulin, calnexin and BiP in the retention of glycoproteins with C-terminal truncations. *Mol Biol Cell* 8, 1943-1954
289. Harding, H.P., *et al.* (1999) Protein translation and folding are coupled by an endoplasmic-reticulum-resident kinase. *Nature* 397, 271-274
290. Friedlander, R., *et al.* (2000) A regulatory link between ER-associated protein degradation and the unfolded-protein response. *Nat Cell Biol* 2, 379-384
291. Travers, K.J., *et al.* (2000) Functional and genomic analyses reveal an essential coordination between the unfolded protein response and ER-associated degradation. *Cell* 101, 249-258
292. Scheuner, D., *et al.* (2001) Translational control is required for the unfolded protein response and in vivo glucose homeostasis. *Mol Cell* 7, 1165-1176
293. Harding, H.P., *et al.* (2003) An integrated stress response regulates amino acid metabolism and resistance to oxidative stress. *Mol Cell* 11, 619-633
294. Calfon, M., *et al.* (2002) IRE1 couples endoplasmic reticulum load to secretory capacity by processing the XBP-1 mRNA. *Nature* 415, 92-96
295. Iwakoshi, N.N., *et al.* (2003) Plasma cell differentiation and the unfolded protein response intersect at the transcription factor XBP-1. *Nat Immunol* 4, 321-329
296. Gething, M.J. (1999) Role and regulation of the ER chaperone BiP. *Semin Cell Dev Biol* 10, 465-472
297. Hendershot, L.M., *et al.* (1988) Identity of the immunoglobulin heavy-chain-binding protein with the 78,000-dalton glucose-regulated protein and the role of posttranslational modifications in its binding function. *Mol Cell Biol* 8, 4250-4256
298. Blond-Elguindi, S., *et al.* (1993) Peptide-dependent stimulation of the ATPase activity of the molecular chaperone BiP is the result of conversion of oligomers to active monomers. *J Biol Chem* 268, 12730-12735
299. Bertolotti, A., *et al.* (2000) Dynamic interaction of BiP and ER stress transducers in the unfolded-protein response. *Nat Cell Biol* 2, 326-332
300. Ma, K., *et al.* (2002) Dimerization and release of molecular chaperone inhibition facilitate activation of eukaryotic initiation factor-2 kinase in response to endoplasmic reticulum stress. *J Biol Chem* 277, 18728-18735
301. Shamu, C.E., and Walter, P. (1996) Oligomerization and phosphorylation of the Ire1p kinase during intracellular signaling from the endoplasmic reticulum to the nucleus. *Embo J* 15, 3028-3039
302. Liu, C.Y., *et al.* (2002) The protein kinase/endoribonuclease IRE1alpha that signals the unfolded protein response has a luminal N-terminal ligand-independent dimerization domain. *J Biol Chem* 277, 18346-18356
303. Shen, J., *et al.* (2002) ER stress regulation of ATF6 localization by dissociation of BiP/GRP78 binding and unmasking of Golgi localization signals. *Dev Cell* 3, 99-111
304. Chen, X., *et al.* (2002) The luminal domain of ATF6 senses endoplasmic reticulum (ER) stress and causes translocation of ATF6 from the ER to the Golgi. *J Biol Chem* 277, 13045-13052

305. Mori, K., *et al.* (1993) A transmembrane protein with a cdc2+/CDC28-related kinase activity is required for signaling from the ER to the nucleus. *Cell* 74, 743-756
306. Lee, A.H., *et al.* (2003) XBP-1 regulates a subset of endoplasmic reticulum resident chaperone genes in the unfolded protein response. *Mol Cell Biol* 23, 7448-7459
307. Ma, Y., *et al.* (2002) Two distinct stress signaling pathways converge upon the CHOP promoter during the mammalian unfolded protein response. *J Mol Biol* 318, 1351-1365
308. Yamamoto, K., *et al.* (2004) Differential contributions of ATF6 and XBP1 to the activation of endoplasmic reticulum stress-responsive cis-acting elements ERSE, UPRE and ERSE-II. *J Biochem (Tokyo)* 136, 343-350
309. Hosokawa, N., *et al.* (2003) Enhancement of endoplasmic reticulum (ER) degradation of misfolded Null Hong Kong alpha1-antitrypsin by human ER mannosidase I. *J Biol Chem* 278, 26287-26294
310. Shi, Y., *et al.* (1999) Characterization of a mutant pancreatic eIF-2alpha kinase, PEK, and co-localization with somatostatin in islet delta cells. *J Biol Chem* 274, 5723-5730
311. Cullinan, S.B., *et al.* (2003) Nrf2 is a direct PERK substrate and effector of PERK-dependent cell survival. *Mol Cell Biol* 23, 7198-7209
312. Venugopal, R., and Jaiswal, A.K. (1998) Nrf2 and Nrf1 in association with Jun proteins regulate antioxidant response element-mediated expression and coordinated induction of genes encoding detoxifying enzymes. *Oncogene* 17, 3145-3156
313. Hinnebusch, A.G. (1997) Translational regulation of yeast GCN4. A window on factors that control initiator-trna binding to the ribosome. *J Biol Chem* 272, 21661-21664
314. Harding, H.P., *et al.* (2000) Regulated translation initiation controls stress-induced gene expression in mammalian cells. *Mol Cell* 6, 1099-1108
315. Oyadomari, S., *et al.* (2002) Targeted disruption of the Chop gene delays endoplasmic reticulum stress-mediated diabetes. *J Clin Invest* 109, 525-532
316. Ma, Y., and Hendershot, L.M. (2003) Delineation of a negative feedback regulatory loop that controls protein translation during endoplasmic reticulum stress. *J Biol Chem* 278, 34864-34873
317. Kojima, E., *et al.* (2003) The function of GADD34 is a recovery from a shutoff of protein synthesis induced by ER stress: elucidation by GADD34-deficient mice. *Faseb J* 17, 1573-1575
318. Jiang, H.Y., *et al.* (2004) Activating transcription factor 3 is integral to the eukaryotic initiation factor 2 kinase stress response. *Mol Cell Biol* 24, 1365-1377
319. Ye, J., *et al.* (2000) ER stress induces cleavage of membrane-bound ATF6 by the same proteases that process SREBPs. *Mol Cell* 6, 1355-1364
320. Haze, K., *et al.* (1999) Mammalian transcription factor ATF6 is synthesized as a transmembrane protein and activated by proteolysis in response to endoplasmic reticulum stress. *Mol Biol Cell* 10, 3787-3799
321. Yoshida, H., *et al.* (1998) Identification of the cis-acting endoplasmic reticulum stress response element responsible for transcriptional induction of mammalian glucose-regulated proteins. Involvement of basic leucine zipper transcription factors. *J Biol Chem* 273, 33741-33749
322. Kokame, K., *et al.* (2001) Identification of ERSE-II, a new cis-acting element responsible for the ATF6-dependent mammalian unfolded protein response. *J Biol Chem* 276, 9199-9205

323. Wang, Y., *et al.* (2000) Activation of ATF6 and an ATF6 DNA binding site by the endoplasmic reticulum stress response. *J Biol Chem* 275, 27013-27020
324. Yoshida, H., *et al.* (2000) ATF6 activated by proteolysis binds in the presence of NF-Y (CBF) directly to the cis-acting element responsible for the mammalian unfolded protein response. *Mol Cell Biol* 20, 6755-6767
325. Shen, X., *et al.* (2001) Complementary signaling pathways regulate the unfolded protein response and are required for C. elegans development. *Cell* 107, 893-903
326. Lee, K., *et al.* (2002) IRE1-mediated unconventional mRNA splicing and S2P-mediated ATF6 cleavage merge to regulate XBP1 in signaling the unfolded protein response. *Genes Dev* 16, 452-466
327. Rutkowski, D.T., and Kaufman, R.J. (2004) A trip to the ER: coping with stress. *Trends Cell Biol* 14, 20-28
328. Yoshida, H., *et al.* (2003) A time-dependent phase shift in the mammalian unfolded protein response. *Dev Cell* 4, 265-271
329. Nishitoh, H., *et al.* (2002) ASK1 is essential for endoplasmic reticulum stress-induced neuronal cell death triggered by expanded polyglutamine repeats. *Genes Dev* 16, 1345-1355
330. Urano, F., *et al.* (2000) Coupling of stress in the ER to activation of JNK protein kinases by transmembrane protein kinase IRE1. *Science* 287, 664-666
331. Orrenius, S., *et al.* (2003) Regulation of cell death: the calcium-apoptosis link. *Nat Rev Mol Cell Biol* 4, 552-565
332. McCullough, K.D., *et al.* (2001) Gadd153 sensitizes cells to endoplasmic reticulum stress by down-regulating Bcl2 and perturbing the cellular redox state. *Mol Cell Biol* 21, 1249-1259
333. Araki, E., *et al.* (2003) Impact of endoplasmic reticulum stress pathway on pancreatic beta-cells and diabetes mellitus. *Exp Biol Med (Maywood)* 228, 1213-1217
334. Yoshioka, M., *et al.* (1997) A novel locus, Mody4, distal to D7Mit189 on chromosome 7 determines early-onset NIDDM in nonobese C57BL/6 (Akita) mutant mice. *Diabetes* 46, 887-894
335. Ron, D. (2002) Proteotoxicity in the endoplasmic reticulum: lessons from the Akita diabetic mouse. *J Clin Invest* 109, 443-445
336. Butler, A.E., *et al.* (2003) Beta-cell deficit and increased beta-cell apoptosis in humans with type 2 diabetes. *Diabetes* 52, 102-110
337. Harding, H.P., *et al.* (2001) Diabetes mellitus and exocrine pancreatic dysfunction in perk-/- mice reveals a role for translational control in secretory cell survival. *Mol Cell* 7, 1153-1163
338. Scheuner, D., *et al.* (2005) Control of mRNA translation preserves endoplasmic reticulum function in beta cells and maintains glucose homeostasis. *Nat Med* 11, 757-764
339. Kaufman, R.J., *et al.* (2002) The unfolded protein response in nutrient sensing and differentiation. *Nat Rev Mol Cell Biol* 3, 411-421
340. Itoh, N., and Okamoto, H. (1980) Translational control of proinsulin synthesis by glucose. *Nature* 283, 100-102
341. Merglen, A., Theander, S., Rubi, B., Chaffard, G., Wollheim, C.B., and Maechler, P. (2004) Glucose Sensitivity and Metabolism-Secretion Coupling Studied during Two-Year Continuous Culture in INS-1E Insulinoma Cells. *Endocrinology* 145, 667-678
342. Bhathena, S.J., *et al.* (1984) Insulin, glucagon, and somatostatin secretion by cultured rat islet cell tumor and its clones. *Proc Soc Exp Biol Med* 175, 35-38

343. Nielsen, D.A., *et al.* (1985) Control of insulin gene expression in pancreatic beta-cells and in an insulin-producing cell line, RIN-5F cells. I. Effects of glucose and cyclic AMP on the transcription of insulin mRNA. *J Biol Chem* 260, 13585-13589
344. Oie, H.K., *et al.* (1983) Clonal analysis of insulin and somatostatin secretion and L-dopa decarboxylase expression by a rat islet cell tumor. *Endocrinology* 112, 1070-1075
345. Poitout, V., *et al.* (1996) Insulin-secreting cell lines: classification, characteristics and potential applications. *Diabetes Metab* 22, 7-14
346. Praz, G.A., *et al.* (1983) Regulation of immunoreactive-insulin release from a rat cell line (RINm5F). *Biochem J* 210, 345-352
347. Brant, A.M., *et al.* (1992) Analysis of the glucose transporter content of islet cell lines: implications for glucose-stimulated insulin release. *Cell Signal* 4, 641-650
348. Hohmeier, H.E., *et al.* (1997) Regulation of insulin secretion from novel engineered insulinoma cell lines. *Diabetes* 46, 968-977
349. Swanston-Flatt, S.K., and Flatt, P.R. (1988) Effects of amino acids, hormones and drugs on insulin release and 45Ca uptake by transplantable rat insulinoma cells maintained in tissue culture. *Gen Pharmacol* 19, 239-242
350. Ribalet, B., and Ciani, S. (1987) Regulation by cell metabolism and adenine nucleotides of a K channel in insulin-secreting B cells (RIN m5F). *Proc Natl Acad Sci U S A* 84, 1721-1725
351. Montrose-Rafizadeh, C., *et al.* (1994) Incretin hormones regulate glucose-dependent insulin secretion in RIN 1046-38 cells: mechanisms of action. *Endocrinology* 135, 589-594
352. Wang, Y., *et al.* (1996) GIP regulates glucose transporters, hexokinases, and glucose-induced insulin secretion in RIN 1046-38 cells. *Mol Cell Endocrinol* 116, 81-87
353. Hribal, M.L., *et al.* (2003) Chronic hyperglycemia impairs insulin secretion by affecting insulin receptor expression, splicing, and signaling in RIN beta cell line and human islets of Langerhans. *Faseb J* 17, 1340-1342
354. Lee, B., *et al.* (2003) Inhibition of mitochondrial Na+-Ca2+ exchanger increases mitochondrial metabolism and potentiates glucose-stimulated insulin secretion in rat pancreatic islets. *Diabetes* 52, 965-973
355. Harapanhalli, R.S., *et al.* (1996) Antioxidant effects of vitamin C in mice following X-irradiation. *Res Commun Mol Pathol Pharmacol* 94, 271-287
356. Kharroubi, I., *et al.* (2004) Free fatty acids and cytokines induce pancreatic beta-cell apoptosis by different mechanisms: role of nuclear factor-kappaB and endoplasmic reticulum stress. *Endocrinology* 145, 5087-5096
357. Fiedorek, F.T., Jr., *et al.* (1990) Selective expression of the insulin I gene in rat insulinoma-derived cell lines. *Mol Endocrinol* 4, 990-999
358. Sossin, W.S., *et al.* (1990) Dale's hypothesis revisited: different neuropeptides derived from a common prohormone are targeted to different processes. *Proc Natl Acad Sci U S A* 87, 4845-4848
359. Lukinius, A., *et al.* (2003) Cellular expression and specific intragranular localization of chromogranin A, chromogranin B, and synaptophysin during ontogeny of pancreatic islet cells: an ultrastructural study. *Pancreas* 27, 38-46
360. Yoo, S.H. (1996) pH- and Ca(2+)-dependent aggregation property of secretory vesicle matrix proteins and the potential role of chromogranins A and B in secretory vesicle biogenesis. *J Biol Chem* 271, 1558-1565
361. Zhang, K., and Kaufman, R.J. (2006) The unfolded protein response: a stress signaling pathway critical for health and disease. *Neurology* 66, S102-109

362. Mitchell, K.J., *et al.* (2001) Dense core secretory vesicles revealed as a dynamic Ca(2+) store in neuroendocrine cells with a vesicle-associated membrane protein aequorin chimaera. *J Cell Biol* 155, 41-51
363. Mitchell, K.J., *et al.* (2003) Ryanodine receptor type I and nicotinic acid adenine dinucleotide phosphate receptors mediate Ca2+ release from insulin-containing vesicles in living pancreatic beta-cells (MIN6). *J Biol Chem* 278, 11057-11064
364. Sombers, L.A., *et al.* (2005) Loaded dopamine is preferentially stored in the halo portion of PC12 cell dense core vesicles. *J Neurochem* 93, 1122-1131
365. Nielsen, J.H. (1989) Mechanisms of pancreatic beta-cell growth and regeneration: studies on rat insulinoma cells. *Exp Clin Endocrinol* 93, 277-285
366. DeAizpurua, H.J., *et al.* (1997) Expression of mixed lineage kinase-1 in pancreatic beta-cell lines at different stages of maturation and during embryonic pancreas development. *J Biol Chem* 272, 16364-16373
367. Cram, D.S., *et al.* (1999) Differential mRNA display analysis of two related but functionally distinct rat insulinoma (RIN) cell lines: identification of CD24 and its expression in the developing pancreas. *Differentiation* 64, 237-246
368. Schwitzgebel, V.M. (2001) Programming of the pancreas. *Mol Cell Endocrinol* 185, 99-108
369. Arvan, P., *et al.* (2002) Lumenal protein multimerization in the distal secretory pathway/secretory granules. *Curr Opin Cell Biol* 14, 448-453
370. Rustom, A., *et al.* (2002) Selective delivery of secretory cargo in Golgi-derived carriers of nonepithelial cells. *Traffic* 3, 279-288
371. Orci, L., *et al.* (1987) Proteolytic maturation of insulin is a post-Golgi event which occurs in acidifying clathrin-coated secretory vesicles. *Cell* 49, 865-868
372. Tian, J.H., *et al.* (2003) Ca2+-dependent phosphorylation of syntaxin-1A by DAP-kinase regulates its interaction with Munc-18. *J Biol Chem*
373. Reetz, A., *et al.* (1991) GABA and pancreatic beta-cells: colocalization of glutamic acid decarboxylase (GAD) and GABA with synaptic-like microvesicles suggests their role in GABA storage and secretion. *Embo J* 10, 1275-1284
374. Gaskins, H.R., *et al.* (1995) Glucose modulates gamma-aminobutyric acid release from the pancreatic beta TC6 cell line. *J Biol Chem* 270, 30286-30289
375. Braun, M., *et al.* (2004) Regulated exocytosis of GABA-containing synaptic-like microvesicles in pancreatic beta-cells. *J Gen Physiol* 123, 191-204
376. Brice, N.L., *et al.* (2002) Metabotropic glutamate and GABA(B) receptors contribute to the modulation of glucose-stimulated insulin secretion in pancreatic beta cells. *Diabetologia* 45, 242-252
377. Wang, J., *et al.* (1999) Novel rabphilin-3-like protein associates with insulin-containing granules in pancreatic beta cells. *J Biol Chem* 274, 28542-28548
378. Regazzi, R., *et al.* (1995) VAMP-2 and cellubrevin are expressed in pancreatic beta-cells and are essential for Ca(2+)-but not for GTP gamma S-induced insulin secretion. *Embo J* 14, 2723-2730
379. Mizuta, M., *et al.* (1997) Localization and functional role of synaptotagmin III in insulin secretory vesicles in pancreatic beta-cells. *Diabetes* 46, 2002-2006
380. Sheu, S.S., *et al.* (2006) Targeting antioxidants to mitochondria: a new therapeutic direction. *Biochim Biophys Acta* 1762, 256-265
381. Yu, T., *et al.* (2006) Increased production of reactive oxygen species in hyperglycemic conditions requires dynamic change of mitochondrial morphology. *Proc Natl Acad Sci U S A*

382. Lee, A.S. (2001) The glucose-regulated proteins: stress induction and clinical applications. *Trends Biochem Sci* 26, 504-510
383. Ohara-Imaizumi, M., *et al.* (2004) The cytokine interleukin-1beta reduces the docking and fusion of insulin granules in pancreatic beta-cells, preferentially decreasing the first phase of exocytosis. *J Biol Chem* 279, 41271-41274
384. Cardozo, A.K., *et al.* (2001) A comprehensive analysis of cytokine-induced and nuclear factor-kappa B-dependent genes in primary rat pancreatic beta-cells. *J Biol Chem* 276, 48879-48886
385. Knoch, K.P., *et al.* (2004) Polypyrimidine tract-binding protein promotes insulin secretory granule biogenesis. *Nat Cell Biol* 6, 207-214
386. Asfari, M., *et al.* (1992) Establishment of 2-mercaptoethanol-dependent differentiated insulin-secreting cell lines. *Endocrinology* 130, 167-178
387. Bhathena, S.J., *et al.* (1982) Insulin, glucagon, and somatostatin receptors on cultured cells and clones from rat islet cell tumor. *Diabetes* 31, 521-531
388. Efrat, S., *et al.* (1988) Beta-cell lines derived from transgenic mice expressing a hybrid insulin gene-oncogene. *Proc Natl Acad Sci U S A* 85, 9037-9041
389. Kroesen, S., *et al.* (1996) Rat brain: distribution of immunoreactivity of PE-11, a peptide derived from chromogranin B. *Eur J Neurosci* 8, 2679-2689
390. Calegari, F., *et al.* (1999) A regulated secretory pathway in cultured hippocampal astrocytes. *J Biol Chem* 274, 22539-22547
391. Borgonovo, B., *et al.* (2002) Regulated exocytosis: a novel, widely expressed system. *Nat Cell Biol* 4, 955-962
392. Ort, T., *et al.* (2001) Dephosphorylation of beta2-syntrophin and Ca2+/mu-calpain-mediated cleavage of ICA512 upon stimulation of insulin secretion. *Embo J* 20, 4013-4023
393. Piquer, S., *et al.* (2006) Monoclonal antibody 76F distinguishes IA-2 from IA-2beta and overlaps an autoantibody epitope. *J Autoimmun*
394. Rossner, M., and Yamada, K.M. (2004) What's in a picture? The temptation of image manipulation. *J Cell Biol* 166, 11-15
395. Villa, A., *et al.* (1993) The endoplasmic-sarcoplasmic reticulum of smooth muscle: immunocytochemistry of vas deferens fibers reveals specialized subcompartments differently equipped for the control of Ca2+ homeostasis. *J Cell Biol* 121, 1041-1051
396. Molinete, M., *et al.* (2000) Trafficking of non-regulated secretory proteins in insulin secreting (INS-1) cells. *Diabetologia* 43, 1157-1164
397. Becker, C.M., *et al.* (1989) Sensitive immunoassay shows selective association of peripheral and integral membrane proteins of the inhibitory glycine receptor complex. *J Neurochem* 53, 124-131
398. Malgaroli, A., *et al.* (1987) Fura-2 measurement of cytosolic free Ca2+ in monolayers and suspensions of various types of animal cells. *J Cell Biol* 105, 2145-2155
399. Rossi, A.H., *et al* (2004) Ca2+ dependency of 'Ca2+-independent' exocytosis in SPOC1 airway goblet cells. *J Physiol* 559, 555-565
400. Hanson, D.A., and Ziegler, S.F. (2001) Regulation of ionomycin-mediated granule release from rat basophil leukemia cells. *Mol Immunol* 38, 1329-1335.

ACKNOWLEDGMENTS

I would like to thank Maria Luisa Malosio for her constant supervision and helpfulness. Thanks for her constant support in the ups and downs of our daily working life and for her precious advice, with which I could gradually gain my independence and grow up as a scientist. Many thanks to Prof. Meldolesi, for offering me the possibility to carry out my PhD, for his scientific supervision and the valuable discussion of my data. I am very grateful to Kevin Docherty for his precious advice, his enthusiasm for my work and his constant encouragements. I would like to thank Daniele Zacchetti, who has followed my work over the time and deserves the title of 'underground tutor' for his technical help and his precious explanations. Thanks to Ezio Bonifacio, who has hosted me in his lab, giving me the practical possibility to carry on my work, to join meetings and training courses, and to get in contact with the world of diabetes. Special thanks to Cristina for her valuable help and friendship, especially when we were both as stressed as our cells! Among the people I would like to thank for non-scientific reasons, the first is Wolfgang, for restoring my enthusiasm, for his constant support in my ups and downs, and for giving me strong reasons to conclude soon and well my PhD. Special thanks to all my friends in the two labs where I have worked, for supporting me day by day until the end (and further!), and for making the working place a unique chance for real friendships. Last, but not least, special thanks to my examiners, Peter Jones and Ottavio Cremona, for the very positive feed back that I got during my 'Viva' about the results of my PhD training, and because my examination gave me new enthusiasm for a new adventure as a post doc. The list would still be long, however I think I can well include everybody thanking for the coffee-breaks and the huge smiles in the corridors... if the walls could only talk!